Therapeutic Potential of Histone Deacetylase 6 Selective Inhibitor, CKD-506 in Inflammatory Bowel Disease

Jaebum Ahn

Department of Medicine

The Graduate School, Yonsei University

Therapeutic Potential of Histone Deacetylase 6 Selective Inhibitor, CKD-506 in Inflammatory Bowel Disease

Directed by Professor Jae Hee Cheon

Doctoral Dissertation
submitted to the Department of Medicine,
the Graduate School of Yonsei University
in partial fulfillment of the requirements for the degree of
Doctor of Philosophy in Medical Science

Jaebum Ahn

December 2023

This certifies that the Doctoral Dissertation of
Jaebum Ahn is approved.

Thesis Supervisor : Jae Hee Cheon

Thesis Committee Member#1 : Jihye Park

Thesis Committee Member#2 : Soo Jung Park

Thesis Committee Member#3: Hyung Jung Lee

Thesis Committee Member#4: Seung Won Kim

The Graduate School
Yonsei University

December 2023

ACKNOWLEDGEMENTS

I want to express my sincere gratitude to my supervisor, Professor Jae Hee Cheon, for his invaluable guidance and support throughout my graduate studies.

I am also deeply grateful to Dr. Seung Won Kim, for his insightful suggestions and warm encouragement on my research.

I would also like to thank my thesis committee members for their thoughtful comments and feedback on my research.

I am also grateful to all the lab members who have provided me with an academic environment and emotional support. Special thanks to Ji Hyung Kim, who generously shared her time and expertise with me.

I would also like to express special thanks to the Bioinformatics Collaboration Unit (BiCU) in the Department of Biomedical Systems Informatics, Yonsei University College of Medicine for analysis support.

Finally, I would like to dedicate this work to my family who always believed in me and inspired me to achieve my goals.

December 2023
Jaebum Ahn

<TABLE OF CONTENTS>

LIST OF FIGURES

LIST OF TABLES

ABSTRACT

Therapeutic Potential of Histone Deacetylase 6 Selective Inhibitor, CKD-506 in Inflammatory Bowel Disease

Jaebum Ahn

Department of Medicine
The Graduate School, Yonsei University

(Directed by Professor Jae Hee Cheon)

Inflammatory bowel disease (IBD) is a chronic, intractable inflammatory disease of unknown cause that occurs in the gastrointestinal tract. Anti-tumor necrosis factor-α (TNF-α) inhibitors can be an alternative treatment for refractory patients to conventional therapy, however, there are limited drug options for primary or secondary non-responders to anti-TNF- α inhibitors.

Histone deacetylase inhibitors have been recognized as potential therapeutic agents for various autoimmune diseases. In particular, CKD-506, a selective inhibitor of histone deacetylase 6 (HDAC6), has been confirmed to have protective effects in animal models of IBD, but there are no studies on human-derived samples.

In this study, the expression pattern of histone deacetylase 6 was investigated through immunohistochemistry staining of human colon tissues. The ex-vivo culture system was established for both mouse and human colon samples, and several inflammatory cytokines and epithelial barrier markers were analyzed after CKD-506 treatment. IBD patients refractory to conventional drugs or anti-TNF-α inhibitors with active inflammation were recruited and colon biopsy samples were incubated with CKD-506 ex-vivo for RNA sequencing and analysis. The transcriptional level of candidate targets of CKD-506 were validated in the human colon cell line and the mouse colon ex-vivo culture system.

We observed an increased expression and activity of HDAC6 in IBD patients compared to healthy control. The disease activity rather than treatment response was correlated with

HDAC6 expression levels in subgroup analysis. After the successful installation of the ex-vivo culture platform, the anti-inflammatory potentials of CKD-506 were confirmed through quantitative real-time polymerase chain reaction. RNA-sequencing of treatment-refractory patient-derived colon samples provided possible downstream targets and elucidated the underlying mechanism of CKD-506. The transcription levels of revealed genes were validated in both human in vitro and mouse ex-vivo models.

This research suggested CKD-506 as a potential therapeutic option for inflammatory bowel disease especially, in patients who poorly responded to current treatment with high disease activity.

Keywords: histone deacetylase inhibitor, inflammatory bowel disease, RNA seq

Therapeutic Potential of Histone Deacetylase 6 Selective Inhibitor, CKD-506 in Inflammatory Bowel Disease

Jaebum Ahn

Department of Medicine
The Graduate School, Yonsei University

(Directed by Professor Jae Hee Cheon)

I. INTRODUCTION

Inflammatory bowel diseases (IBD), including ulcerative colitis (UC) and Crohn's disease (CD), are immune-mediated chronic relapsing diseases characterized by progressive and destructive inflammation affecting the gastrointestinal tract.[1] The prevalence of IBD is growing worldwide, across Asia, North America, and Europe. Several studies suggested that genetic, immunologic, and environmental factors seem to be involved in abnormal immune response or barrier dysfunction, however, the etiology of IBD remains unclear.[2,3]

Anti-TNF-α inhibitors and other biologics, as well as conventional agents such as 5-aminosalicylic acids (ASA), immunomodulators (azathioprine, 6-mercaptopurine), corticosteroids, have been considered as treatment options for IBD patients. These drugs may relieve symptoms but there were no successful medications in terms of mucosal healing.[4,5] Furthermore, current remedies including biologics do not work for one-third of IBD patients and even beneficial patient groups showed less response to medications as time goes by.[6-8] The absence of therapeutics with the small molecule is a huge unmet need for patients and a multidimensional approach is being made to search for potential therapeutic candidates.[9] However, patients who have been prescribed immunosuppressant or biologics are continuously increasing in Korea (Figure 1).

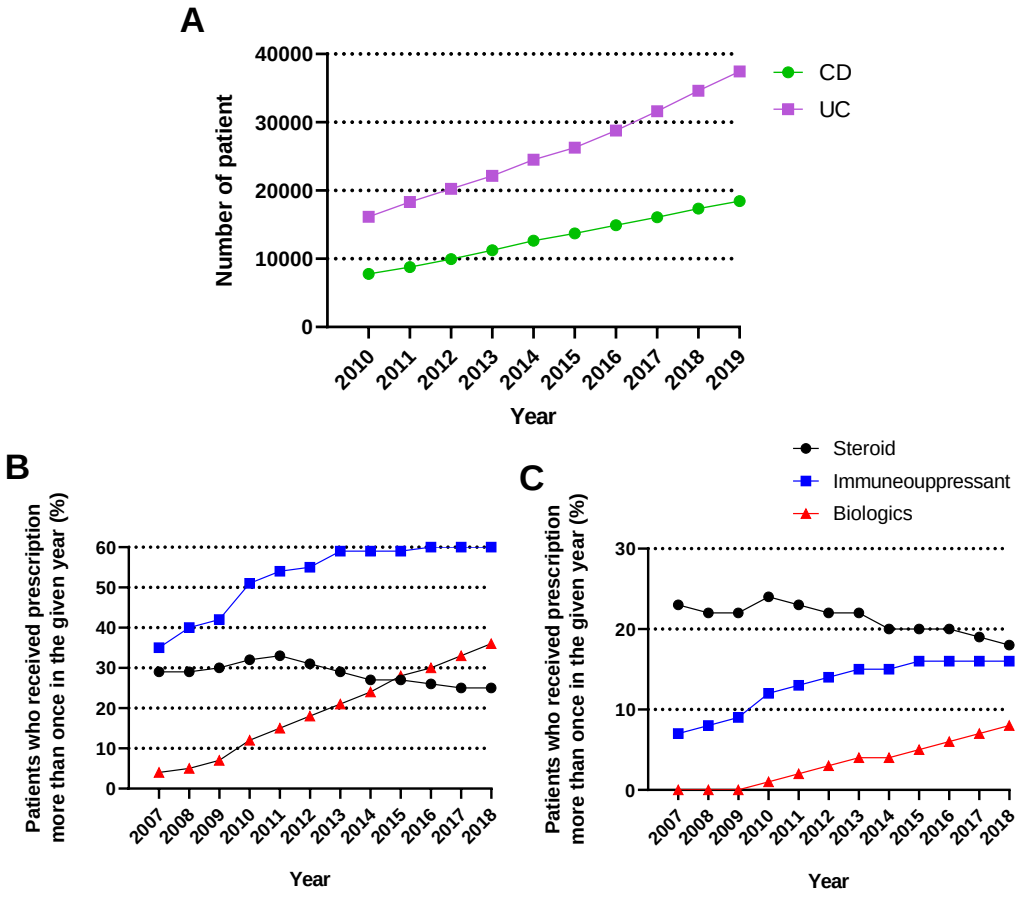

Figure 1. Prevalence and medication usage of inflammatory bowel disease in Korea[10]
Prevalence of Crohn's disease (CD) and ulcerative colitis (UC) in Korea for the past 10 years (A). The percentage of patients who have been prescribed immunosuppressant or biologics are increasing in CD (B) and UC (C).

Histone deacetylase (HDAC) inhibitor is one of the possible treatments, of which anti-cancer and anti-inflammatory effects have been revealed for various autoimmune diseases.[11-14] Especially, HDAC6 is evenly distributed in the cytoplasm and nucleus, which binds not only to histones but also proteins related to cell growth, death, and inflammation. HDAC6 directly controls the expression and regulation of certain targets as well as epigenetic mechanisms.[15]

CKD-506, a recently developed highly selective inhibitor of histone deacetylase 6, has been proven to have anti-inflammatory effects in an IBD animal model.[16] In addition, a phase 2 clinical trial is ongoing to confirm the safety and effectiveness of CKD-506 in rheumatoid arthritis patients who do not respond to methotrexate.[17,18] In a previous study, colitis was alleviated by CKD-506 in the IBD mouse model and was associated with the NF-κB pathway.[19] However, there has never been any research on the effect of HDAC6 inhibitors from human materials or a detailed mechanism study.

To reveal intestinal pathophysiologies of humans, in vitro cell culture or in vivo animal model systems were commonly adopted mimicking in vivo gut physiology. Transformed cell lines have been granted as the most cost-effective and accessible form due to indefinite passages and homogeneity. At the same time, most of these cells are of cancerous origin and poorly reproduce in normal intestinal environments.[20] Furthermore, the normal intestinal epithelium consists of various types of cells such as enterocytes, goblet cells, enteroendocrine cells, Paneth cells, and immune blood cells, unlike single cell lines. Though co-culture enabled the reproduction of more complex cell-cell interactions and physiologic situations, it is still insufficient to imitate in-vivo surroundings and difficult to control culture conditions for multiple types of cells. In-vivo animal model as well as an in-vitro model has a critical drawback in terms of species differences.

The colon is a complicated multicellular tube with a diverse cellular distribution. The cellular heterogeneity contributed to the immunological defense and intestinal barrier. Ex-vivo systems are models cultured outside of an organism, but containing live tissues with complex cellular compositions found in vivo.[21] Human colon explants culture has been

endeavored for several decades.[22] However, there were issues of cell survival and integrity due to exclusive characteristics of the human colon, including oxygen permeability across the intestinal wall and microbial communities.[23,24] Previous studies presented a human colon tissue ex-vivo culture model with various levels of oxygen supply, with or without antibiotics and growth factors.[25]

First of all, HDAC6 expression and activity were confirmed in human colon biopsy samples to estimate the potential effects of HDAC suppressor, CKD-506. Then human colon tissue ex-vivo culture system was established, especially for colon biopsy samples. To define whether CKD-506 could be a protective or therapeutic drug for IBD, CKD-506-treated human biopsy samples were collected and executed in RNA-seq.

In detail, based on clinical and endoscopic findings, healthy control, CD patients, and UC patients were recruited. Patients were divided into conventional treatment or anti-TNF-α inhibitor treatment groups, then sub-classified as treatment responders and non-responders according to current medication status. HDAC6 and α-tubulin acetylation expression levels were confirmed through immunohistochemistry (IHC) staining of paraffin-sectioned colon biopsy samples. To establish a colon biopsy ex-vivo culture system, pre-experiments were conducted with a mouse model, and then applied to human biopsy samples. To investigate potential targets of CKD-506, several inflammations and epithelial barrier markers were observed through quantitative real-time reverse transcription polymerase chain reaction (qRT-PCR) and cytometric bead array (CBA) using colitis mouse models.[26] RNA-seq analysis with isolated RNA from human colon biopsy samples was performed, and DEGs (differentially expressed genes) were extracted. Through the volcano plot, Venn diagram, and network-based pathway analysis, potential therapeutic targets as well as markers related to IBD or HDAC pathway were specified. Possible downstream targets and related pathways were suggested with further gene set enrichment analysis (GSEA) and confirmed with literature research and data-based analysis.

II. MATERIALS AND METHODS

1. Patients and sample collection

Human colonoscopic biopsy samples were collected at the gastroenterology clinic of Yonsei University College of Medicine, Severance Hospital, Seoul, Korea. The diagnosis of UC and CD was based on previously established criteria based on clinical, endoscopic, histopathologic, and radiologic evaluation.[27,28] To be included in the IBD group, patients must have met the following criteria: i) age over 19 years; ii) planned to undergo colonoscopy; iii) able to give informed consent. The following IBD patients were excluded: i) suspected pregnancy or ongoing lactation, ii) unclear diagnosis of either CD or UC, iii) unable to give informed consent. To be included in the healthy control group, individuals must have met the following criteria: i) age over 19 years; ii) planned to undergo colonoscopy due to regular check-ups or intestinal symptoms, iii) able to give informed consent. The following healthy control individuals were excluded: i) suspected pregnancy or ongoing lactation, ii) unable to give informed consent.

IBD patients were classified into conventional treatment groups without anti-TNF-α exposure and anti-TNF-α treatment group. Each group was subdivided into responders and non-responders to the given treatment. There is no concrete agreement on the definition of treatment response. Several IBD research groups suggested different guidelines and interpretation of response varies on clinical symptom, endoscopic finding, or pathological review. In this study, responders and non-responders were classified mainly based on clinical manifestations and endoscopic results following the guidance addressed by the U.S. Department of Health and Human Services, food and drug administration with few modifications.[29,30] Response for UC was defined as a decrease from baseline in the Mayo score of greater than or equal to 3 points and at least a 30 percent reduction from baseline, and a decrease in rectal bleeding subscore of greater than or equal to 1 or an absolute rectal bleeding subscore of 0 or 1. In addition,

the endoscopic subscore was 0 or 1.[31,32] Response for CD was defined as a decrease from baseline of at least 70 points on the Crohn's disease activity index (CDAI) and at least a 25% reduction in the total score, and simple endoscopic score (SES-CD) of 0 or 1.[33-35] Otherwise, patients were assigned as non-responders and response was evaluated after at least 12 weeks of given treatment.

The baseline characteristics of the patients and healthy individuals were obtained from the collected electronic medical data, including smoking and alcohol history, comorbidities, IBD-related symptoms, previous surgery, and prescription history. Laboratory findings such as white blood cell (WBC) count, red blood cell (RBC) count, hemoglobin level, platelet count, electrolyte sedimentation rate (ESR), C-reactive protein (CRP), and albumin level were also investigated.

This study was conducted according to the ethical guidelines of the Declaration of Helsinki and was approved by the Institutional Review Board of Yonsei University College of Medicine (IRB approved number: 4-2021-0171). Written informed consent was obtained from all participants.

2. Cell culture and mouse model

Human colon carcinoma cell lines HT-29 (Korea Cell Line Bank, Seoul, South Korea) were maintained at 37℃ in a humidified incubator of 5% CO_2. HT-29 cells were cultured in RPMI 1640 medium containing 10% heat-inactivated fetal bovine serum (FBS) and 1% penicillin-streptomycin solution. Cell viability was checked using trypan blue staining under the microscope.

Male C57BL/6 mice (68 weeks old) were acclimatized for 1 week before the experiment. Mice were maintained at a temperature of 22℃ on a 12-hour light/dark cycle in a pathogen-free facility. All experimental animals were reviewed and approved by the Institutional Animal Care and Use Committee of Yonsei University, and all methods were performed according to the guidelines and regulations of the IACUC.

3. Ex-vivo culture and treatment

The large intestine was obtained from the mouse model. After sufficient washing, the colon sample was punched with a 3mm diameter biopsy punch. Punched samples were placed in a well containing high glucose Dulbecco's modified Eagle's medium (DMEM) containing 15% fetal bovine serum (FBS) and 1% penicillin-streptomycin solution with gentamicin 50 μg/mL antibiotics with the epithelial surface facing up. For the human samples punching process was skipped and colonoscopic biopsy samples were immediately stored in the same media after intensive rinsing and washing. After 3 hours of ex-vivo culture in a humidified incubator with 5% CO_2, the integrity of the cells was verified through an optical microscope. The outlined procedure is depicted in Figure 2.

CKD-506 was dissolved in dimethyl sulfoxide (DMSO) and diluted in distilled water. CKD-506 1 μM, CKD-506 3 μM, tofacitinib 1 μM, and the same amount of distilled water was treated as a vehicle while incubation. To investigate the response of CKD-506 in inflammation conditions, interferon-γ (IFN-γ) 0 ng/mL, 10 ng/mL, and 50 ng/mL were co-treated in a dose-dependent manner in ex-vivo.

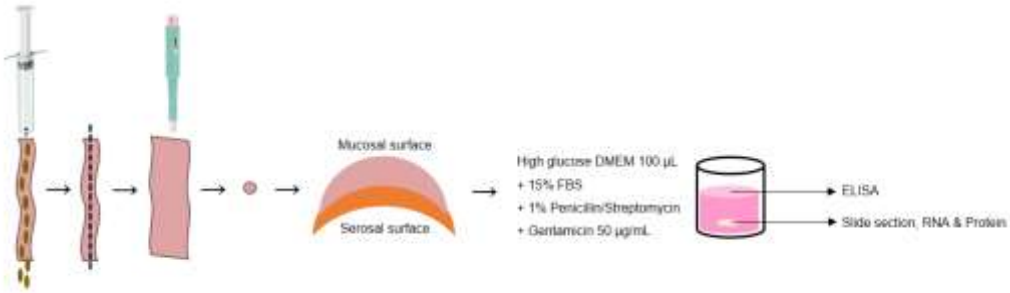

Figure 2. Establishment of colon tissue ex-vivo culture system

The large intestine obtained from the mouse model was sufficiently washed and then dissected longitudinally. A punched sample with a diameter of 3mm was cultured with high glucose DMEM containing FBS and antibiotics, serosa surface facing the bottom.

4. Histological analysis

Colon tissues were fixed in a 10% neutral formalin solution overnight, embedded in paraffin, and stained with periodic acid-Schiff reagent (PAS). Images were acquired using a light microscope. The severity of inflammation and barrier imbalance in mouse models was determined by a modified version of a previously described histomorphological scoring system consisting of inflammatory cell infiltration and overall structural integrity as major criteria (Table 1).[36] For human colon biopsy samples, a simplified Geoboes score was adopted to evaluate intestinal inflammation (Table 2).[37,38]

Table 1. Histomorphological scoring system for mouse colon tissue

Category	Criteria	Definition	Score
Inflammatory cell infiltration	Leukocyte density of lamina propria infiltrated	Mild: <25%	1
		Moderate: 25-50%	2
		Severe: >50%	3
Intestinal architecture	Erosion and ulcer	Focal erosion	1
		Focal ulceration	2
		Extended ulceration	3

Table 2. Histomorphological scoring system for human colon tissue

Grade	Criteria	Score
0	No inflammatory activity	0.0 No abnormalities 0.1 Presence of architectural changes 0.2 Presence of architectural changes and chronic mononuclear cell infiltrate
1	Basal plasma cells	1.0 No increase 1.1 Mild increase 1.2 Marked increase
2A	Eosinophils in lamina propria	2A.0 No increase 2A.1 Mild increase 2A.2 Marked increase
2B	Neutrophils in lamina propria	2B.0 No increase 2B.1 Mild increase 2B.2 Marked increase
3	Neutrophils in epithelium	3.0 None 3.1 <50% crypts involved 3.2 >50% crypts involved
4	Epithelial injury	4.0 None 4.1 Marked attenuation 4.2 Probable crypt destruction: probable erosion 4.3 Unequivocal crypt destruction: unequivocal erosion 4.4 Ulcer or granulation tissue

5. Immunohistochemistry assay

Formalin-fixed, paraffin-embedded colon sections were deparaffinized in xylene and ethanol and then rehydrated in water. After antigen retrieval, sections were washed with distilled water, quenched in 0.3% hydrogen peroxide, and blocked in 3% bovine serum albumin (BSA) diluted in Tris-buffered saline plus 0.1% Tween-20 (TBS-T). Then sections were incubated with primary and secondary antibodies. Staining was visualized using the DAB Substrate Kit (Vector Laboratories, Inc., CA, California, USA). Slides were counterstained with hematoxylin and observed under a microscope. Staining intensity was analyzed and scored by ImageJ software.

6. Quantitative real-time reverse-transcription polymerase chain reaction

Total RNA was extracted using TRIzol Reagent (Invitrogen, Carlsbad, CA, USA) or Geneall Ribospin II (Gene All Biotechnology, Seoul, South Korea). Then, RNA was reverse transcribed using a high-capacity cDNA Reverse Transcription (Applied Biosystems, Foster City, CA, USA) according to the manufacturer's protocol.

Amplification was performed using StepOne Plus real-time PCR system (Applied Biosystems, Foster City, CA, USA) for 45 cycles using the following thermocycling steps: 95℃ for 30 sec, 59-61℃ for 30 sec, and 72℃ for 40 sec. Gene expression levels were reported as the relative expression fold change compared to that of *Gapdh* after normalization.

Table 3. Mouse primers used for quantitative real-time PCR

Gene	Sequence (5' to 3')
Hdac6	F: AGCTTACTTTGCTGCGACCG, R: CGCAAACTGCGCCAGTATTT
Tuba1a	F: CTGGAACCCACGGTCATC, R: GTGGCCACGAGCATAGTTATT
Il10	F: TGAATTCCCTGGGTGAGAAG, R: TCACTCTTCACCTGCTCCACT
Muc2	F: GGTCCAGGGTCTGGATCACA, R: GCTCAGCTCACTGCCATCTG
Tnfa	F: CAAAGGGAGAGTGGTCAGGT, R: ATTGCACCTCAGGGAAGAGT
Il33	F: TCCAACTCCAAGATTTCCCCG, R: CATGCAGTAGACATGGCAGAA
Il1b	F: GCAACTGTTCCTGAACTCAACT, R: ATCTTTTGGGGTCCGTCAACT
Lrg1	F: TTGGCAGCATCAAGGAAGC, R: CAGATGGACAGTGTCGGCA
C-myc	F: CATTCAAGCAGACGAGCA, R: CGAGTTAGGTCAGTTTATGCAC
Jak2	F: CAATGATAAACAAGGGCAAATGAT, R: CTTGGCAATCTTCCGTTGCT
Stat3	F: CCCCGTACCTGAAGACCAAGT, R: CCGTTATTTCCAAACTGCATCA
Pi3kca	F: ACACCACGGTTTGGACTATGG, R: GGCTACAGTAGTGGGCTTGG
Akt1	F: AGAAGAGACGATGGACTTCCG, R: TCAAACTCGTTCATGGTCACAC
mTOR	F: CACCAGAATTGGCAGATTTGC, R: CTTGGACGCCATTTCCATGAC
Slc26a2	F: CAGCACTGTGACCTTCATGGCT, R: CTGAGACGTGAGGATGGTGAAG
Has3	F: CCTTGGCAACTCAGTGGACTAC, R: TGGACATCTCCTCCAACACCTC
Yod1	F: GTCAGCGAATCCTCGTTGGCTA, R: CGCAGGTGAAGCTTTTGGTCTG
Il1r2	F: CAGTGCAGCAAGACTCTGGTAC, R: GCAAGTAGGAGACATGAGGCAG
Mier3	F: GAAACGGACAGTGGTAACTCACC, R: AGGATGCCACAGTAACTGGTCC
Cd177	F: ATACCAGTGCTGACCCTTCTG, R: CCTCGCAGGTTTTCTCACCA

F: forward primer, R: reverse primer

Table 4. Human primers used for quantitative real-time PCR

Gene	Sequence (5' to 3')
C-MYC	F: TACCCTCTCAACGACAGCAG, R: TCTTGACATTCTCCTCGGTG
JAK2	F: AGCCTATCGGCATGGAATATCT, R: TAACACTGCCATCCCAAGACA
STAT3	F: ACCAGCAGTATAGCCGCTTC, R: GCCACAATCCGGGCAATCT
PI3KCA	F: GGTTGTCTGTCAATCGGTGACTGT, R: GAACTGCAGTGCACCTTTCAAGC
AKT1	F: TTCTGCAGCTATGCGCAATGTG, R: TGGCCAGCATACCATAGTGAGGTT
mTOR	F: GCTTGATTTGGTTCCCAGGACAGT, R: GTGCTGAGTTTGCTGTACCCATGT
SLC26A2	F: ATGTCAGTGGGACTTGTGCTGC, R: AACTCAGCCACCATGAACCAGG
HAS3	F: AGCACCTTCTCGTGCATCATGC, R: TCCTCCAGGACTCGAAGCATCT
YOD1	F: CCATTCTGGAAGACTTGCCCATC, R: ACCACGGTTCTGGTAAGCACAG
IL1R2	F: GGCTATTACCGCTGTGTCCTGA, R: GAGAAGCTGATATGGTCTTGAGG
MIER3	F: TGGGACGGTAAATGCTTCAGCC, R: GACGGTTGCTACACTGTTGGTC
CD177	F: ATGAGCGCGGTATTACTGCTG, R: GGTCGGACACCTTCCACAC

F: forward primer, R: reverse primer

7. Cytometric bead array assay

Mouse and human cytokine concentrations from tissue culture media were measured using the CBA Mouse Th1/Th2/Th17 Cytokine Kit (BD Biosciences, San Jose, CA, USA) and Human Th1/Th2/Th17 CBA Kit (BD Biosciences, San Jose, CA, USA) according to the manufacturer's protocol. Samples were analyzed by flow cytometry.

8. RNA-seq and differentially expressed gene (DEG) analysis

For RNA quantity and integrity evaluation, Agilent TapeStation 4200 (Agilent Technologies, Santa Clara, CA) was used to select samples satisfying 28S/18S ribosomal fragment ratio > 1.5 and RNA integrity number (RIN) > 5. RNA-seq was conducted by Macrogen (Seoul, Republic of Korea) and right before the RNA sequencing, RIN and adequacy of the sample were confirmed once again through Agilent Technologies 2100 Bioanalyzer (Agilent Technologies), then only samples meeting the condition were analyzed.

The cDNA was synthesized from the isolated RNA and the NGS library was prepared according to the manufacturer's protocol of the TruSeq Stranded Total RNA Library Prep Gold Kit (Illumina, San Diego, USA), and the paired-end-sequencing method HiSequation 2000 (Illumina, San Diego, USA) was used.

Data quality control was performed with FastQC (version 0.11.7) and trimming was done by Trimmomatic (version 0.38).[39] For alignment, the reference genome used was Homo sapiens GRCh38. Accurate alignment was executed using HISAT2 (version 2.1.0) and Bowtie2 (version 2.3.4.1).[40,41] Assembly and quantification was performed through StringTie2 (version 2.1.3b).[42] Differential expression analysis was done by Ballgown (Version 2.14.1).[43]

As a DEG analysis, the expression profile was extracted from the fragments per kilobase of transcript per million mapped reads (FPKM) / reads per kilobase of transcript

per million mapped reads (RPKM) values and the transcripts per kilobase million (TPM). The differentially expressed genes or transcripts were selected through statistical hypothesis among expression values of two or more groups with different conditions. To examine the effect on CKD-506 and the target genes, group analysis was performed between the group treated with CKD-506 1 μM or CKD-506 3 μM compared to the sample treated with vehicle, and the genes with significant fold change were selected. If the expression value of listed genes was 0 for more than 30% of total samples, those genes were excluded from the analysis. The overall cutoff value was based on a *p*-value of less than 0.05 and the absolute value of the log2 fold change more than 1.0. Volcano plot was depicted web-based analysis tool called VolcaNoseR.[44] Venn diagrams of DEGs by treatment response or disease type were demonstrated with Venny (version 2.0).[45] Cell population analysis from bulk RNA-seq data was done by xCell.[46]

Network-based gene ontology (GO) analysis was done by using STRING protein-protein interaction network database (version 11.0) and GO annotation database (release date 2021.12.15).[47,48] At first, query genes were extended to neighbors that had at least two connections with DEGs in the STRING database. The major components were constructed by removing singletons and very small networks from subnetworks composed of query genes. Spatial analysis of functional enrichment, SAFE1 (version 1.0.0 beta 7) supported by Cytoscape3 (version 3.8.2) was done by parameters prepared by following methods.[49,50] Inferring the enrichment score of each node, edge weight was not considered, and underweight nodes were excluded. The identical term distributed in more than 10 multi-regions were removed. Functional modules with Jaccard similarity over 0.75 were merged. The merged module was defined as a single domain, and each domain contained at least one GO term.

In the visualized network, each domain was depicted in a unique color, and node size was determined by the maximal enrichment score. The brightness and saturation of each node in a certain domain varied based on the enrichment score. The multi-functional nodes were colored with the sum of the unique colors of the domains.

Additional general GO analysis was performed based on gene ontology biological process (GOBP) or Kyoto encyclopedia genes and genomes (KEGG) database via clusterProfiler and enrich plot in R package.[51,52]

The gene set enrichment assay (GSEA) was executed by all the analyzed genes from the total patients including both conventional non-responders and anti-TNF non-responders. The investigation was carried out by implication of different gene sets including hallmark, ontology, immunologic signature, regulatory target, and cell type signature provided by the MSigDB database (version 2022.1, UC San Diego and Broad Institute).

9. Statistical analysis

GraphPad Prism 5.0 software was used for statistical analyses. The significance of the differences between the test conditions was assessed using two-way or one-way analysis of variance (ANOVA) for multiple comparisons. Statistical significance was set at $p < 0.05$.

III. RESULTS

1. HDAC6 expression and activity in inflammatory bowel disease colon tissue

A total of 10 healthy controls, 47 CD patients, and 63 UC patients participated in this study. The baseline characteristics of the control group and IBD patients are summarized in Table 5. There were significant differences among healthy control, CD, and UC patients in age (49 vs. 28.7 vs. 46.6 years; $p < 0.001$) and Gebeos score (0.0 vs. 3.9 vs. 3.5; $p < 0.001$). The disease duration of CD patients was significantly shorter than UC patients (4.9 vs. 7.4 years; $p < 0.019$), and more CD than UC patients used an immunomodulator (74.6% vs 27.7%; $p < 0.001$).

The CD and UC patients were subdivided into conventional medication or anti-TNF-α inhibitor-treated group, then responders or non-responders. For CD, 11 treatment naïve patients, 10 conventional treatment responders, 11 conventional treatment non-responders, 8 anti-TNF responders, and 7 anti-TNF non-responders were included. Baseline characteristics are summarized in Table 6. For UC, 10 treatment naïve patients, 15 conventional treatment responders, 14 conventional treatment non-responders, 11 anti-TNF responders, and 13 anti-TNF non-responders were included. Baseline characteristics are summarized in Table 7.

Multiple linear regression analysis of significant variables such as age, immunomodulator use, and Gebeos score with histological scores of Hdac6 and Tuba1a showed that there was no association except disease status (healthy control vs. CD or UC).

In comparison to the healthy control group, patients with CD exhibited elevated HDAC6 expression in both the epithelium (Figure 6A) and lamina propria (Figure 6B). Following classification based on treatment response, it appeared that every subgroup within the CD population demonstrated elevated HDAC6 expression compared to the healthy control group. Considering solely statistically significant differences, increased HDAC6 expression was observed in patients who responded to conventional treatment and in treatment-naive patients compared to the healthy control group (Figure 3B and 3C).

Compared to the healthy control, UC patients presented higher expression of Hdac6 in both epithelium (Figure 6A) and lamina propria (Figure 6B). After subclassification according to treatment response, all the UC population seemed to exhibit superior HDAC6 expression than the healthy control. Considering only statistically significant disparities, elevated Hdac6 expression was detected in individuals who did not respond to conventional treatment and those who did not respond to anti-TNF treatment (Figure 4B and 4C). Also, treatments naive patients demonstrated significantly elevated HDAC6 only in epithelium (Figure 4B).

There were no considerable correlations between HDAC6 expression level and response of conventional regimen or anti-TNF-α inhibitor. Following sub-analysis

according to disease activity showed that active status compared to remission status showed higher HDAC6 expression in both CD and UC, an especially significant increment was observed in UC patients (Figure 5A and 5B).

HDAC6 is known to deacetylate one of the well-known substrates, TUBA1A or α-tubulin. Patients diagnosed with CD and UC displayed heightened levels of acetylated α-tubulin in both the epithelium (Figure 6C) and lamina propria (Figure 6D) when contrasted with the healthy control group. Even upon stratification based on therapeutic modalities and treatment responses, CD and UC patients appeared to exhibit elevated acetylated α-tubulin expression. However, noteworthy increases were detected across the entire cellular population in treatment-naive CD patients, and solely within the epithelium of CD patients who responded to conventional treatment (Figure 3D and 3E). There were no statistically meaningful changes in UC subpopulations (Figure 4D and 4E).

Instead of comparing the expression of HDAC6 and acetylated α-tubulin on a gene-by-gene basis, a comparative analysis of HDAC6 and α-tubulin acetylation was also conducted on a patient-by-patient basis (Figure 6E). While both HDAC6 and α-tubulin acetylation demonstrated an upward trend in IBD compared to healthy controls, a closer examination of paired patient samples revealed a notable decline in the relative increase of α-tubulin acetylation compared to that of HDAC6.

Table 5. Clinical characteristics of healthy controls and IBD patients

Characteristic	Healthy control	CD	UC	*p*-value
No. of patients	10	47	63	-
Age(year)	49 ± 13	28.7 ± 10.1	46.6 ± 17.2	< 0.001
Sex				
Male	5 (50.0)	31 (66.0)	39 (61.9)	0.662
Female	5 (50.0)	16 (34.0)	24 (38.1)	
Smoking				
Never-smoker	7 (70.0)	35 (74.5)	43 (68.3)	0.437
Ex-smoker	2 (20.0)	10 (21.3)	19 (30.2)	
Current smoker	1 (10.0)	2 (4.3)	1 (1.6)	
Disease duration(year)	-	4.9 ± 5.1	7.4 ± 5.8	0.019
Steroid use	-	16 (34.0)	24 (38.1)	0.662
5-ASA use	-	34 (72.3)	52 (82.5)	0.614
Immunomodulator				
None	-	13 (27.7)	47 (74.6)	< 0.001
AZA		29 (61.7)	16 (25.4)	
MTX		2 (4.3)	0 (0.0)	
6-MP		1 (2.1)	0 (0.0)	
AZA + MTX or 6-MP		2 (4.3)	0 (0.0)	
Biologics use				
Infliximab	-	8 (17.0)	16 (25.4)	0.113
Adalimumab		7 (14.9)	4 (6.3)	
Golimumba		0 (0.0)	4 (6.3)	
Biologics duration(year)	-	2.9 ± 1.5	7.5 ± 23.4	0.454
CRP(mg/dL)	0.6 ± 0.4	13.5 ± 20.4	10.4 ± 32.5	0.620
ESR(mm/hr)	4.0 ± 4.0	32.5 ± 29.1	27.9 ± 0.5	0.152

Albumin(g/dL)	4.2 ± 2.8	4.2 ± 0.5	4.3 ± 0.5	0.853
Montreal behavior				
B1 – inflammatory	-	39 (83.0)	-	-
B2 – Stricturing		4 (8.5)		
B3 – Penetrating		4 (8.5)		
Montreal location (CD)				
L1 – ileal		9 (19.1)		
L2 – colonic	-	2 (4.3)	-	-
L3 – ileocolonic		36 (76.6)		
L4 – upper GI		0 (0.0)		
Montreal location (UC)				
E1 – proctitis	-	-	3 (4.8)	-
E2 – distal proctitis			24 (38.1)	
E3 – pancolitis			36 (57.1)	
Endoscopic finding (UC)				
0 – normal			15 (23.8)	
1 – mild disease	-	-	12 (19.0)	-
2 – moderate disease			19 (30.2)	
3 – severe disease			17 (27.0)	
Mayo score	-	-	5.5 ± 3.9	-
CDAI	-	142.3 ± 97.9	-	-
Geboes score	0.0 ± 0.0	3.9 ± 0.7	3.5 ± 1.3	< 0.001

Data are expressed as either mean (± S.D.) or n (%)

Table 6. Clinical characteristics of Crohn's disease patients and treatment response

Characteristic	Naïve	Conventional treatment responder	Conventional treatment non-responder	Anti-TNF responder	Anti-TNF non-responder
No. of patients	11	10	11	8	7
Age(year)	27.4 ± 8.6	28.6 ± 13.2	30.9 ± 13.6	28.6 ± 5.3	27.3 ± 6.7
Sex					
Male	8 (72.7)	7 (70.0)	9 (81.8)	5 (62.5)	2 (28.6)
Female	3 (27.3)	3 (30.0)	2 (18.2)	3 (37.5)	5 (71.4)
Smoking					
Never-smoker	7 (63.6)	6 (60.0)	8 (72.7)	7 (87.5)	7 (100.0)
Ex-smoker	2 (18.2)	4 (40.0)	2 (27.3)	1 (12.5)	0 (0.0)
Current smoker	2 (18.2)	0 (0.0)	0 (0.0)	0 (0.0)	0 (0.0)
Disease duration(year)	0.1 ± 0.2	5.6 ± 4.8	6.6 ± 5.3	4.5 ± 2.4	9.3 ± 6.1
Steroid use	0 (0.0)	1 (10.0)	2 (18.2)	6 (75.0)	7 (100.0)
5-ASA use	2 (18.2)	10 (100.0)	10 (90.9)	7 (87.5)	7 (100.0)
Immunomodulator					
None	11 (100.0)	1 (10.0)	1 (9.1)	0 (0.0)	0 (0.0)
AZA	0 (0.0)	9 (10.0)	9 (81.8)	8 (100.0)	4 (57.1)
MTX	0 (0.0)	0 (0.0)	0 (0.0)	0 (0.0)	1 (14.3)
6-MP	0 (0.0)	0 (0.0)	0 (0.0)	0 (0.0)	0 (0.0)
AZA + MTX or 6-MP	0 (0.0)	0 (0.0)	0 (0.0)	0 (0.0)	2 (28.6)
Biologics use					
Infliximab	-	-	-	7 (87.5)	1 (14.3)
Adalimumab				1 (12.5)	6 (85.7)
Golimumab				0 (0.0)	0 (0.0)
Biologics duration(year)	-	-	-	2.9 ± 1.4	2.9 ± 1.7
CRP(mg/dL)	28.5 ± 31.8	1.9 ± 2.6	16.8 ± 11.7	2.8 ± 2.5	13.4 ± 21.3
ESR(mm/hr)	52.5 ± 29.1	16.1 ± 20.0	36.1 ± 34.8	21.2 ± 15.1	31.7 ± 28.7

Albumin(g/dL)	3.8 ± 0.6	4.5 ± 0.3	4.3 ± 0.3	4.3 ± 0.2	4.1 ± 0.7
Montreal behavior					
B1 – inflammatory	8 (72.7)	10 (100.0)	8 (72.7)	8 (100.0)	5 (71.4)
B2 – Stricturing	2 (18.2)	0 (0.0)	2 (18.2)	0 (0.0)	0 (0.0)
B3 – Penetrating	1 (9.1)	0 (0.0)	1 (9.1)	0 (0.0)	2 (28.6)
Montreal location					
L1 – ileal	4 (36.4)	2 (20.0)	2 (18.2)	0 (0.0)	1 (14.3)
L2 – colonic	0 (0.0)	0 (0.0)	0 (0.0)	2 (25.0)	0 (0.0)
L3 – ileocolonic	7 (63.6)	8 (80.0)	9 (81.8)	6 (75.0)	6 (85.7)
L4 – upper GI	0 (0.0)	0 (0.0)	0 (0.0)	0 (0.0)	0 (0.0)
CDAI	181.2 ± 106.0	57.3 ± 31.1	193.6 ± 93.6	82.1 ± 32.1	190.9 ± 101.2
Geboes score	4.0 ± 0.0	3.6 ± 1.3	3.7 ± 0.9	4.0 ± 0.0	4.0 ± 0.0

Data are expressed as either mean (± S.D.) or n (%)

Table 7. Clinical characteristics of ulcerative colitis patients and treatment response

Characteristic	Naïve	Conventional treatment responder	Conventional treatment non-responder	Anti-TNF responder	Anti-TNF non-responder
No. of patients	10	15	14	11	13
Age(year)	37.6 ± 14.0	54.0 ± 15.2	44.6 ± 15.8	50.3 ± 19.2	43.8 ± 19.2
Sex					
Male	6 (60.0)	10 (66.7)	8 (57.1)	8 (72.7)	8 (53.8)
Female	4 (40.0)	5 (33.3)	6 (42.9)	3 (27.3)	6 (46.2)
Smoking					
Never-smoker	7 (70.0)	9 (60.0)	11 (78.6)	7 (63.6)	9 (69.2)
Ex-smoker	2 (20.0)	6 (40.0)	3 (21.4)	4 (36.4)	4 (30.8)
Current smoker	1 (10.0)	0 (0.0)	0 (0.0)	0 (0.0)	0 (0.0)
Disease duration(year)	0.0 ± 0.1	9.1 ± 5.4	7.7 ± 5.7	10.2 ± 4.0	8.5 ± 6.0
Steroid use	1 (10.0)	5 (33.3)	5 (35.7)	5 (45.5)	8 (61.5)
5-ASA use	0 (0.0)	15 (100.0)	14 (100.0)	10 (90.9)	13 (100.0)
Immunomodulator					
None	10 (100.0)	12 (80.0)	11 (78.6)	8 (72.7)	6 (46.2)
AZA	0 (0.0)	3 (20.0)	3 (21.4)	3 (27.3)	7 (53.8)
MTX	0 (0.0)	0 (0.0)	0 (0.0)	0 (0.0)	0 (0.0)
6-MP	0 (0.0)	0 (0.0)	0 (0.0)	0 (0.0)	0 (0.0)
AZA + MTX or 6-MP	0 (0.0)	0 (0.0)	0 (0.0)	0 (0.0)	0 (0.0)
Biologics use					
Infliximab	-	-	-	7 (63.6)	9 (69.2)
Adalimumab				3 (27.3)	1 (7.7)
Golimumab				1 (9.1)	3 (23.1)
Biologics duration(year)	-	-	-	3.3 ± 2.1	2.4 ± 1.2
CRP(mg/dL)	23.8 ± 70.0	6.0 ± 19.3	10.1 ± 22.8	2.3 ± 2.9	12.6 ± 22.2
ESR(mm/hr)	29.6 ± 25.9	26.0 ± 26.0	24.3 ± 20.0	24.6 ± 28.7	41.8 ± 33.4

Albumin(g/dL)	4.1 ± 0.8	4.5 ± 0.2	4.2 ± 0.5	4.4 ± 0.3	4.0 ± 0.3
Montreal behavior					
B1 – inflammatory	1 (10.0)	1 (6.7)	0 (0.0)	0 (0.0)	1 (7.7)
B2 – Stricturing	3 (30.0)	6 (40.0)	6 (42.9)	5 (45.5)	4 (30.8)
B3 – Penetrating	6 (60.0)	8 (53.3)	8 (57.1)	6 (54.5)	8 (61.5)
Montreal location					
L1 – ileal	0 (0.0)	9 (60.0)	0 (0.0)	6 (54.5)	0 (0.0)
L2 – colonic	1 (10.0)	6 (40.0)	0 (0.0)	5 (45.5)	0 (0.0)
L3 – ileocolonic	7 (70.0)	0 (0.0)	7 (50.0)	0 (0.0)	5 (38.5)
L4 – upper GI	2 (20.0)	0 (0.0)	7 (50.0)	0 (0.0)	8 (61.5)
CDAI	8.2 ± 2.7	1.3 ± 0.7	8.6 ± 1.2	1.2 ± 0.8	8.6 ± 1.5
Geboes score	3.2 ± 1.7	3.3 ± 1.5	3.7 ± 1.1	3.4 ± 1.4	4.0 ± 0.0

Data are expressed as either mean (± S.D.) or n (%)

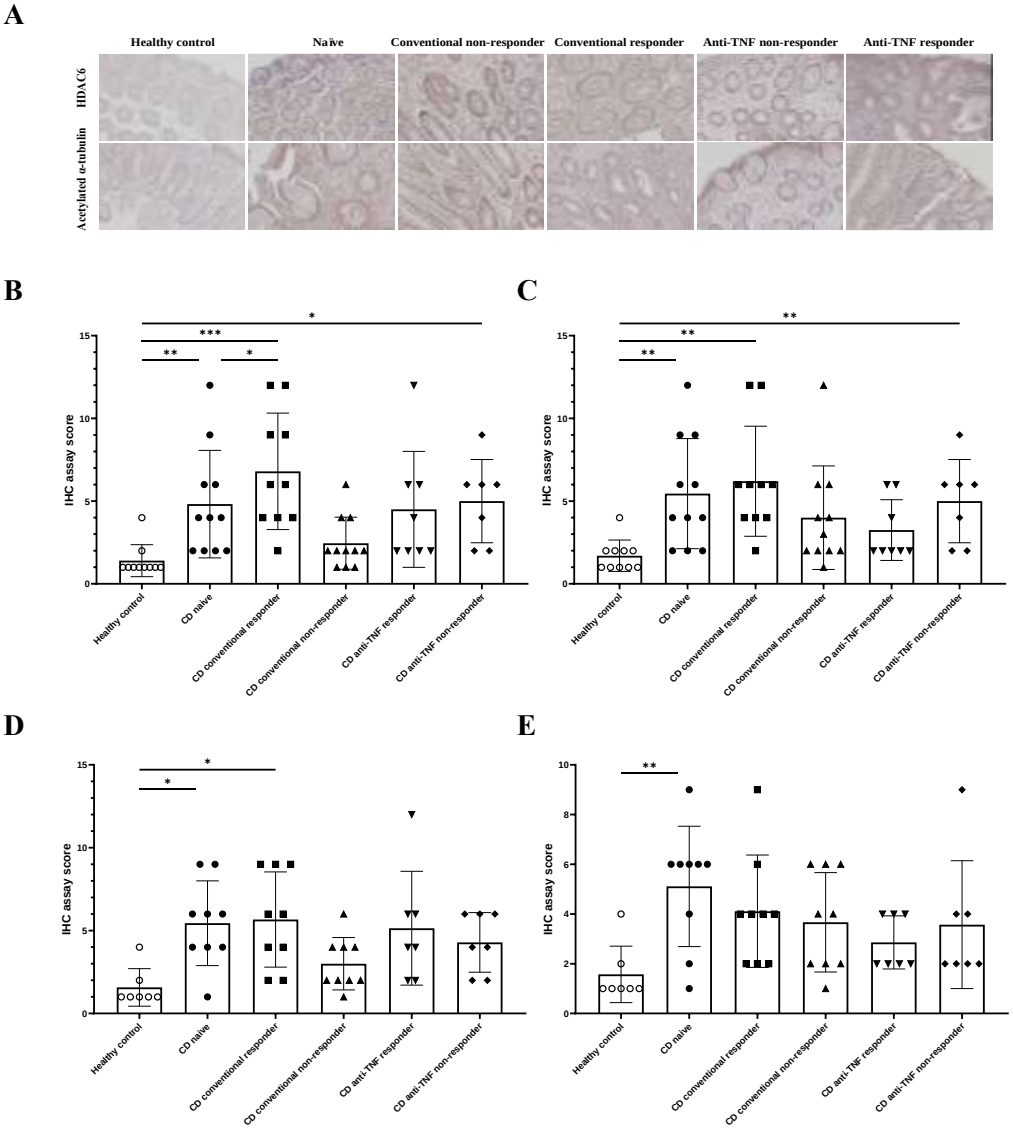

Figure 3. HDAC6 and acetylated α-tubulin expression in CD patients

Microscopic evaluation of IHC staining of HDAC6 and acetylated α-tubulin expression in colon biopsy samples of Crohn's disease (CD) patients (A). HDAC6 expression in epithelium (B) and lamina propria (C), and acetylated α-tubulin expression in epithelium (D) and lamina propria (E) were analyzed separately. Magnification ×200. Significance is indicted by * $p < 0.05$, ** $p < 0.005$, *** $p < 0.0005$.

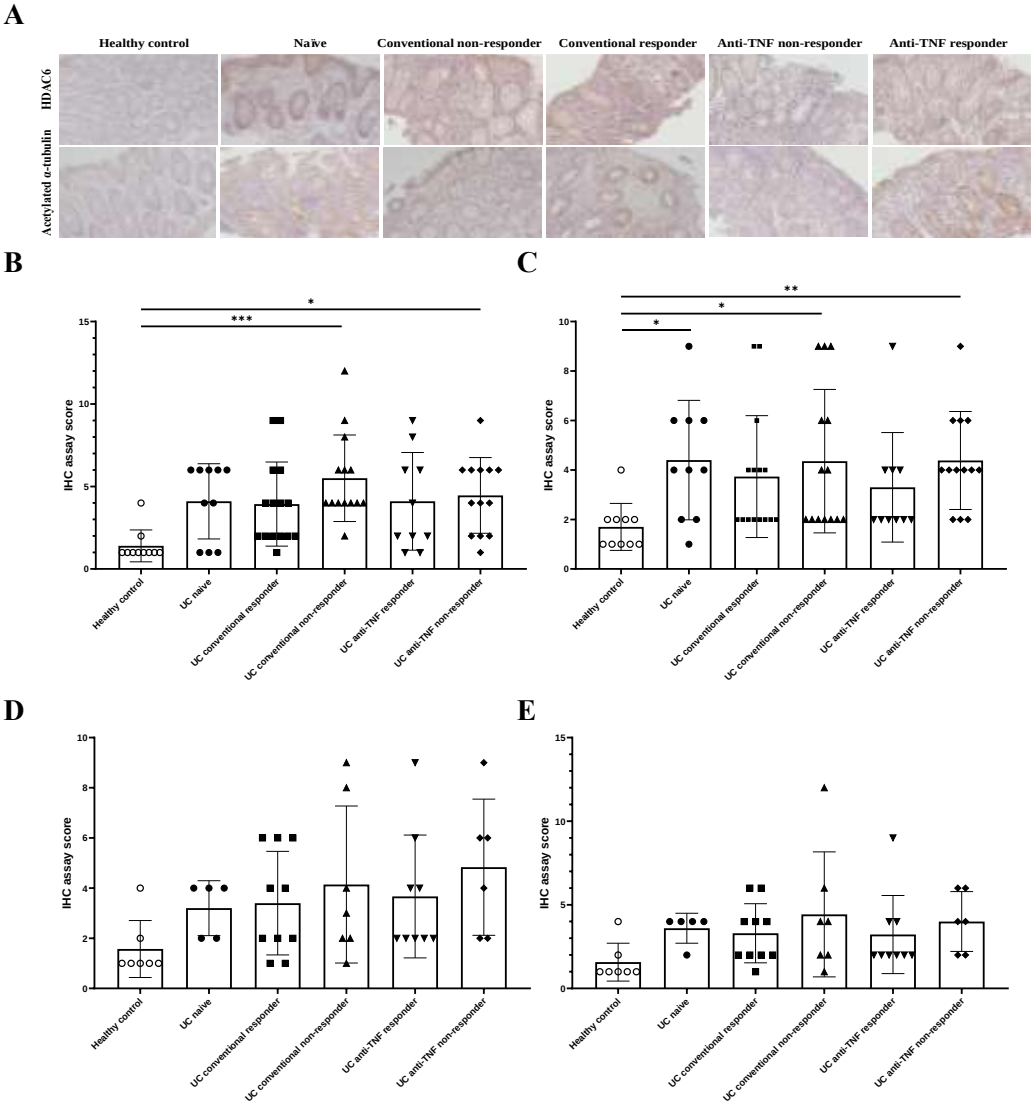

Figure 4. HDAC6 and acetylated α-tubulin expression in UC patients

Microscopic evaluation of IHC staining of HDAC6 and acetylated α-tubulin expression in colon biopsy samples of ulcerative colitis (UC) patients (A). HDAC6 expression in epithelium (B) and lamina propria (C), and acetylated α-tubulin expression in epithelium (D) and lamina propria (E) were analyzed separately. Magnification ×200. Significance is indicted by * $p < 0.05$, ** $p < 0.005$, *** $p < 0.0005$.

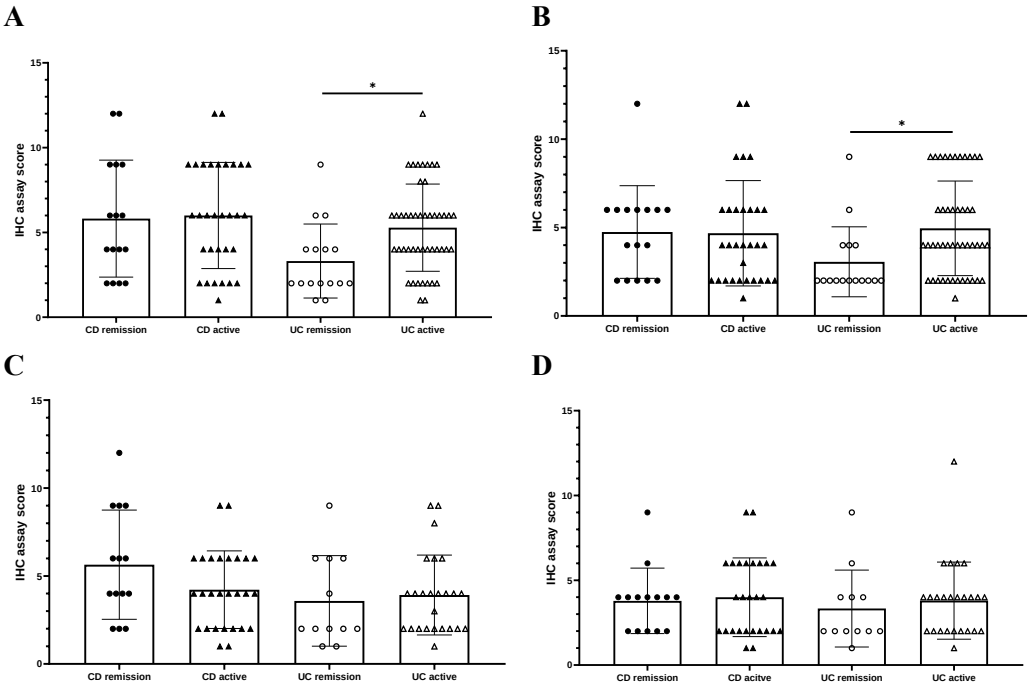

Figure 5. HDAC6 and acetylated α-tubulin expression in remission or active IBD patients

Instead of treatment response, integrated Crohn's disease (CD) and ulcerative colitis (UC) patients were divided into remission and activation status. HDAC6 expression in epithelium (A) and lamina propria (B), and acetylated α-tubulin expression in epithelium (C) and lamina propria (D) were analyzed separately. Significance is indicated by * $p < 0.05$.

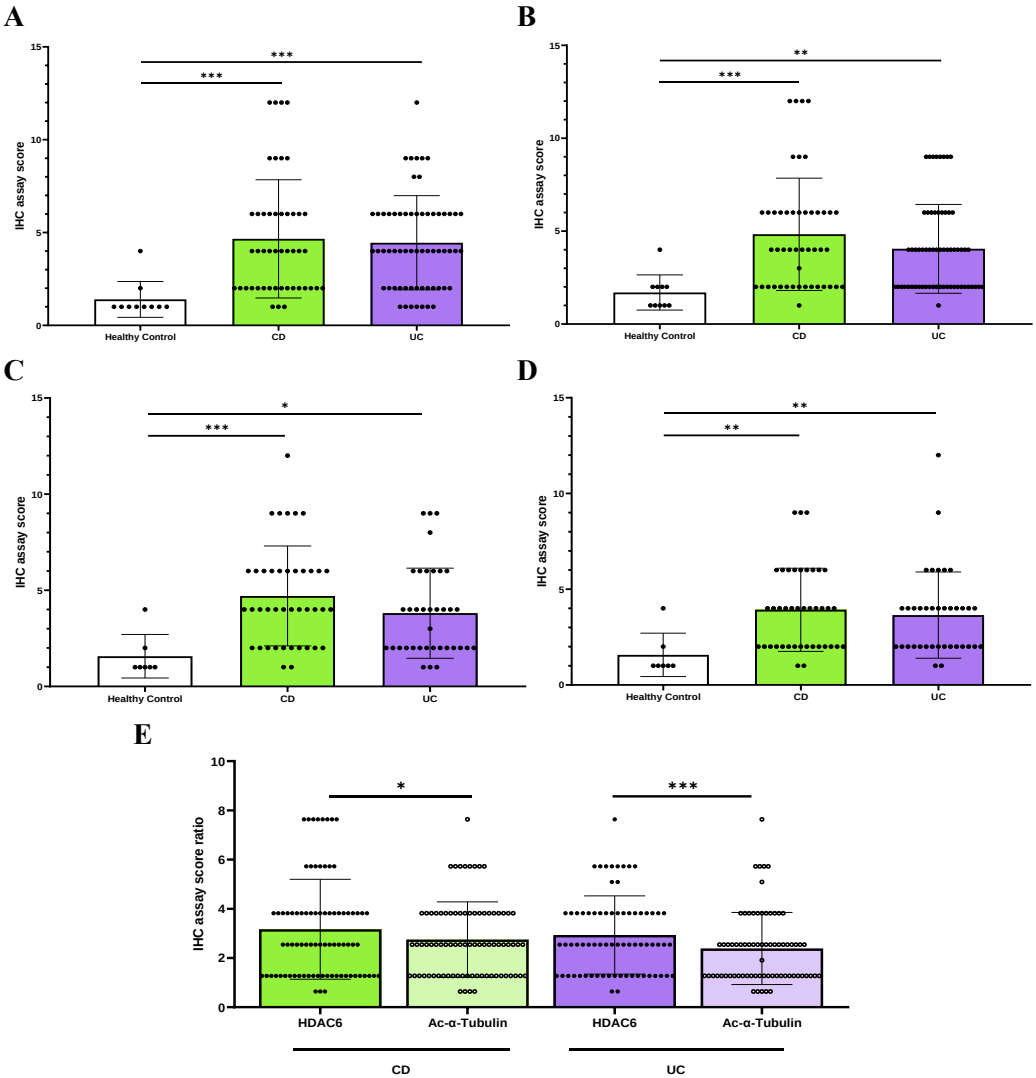

Figure 6. HDAC6 and acetylated α-tubulin expression in IBD patients

Instead of treatment response subtypes, integrated Crohn's disease (CD) and ulcerative colitis (UC) patients were analyzed. HDAC6 expression in epithelium (A) and lamina propria (B), and acetylated α-tubulin expression in epithelium (C) and lamina propria (D) were analyzed separately. Proportional IHC score in paired samples presented a decreased level of acetylated α-tubulin compared to HDAC6 (E). Significance is indicted by * p <0.05, ** p <0.005, *** p <0.0005.

2. Establishment of an ex-vivo culture system

When utilizing ex-vivo cultures of mouse colon tissue, it was determined that maintaining cell integrity challenging after a cultivation time exceeding 3 hours by optical microscopy. Particularly, when the ex-vivo cultures were extended beyond 24 hours, discerning cell morphology became arduous (Figure 7A).

As the concentration of IFN-γ increased, the preservation of cellular morphology was compromised. Visual observation revealed that the cellular morphology tended to remain relatively stable in groups treated with CKD-506 3 μM or tofacitinib 1 μM in contrast to the group treated with CKD-506 1 μM (Figure 7B). Through histomorphological scoring, a significant reduction in inflammation score was evident in colonic tissues induced with inflammation by treatment with IFN-γ at 10 ng/mL and 50 ng/mL, when co-treated with CKD-506 1 μM and 3 μM compared to the vehicle group (Figure 7C).

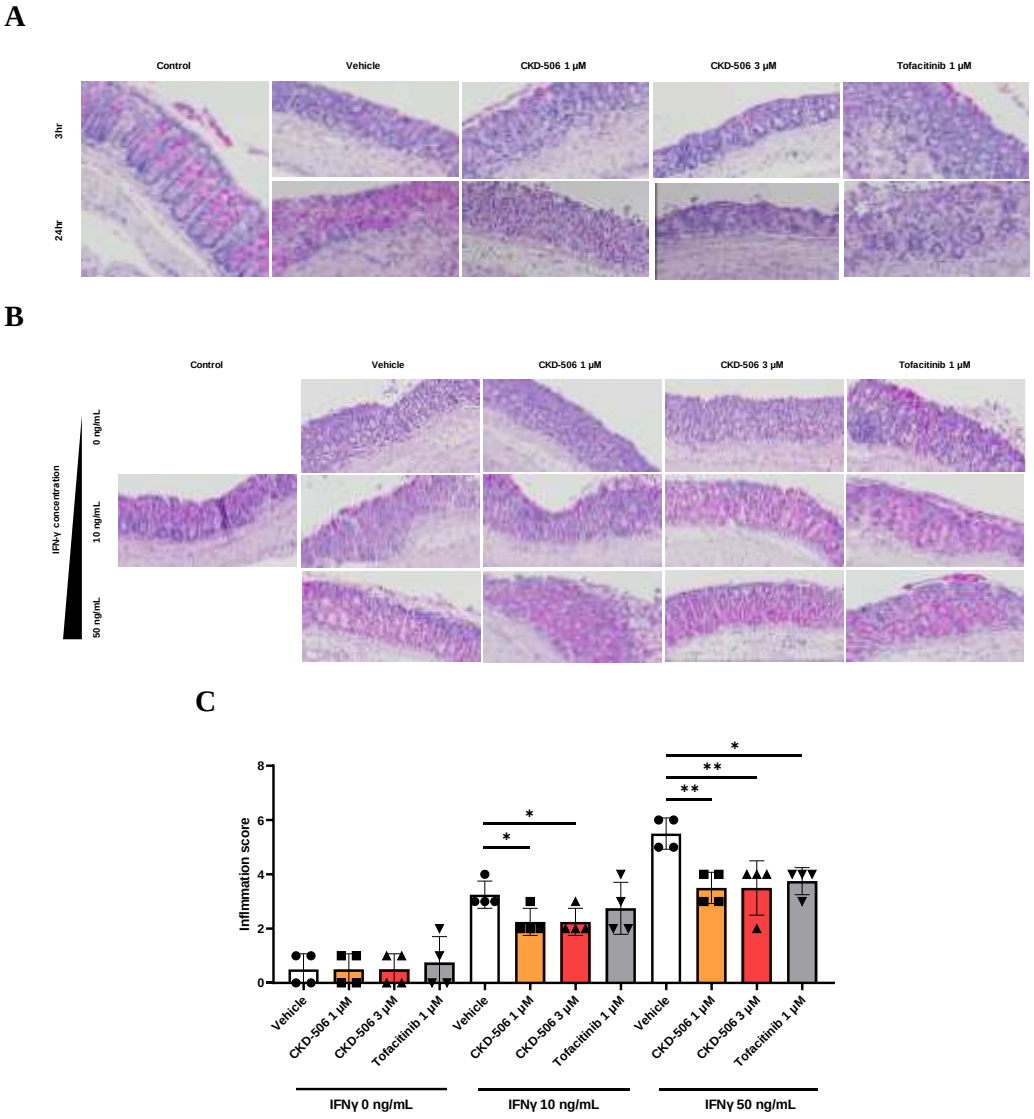

Figure 7. Phenotype and inflammation score of colon ex-vivo culture of murine colitis models after CKD-506 treatment

The phenotypic architecture was preserved in the ex-vivo culture of murine colitis after 3 hours instead of 24 hours (A). Phenotypic degradation (B) and inflammation score (C) were reduced in the IFN-γ colitis model in the CKD-506 treatment group compared to the vehicle. Magnification ×200. Significance is indicated by * $p < 0.05$, ** $p < 0.005$.

3. Effects of CKD-506 on inflammatory cytokines and epithelial barrier function in murine colitis tissue

Several inflammation and epithelial barrier markers were observed by qRT-PCR after ex-vivo culture of IFN-γ-induced mice colitis colon biopsy samples. There was no significant difference in the transcription level of interleukin-10 (IL-10) depending on the concentration of IFN-γ. When treated with CKD-506, *Il10* significantly increased and reached higher levels than tofacitinib. As the concentration of IFN-γ increased, the enhancing effect of CKD-506 became more pronounced (Figure 8A). While there was an observable trend of mucin 2 (MUC2) decline with increasing IFN-γ levels, it did not reach statistical significance. There was a notable increase in transcription compared to tofacitinib in CKD-506 treated samples. Although this trend was evident across all IFN-γ concentrations, the statistically considerable results were only found in the IFN-γ 10 ng/mL treated group (Figure 8B). In this qRT-PCR results, tumor necrosis factor-alpha (TNF-α) levels increased in a dose-dependent manner with IFN-γ. CKD-506 significantly reduced TNF-α to a similar extent as tofacitinib, and this effect was more pronounced as inflammation became more severe (Figure 8C). The interleukin-33 (IL-33) level increased simultaneously with the IFN-γ concentration. CKD-506 markedly decreased *Il33* to a comparable extent as tofacitinib (Figure 8D). As the concentration of IFN-γ increased, the transcription level of Interleukin-1 beta (IL-1β) also exhibited an elevation. Both CKD-506 and tofacitinib demonstrated a statistically significant and remarkable reduction in *Il1β* (Figure 8E). The correlation between leucine-rich α-2 glycoprotein 1 (LRG1) and IFN-γ was not established. In addition, a high dose of CKD-506 significantly reduced the transcription level of *Lrg1* compared to the vehicle (Figure 8F).

Through the CBA analysis kit, altered expression levels of several inflammatory cytokines were observed using IFN-γ treated mice colitis colon samples. Interleukin-2 (IL-2) expression level decreased as IFN-γ concentration increased. In CKD-506 treated

groups, a statistically significant reduction in Il-2 was observed, with a similar trend seen in the tofacitinib-treated group (Figure 9A). Interleukin-4 (IL-4) expression decreased as IFN-γ intensity increased. The CKD-506 treatment induced statistically considerable diminishment of Il-4 level, and tofacitinib also provoked a comparable level of decrement (Figure 9B). Interleukin-6 (IL-6) expression demonstrated statistically significant elevation as IFN-γ concentration raised. Escalated CKD-506 concentrations led to a meaningful decline in Il-6, and a similar trend was observed in the tofacitinib-treated group (Figure 9C). Il-10 showed broad sample-to-sample variation, with no statistically significant changes. Expression levels of Il-10 decreased as IFN-γ concentration increased. Notably, some samples treated with CKD-506 or tofacitinib exhibited substantial increases in Il-10 (Figure 9D). As expected, the detected IFN-γ expression level increased with higher IFN-γ treatment concentrations. When incubated with CKD-506 or tofacitinib along with IFN-γ at 10 ng/mL, a statistically significant suppression of IFN-γ was observed compared to the vehicle. At IFN-γ 50 ng/mL treatment set, considerable escalation of expressed IFN-γ was seen in the CKD-506 3 μM and tofacitinib-treated groups than CKD-506 1 μM incubated group. However, there was no definite correlation with the vehicle (Figure 9E). Interleukin-17 (IL-17) expression increased concurrently with amplified IFN-γ concentration. Both CKD-506 and tofacitinib treatment resulted in significant reductions in Il-17 compared to the vehicle group (Figure 9F).

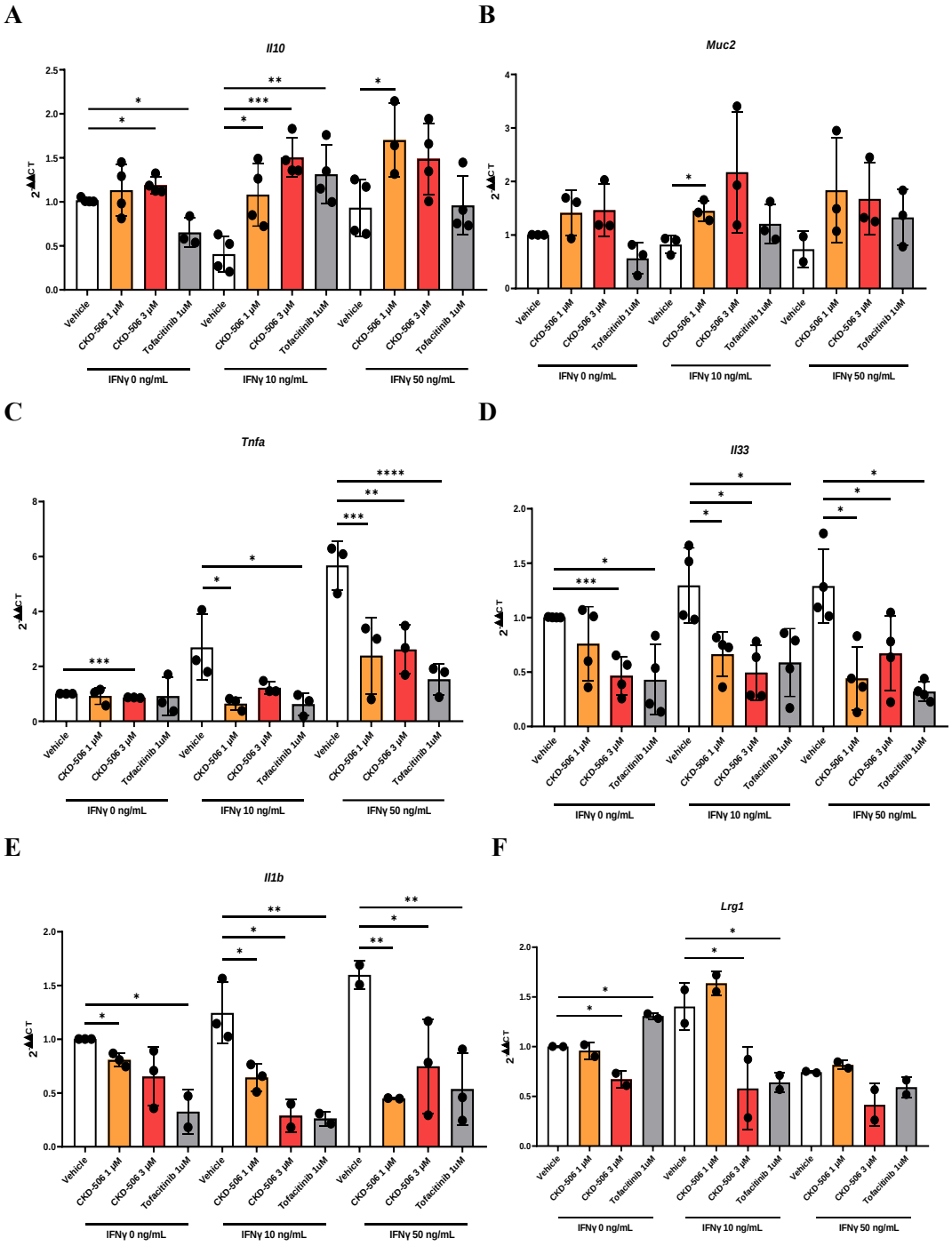

Figure 8. Inflammatory and epithelial barrier marker transcription in murine colitis models after CKD-506 treatment

Several inflammatory cytokines and epithelial barrier markers were investigated by qRT-PCR in murine colitis models after CKD-506 treatment. Increased anti-inflammatory and decreased pro-inflammatory cytokines, and improved epithelial barrier function were observed. Significance is indicted by * $p < 0.05$, ** $p < 0.005$, *** $p < 0.0005$, **** $p < 0.0001$.

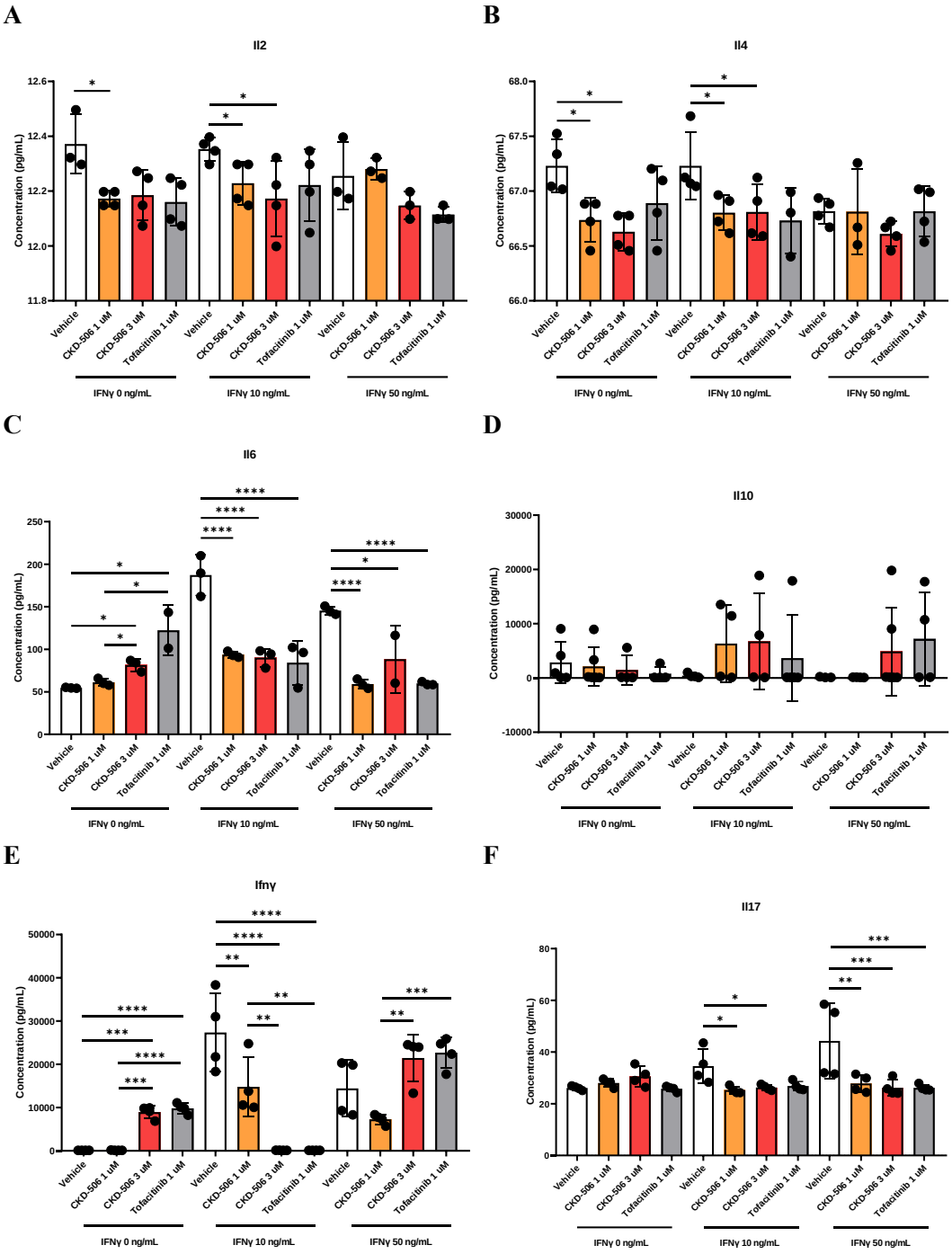

Figure 9. Inflammatory cytokine expression in murine colitis models after CKD-506 treatment

Several inflammatory cytokines were examined by CBA in murine colitis models after CKD-506 treatment. Increased anti-inflammatory and decreased pro-inflammatory cytokines were observed. Significance is indicted by * $p < 0.05$, ** $p < 0.005$, *** $p < 0.0005$.

4. RNA sequencing of CKD-506-treated human colon tissue

A total of 24 patients were enrolled for RNA sequencing. Excluding cases that did not meet the criteria for RNA integrity number (RIN) and ribosomal RNA (rRNA) ratio, or those without clear peaks, a total of 20 samples were included.

The baseline characteristics of CD and UC patients who underwent RNA sequencing are summarized in Table 8. The median age was 40 years and the median disease duration was 6.3 years. The proportion of males to females was 85.0% to 15.0%, and all the subjects were never or ex-smokers. Since all the patients were conventional treatment or anti-TNF inhibitor non-responders, over 75% of patients were exposed to steroids, 5-ASA, and immunomodulators. Especially for anti-TNF non-responders, only infliximab and adalimumab users were recruited with median biologics duration of 4.46 years. Most CD patients were inflammatory, ileocolonic type according to Montreal classification of behavior and location. 60% of UC patients were pancolitis with moderate to severe disease.

Table 8. Clinical characteristics of IBD patients who underwent RNA-seq

Characteristic	CD		UC		Total
	Conventional treatment non-responder	Anti-TNF non-responder	Conventional treatment non-responder	Anti-TNF non-responder	
No. of patients	5	5	5	5	20
Age(year)	45 ± 19	36 ± 16	32 ± 13	46 ± 15	40 ± 16
Sex					
Male	5 (100.0)	5 (100.0)	4 (80.0)	3 (60.0)	17 (85.0)
Female	0 (0.0)	0 (0.0)	1 (20.0)	2 (40.0)	3 (15.0)
Smoking					
Never-smoker	2 (40.0)	1 (20.0)	3 (60.0)	3 (60.0)	9 (45.0)
Ex-smoker	3 (60.0)	4 (80.0)	2 (40.0)	2 (40.0)	11 (55.0)
Current smoker	0 (0.0)	0 (0.0)	0 (0.0)	0 (0.0)	0 (0.0)
Disease duration(year)	3.5 ± 4.3	8.0 ± 4.1	4.0 ± 1.9	9.7 ± 5.0	6.3 ± 4.5
Steroid use	4 (80.0)	5 (100.0)	2 (40.0)	5 (100.0)	15 (75.0)
5-ASA use	5 (100.0)	5 (100.0)	5 (100.0)	5 (100.0)	20 (100.0)
Immunomodulator					
None	0 (0.0)	0 (0.0)	5 (100.0)	0 (0.0)	5 (25.0)
AZA	2 (40.0)	1 (20.0)	0 (0.0)	5 (100.0)	8 (40.0)
MTX	2 (40.0)	1 (20.0)	0 (0.0)	0 (0.0)	3 (15.0)
6-MP	0 (0.0)	0 (0.0)	0 (0.0)	0 (0.0)	0 (0.0)
AZA+MTX or 6-MP	1 (20.0)	3 (60.0)	0 (0.0)	0 (0.0)	4 (20.0)
Biologics use					
Infliximab	-	2 (40.0)	-	5 (100.0)	7 (35.0)
Adalimumab		3 (60.0)		0 (0.0)	3 (15.0)
Golimumba		0 (0.0)		0 (0.0)	0 (0.0)
Biologics duration(year)	-	4.6 ± 2.7	-	4.7 ± 2.9	4.64.7 ± 2.7
CRP(mg/dL)	9.6 ± 7.9	5.3 ± 8.4	5.6 ± 5.5	4.2 ± 3.4	6.2 ± 6.4
ESR(mm/hr)	21.8 ± 16.6	11.2 ± 9.8	9.8 ± 7.2	28.0 ± 17.0	17.7 ± 14.5
Albumin(g/dL)	4.5 ± 0.3	4.3 ± 0.2	4.7 ± 2.8	4.4 ± 0.5	4.5 ± 0.3
Montreal behavior			-	-	

B1 – inflammatory	5 (100.0)	3 (60.0)			8 (80.0)
B2 – Stricturing	0 (0.0)	1 (20.0)			1 (10.0)
B3 – Penetrating	0 (0.0)	1 (20.0)			1 (10.0)
Montreal location (CD)					
L1 – ileal	1 (20.0)	1 (20.0)			2 (20.0)
L2 – colonic	1 (20.0)	0 (0.0)	-	-	1 (10.0)
L3 – ileocolonic	3 (60.0)	4 (80.0)			7 (70.0)
L4 – upper GI	0 (0.0)	0 (0.0)			0 (0.0)
Montreal location (UC)					
E1 – proctitis	-	-	2 (40.0)	0 (0.0)	2 (20.0)
E2 – distal proctitis			0 (0.0)	2 (40.0)	2 (20.0)
E3 – pancolitis			3 (60.0)	3 (60.0)	6 (60.0)
Endoscopic finding (UC)					
0 – normal			0 (0.0)	0 (0.0)	0 (0.0)
1 – mild disease	-	-	1 (20.0)	1 (20.0)	2 (20.0)
2 – moderate disease			2 (40.0)	3 (60.0)	5 (50.0)
3 – severe disease			2 (40.0)	1 (20.0)	3 (30.0)
Mayo score	-	-	7.4 ± 1.5	7.2 ± 1.3	7.3 ± 1.3
CDAI	161.4 ± 16.2	223.4 ± 108.1	-	-	192.4 ± 80.0

Data are expressed as either mean (± S.D.) or n (%)

5. Volcano plot of differentially expressed genes

The DEGs of each group were successfully extracted. Open reading frame (ORF) or uncharacterized LOC genes were excluded. In CD patients, 384 and 1299 DEGs were selected for conventional non-responders and anti-TNF non-responders (Table 9). The DEGs of conventional non-responders and anti-TNF non-responders were 673 and 903 in UC (Table 10).

Volcano plots were illustrated for every single group (Figure 10-11). The top 10 highest fold change DEGs were listed. Excluding pseudogenes and introns, *SMCP, AFM, PLSCR3, CFC1B, ASB11, FAM162B, SNX15, AJM1, RABA3A, GUCA2B, TMEM121, TRIM64C, HAS3, LRRC8A, LAMB3* and *PDXP-DT* were recognized in CD patients. In UC, *MAS1, TRAV41, MSMB, WFDC5, TSSK6, FAM238A, PHOSPHO1, IL36G, NANOS3, OR5D13, OR8J3, FILNC1, GUCA1C, SSC4D and PGBD3* were noticed.

Compared to conventional non-responders, anti-TNF non-responders represented a larger number of DEGs. Furthermore, anti-TNF non-responders presented a higher magnitude of log2 fold change and a more reliable *p*-value than conventional non-responders.

Table 9. Number of DEGs in CKD-506 treated CD and UCpatients

Disease	**CD**			
Subtype	Conventional non-responder		Anti-TNF non-responder	
Compared group (Vehicle vs.)	CKD-506 1 μM	CKD-506 3 μM	CKD-506 1 μM	CKD-506 3 μM
Down-regulation	78	308	130	17
Up-regulation	122	76	148	1004
Total	200	384	278	1021

Table 10. Number of DEGs in CKD-506 treated UC patients

Disease	**UC**			
Subtype	Conventional non-responder		Anti-TNF non-responder	
Compared group (Vehicle vs.)	CKD-506 1 μM	CKD-506 3 μM	CKD-506 1 μM	CKD-506 3 μM
Down-regulation	410	91	340	269
Up-regulation	69	103	76	218
Total	479	194	416	487

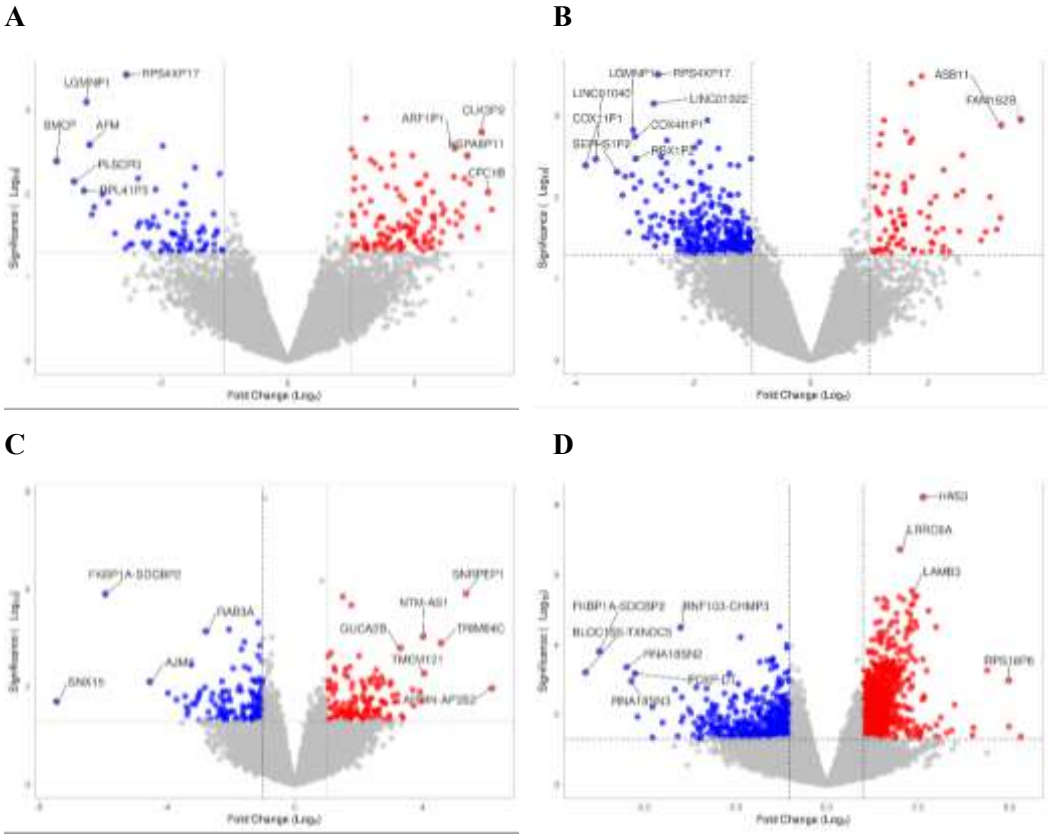

Figure 10. Volcano plot of DEGs in CD

Volcano plots of DEGs were depicted for each group in Crohn's disease (CD) patients. Conventional non-responders were depicted above, CKD-506 1 μM (A), and CKD-506 3 μM (B). Anti-TNF non-responders were demonstrated below, CKD-506 1 μM (C), and CKD-506 3 μM (D).

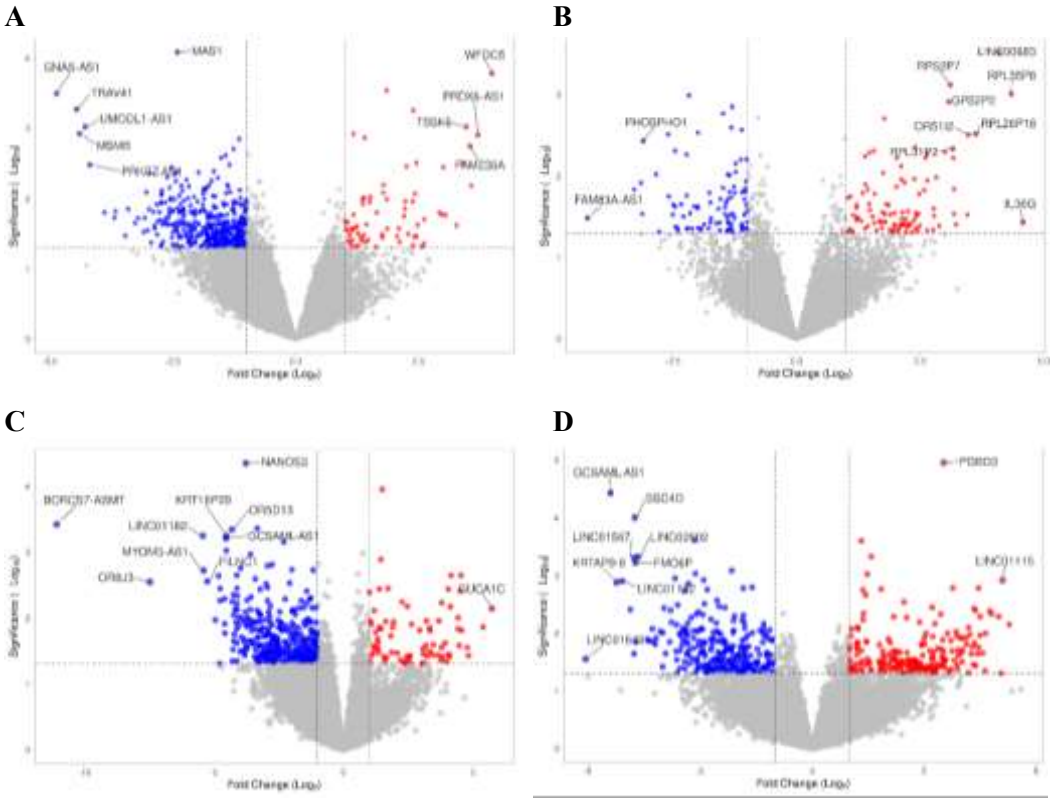

Figure 11. Volcano plot of DEGs in UC

Volcano plots of DEGs were depicted for each group in Crohn's disease (CD) patients. Conventional non-responders were depicted above, CKD-506 1 μM (A), and CKD-506 3 μM (B). Anti-TNF non-responders were demonstrated below, CKD-506 1 μM (C), and CKD-506 3 μM (D).

6. Venn diagram analysis

Venn diagram was illustrated based on either treatment or disease type to elucidate common DEGs shared by different groups. Among anti-TNF non-responders, CKD-506 1 μM and 3 μM treated groups represented 93 common genes in UC and 8 genes in CD (Fig 11A). For conventional non-responders, CKD-506 1 μM and 3 μM displayed 22 common DEGs in UC patients and 40 in CD patients (Fig 11B). At the same concentration of CKD-506 as 1 μM, CD and UC presented 7 mutual DEGs in conventional non-responders and 10 in anti-TNF non-responders. For the CKD-506 3 μM treated samples, overlapping DEGs of CD and UC were 12 in both conventional and anti-TNF non-responders. Considering CKD-506 1 μM treated samples, conventional non-responders, and anti-TNF non responders exhibited mutual DEGs of 7 in both UC and CD (Figure 12C, D). When selecting CKD-506 3 μM treated patients, refractory to conventional and anti-TNF shared 13 DEGs in UC and 5 in CD.

Instead of analyzing the entire set of DEGs, I opted to differentiate between positively regulated and negatively regulated genes. Specifically, I focused on genes that exhibited common changes across at least two groups. The introns and pseudogenes were shaded gray or excluded when listed DEGs over 20.

Comparative analysis of anti-TNF non-responders revealed that among the three groups, *HMGCS2, IL1R2, YOD12, MIER3*, and *HAS3* were consistently upregulated. In the case of two groups, *SLC26A2, SCNN1B, CLCA4, SLC25A51P3, PGBD3, FOXD4L1, UMOD, CLDN18, GUCA2B, CD177, GPAT3, FAM110C, CCNG2, PLCXD1, WEE1, PLAUR, SIRT1, TNS4, B3GNT5*, and *MXD1* were highly transcribed (Figure 13A). Conversely, there were no decreased genes shared by more than three domains. All the overlapping suppressed DEGs were only found in UC patients who were anti-TNF non-responders, treated with CKD-506 at concentrations of 1 μM or 3 μM (Figure 13B).

For conventional non-responders only, there were no up or down-regulated DEGs

shared by more than three different groups. Intersection between two groups, *MARCHF11*, *IGLV4-60*, *ASB11*, *SLC26A2*, *HOXC6*, *IFNA8*, *TMPRSS9*, *TPH1*, *ALDH1A2*, *GLDN*, *TCTEX1D2*, and *HOXD13* were increased (Figure 14A). *KIR2DL4*, *CD164L2*, *KCNH3*, *DRGX*, *ARL4D*, *SP5*, *CBX2*, *HCAR3*, *HCAR2*, *YPEL4*, *PROK2*, *SMCP*, *UCN2*, *TAAR2*, *CSN3*, *INSM2*, *PPEF1*, *GABRA5*, *LRRC3C*, *NPTX2*, *OR52K1*, *PRRT1*, *CHRM1*, *PRND*, and *PHEX* were decreased (Figure 14B).

The Venn diagram analysis of CD patients figured out that there were no common genes in more than three domains. When focusing on just two groups, *TPH1*, *TCTEX1D2*, *HOXD13*, *ALDH1A2*, *GLDN*, *TICAM2*, *CD177*, *YOD1*, *HAS3*, *MIER3*, *IL1R2*, *GPAT3*, *FAM110C*, *HMGCS2*, and *ADAMTS9* were up regulated (Figure 15A). The down-regulated genes were *COL1A1*, *FAM209A*, *HCAR2*, *RNR1*, *RNR2*, *SMCP*, *UCN2*, *TAAR2*, *CSN3*, *INSM2*, *PPEF1*, *GABRA5*, *LRRC3C*, and *NPTX2* (Figure 15B).

In the case of UC patients, there was one gene, *SCL26A2* commonly up-regulated in all the domains. No overlapping DEGs were found among the three different categories. Between any other two groups, *HOXC6*, *IFNA8*, *TMPRSS9*, *SCNN1B*, *CLCA4*, *PGBD3*, *FOXD4L1*, *UMOD*, *HMGCS2*, *CA4*, *CA1*, *OR51I2*, and *TNS4* were escalated (Figure 16A). The suppressed DEGs included *KIR2DL4*, *CD164L2*, *KCNH3*, *DRGX*, *ARL4D*, *SP5*, *CBX2*, *SH3BGR*, *NODAL*, and *SPEM2* (Figure 16B).

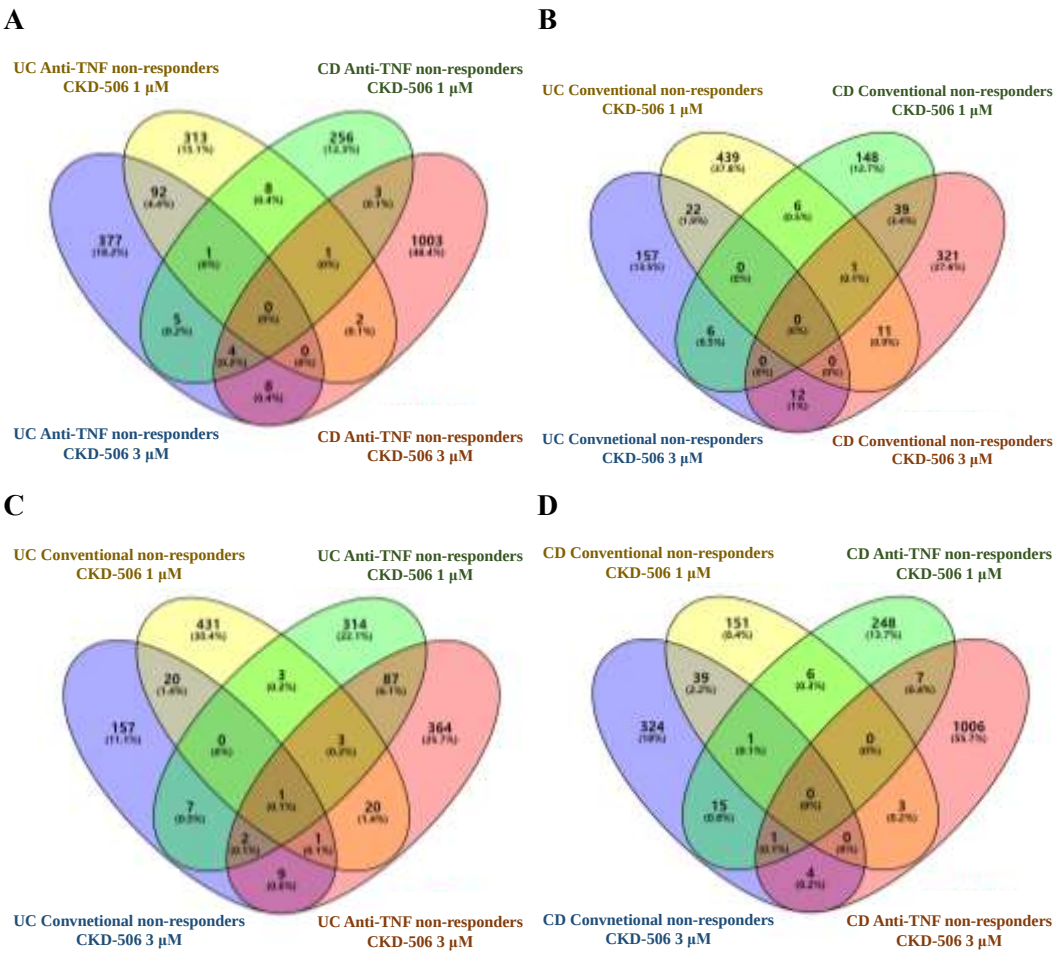

Figure 12. Venn diagram of DEGs overall

Venn diagram delineated the number of DEGs shared by different treatment or disease groups. According to the treatment, anti-TNF non-responders (A) and conventional non-responders (B) of both Crohn's disease (CD) and ulcerative colitis (UC) were presented above. Based on disease type, UC (C) and CD (D) were displayed below.

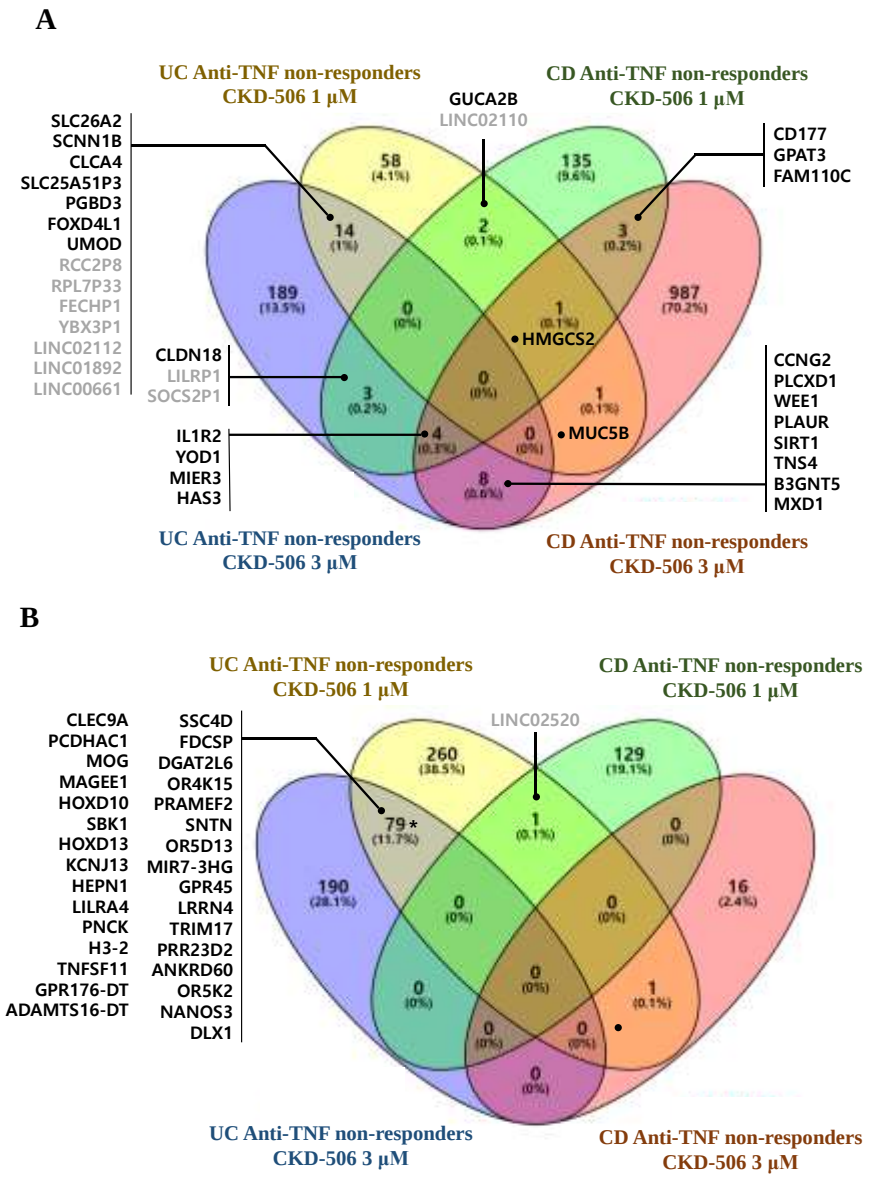

Figure 13. Venn diagram DEGs in anti-TNF non-responders

The number of up-regulated (A) and down-regulated (B) DEGs of anti-TNF non-responders were displayed on the Venn diagram. DEGs of intersecting zones were listed.

* Pseudogenes or non-coding genes were excluded

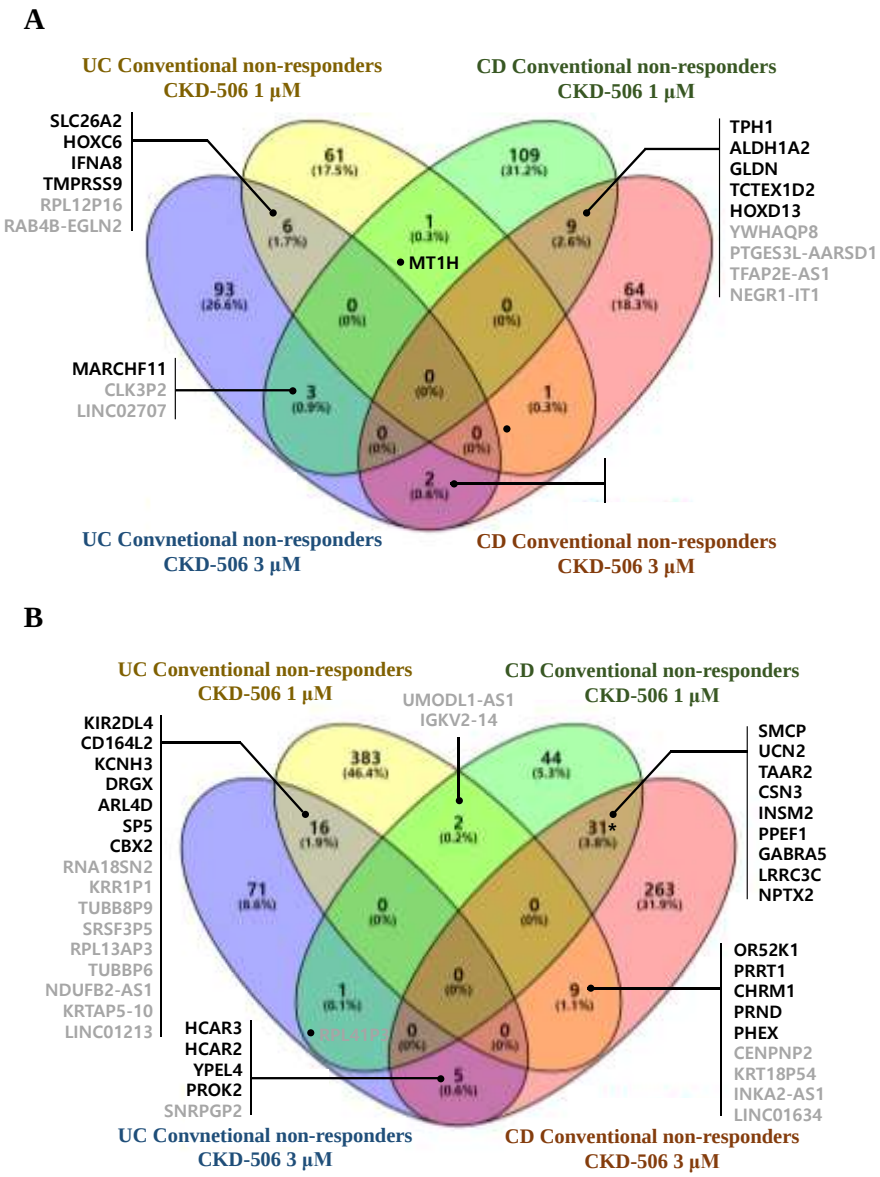

Figure 14. Venn diagram of DEGs in conventional non-responders

The number of up-regulated (A) and down-regulated (B) DEGs of conventional non-responders were displayed on the Venn diagram. DEGs of intersecting zones were listed.

* Pseudogenes or non-coding genes were excluded

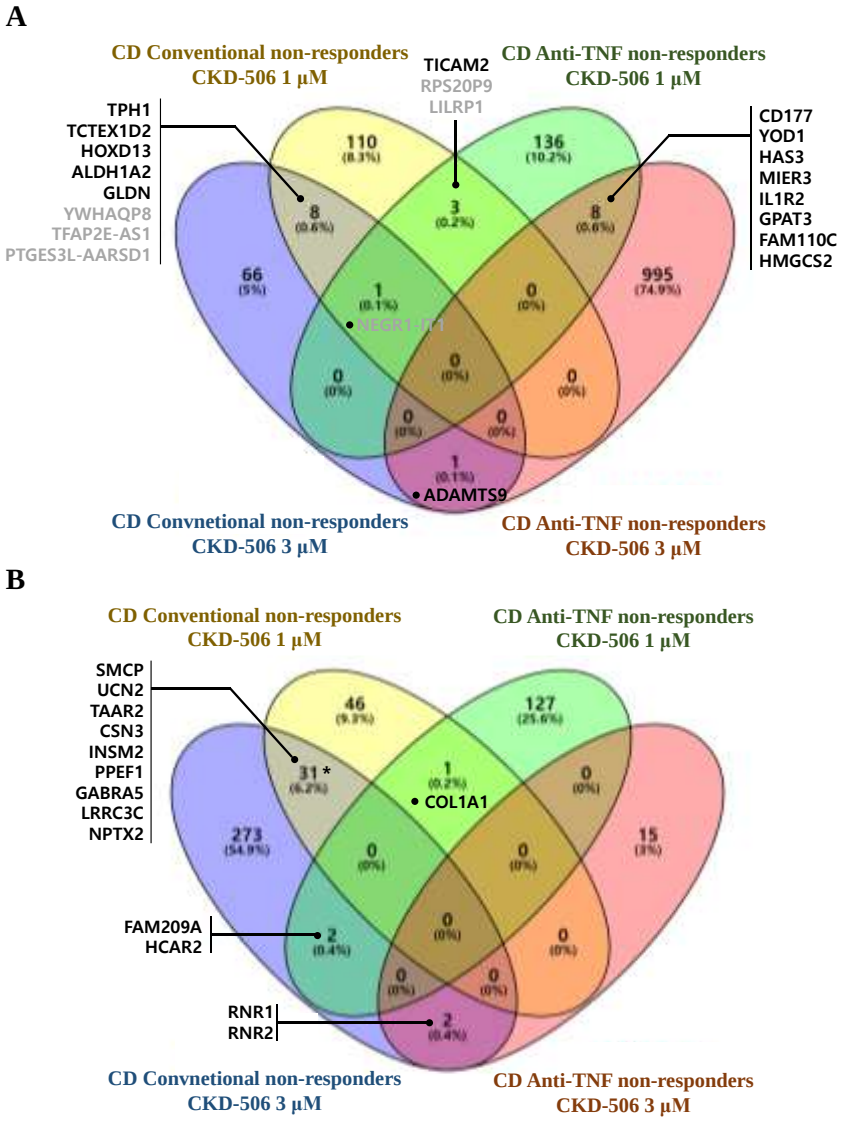

Figure 15. Venn diagram DEGs in CD

The number of up-regulated (A) and down-regulated (B) DEGs of Crohn's disease (CD) patients was displayed on the Venn diagram. DEGs of intersecting zones were listed.

* Pseudogenes or non-coding genes were excluded

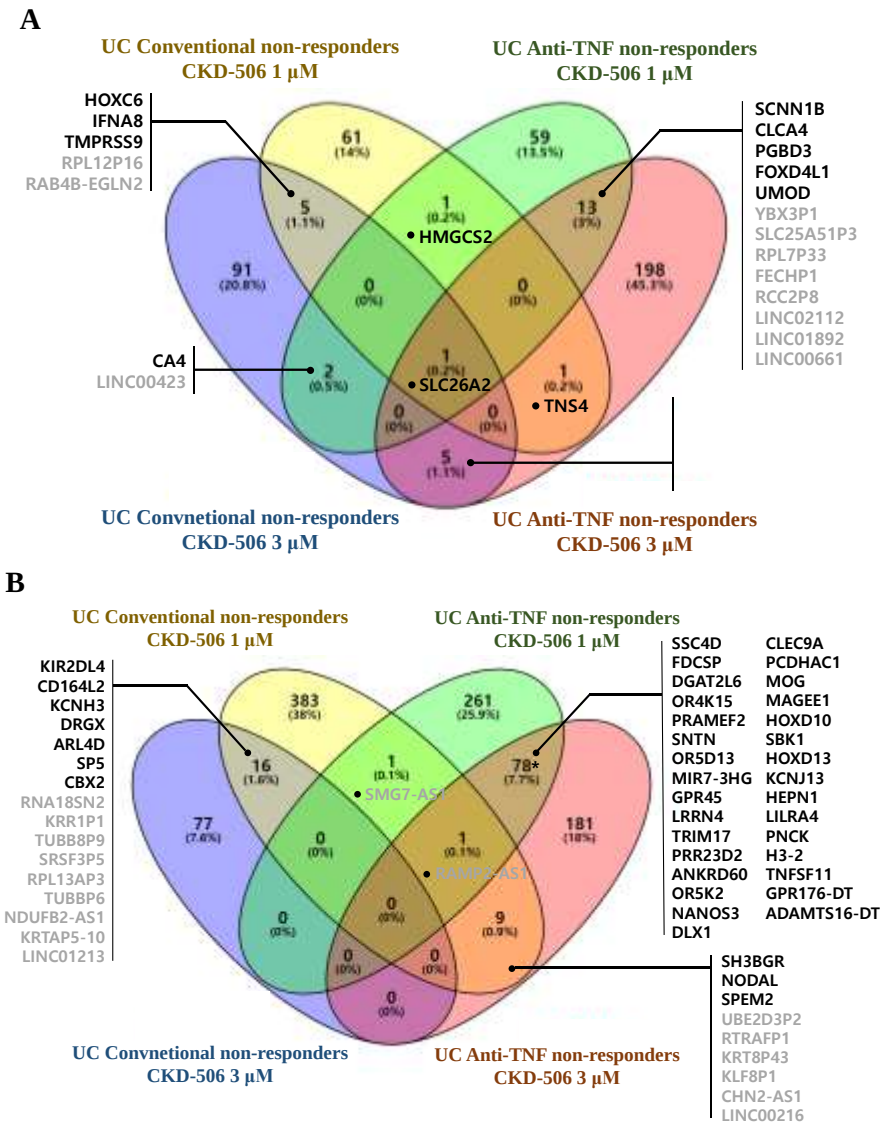

Figure 16. Venn diagram of DEGs in UC

The number of up-regulated (A) and down-regulated (B) DEGs of ulcerative colitis (UC) patients was displayed on the Venn diagram. DEGs of intersecting zones were listed.

* Pseudogenes or non-coding genes were excluded

7. Deconvolution cell population analysis

The xCell deconvolution method is a bioinformatics analytical approach employed to profile cell types using gene expression data. Its purpose is to forecast and examine the proportional occurrences of different cell types present in a biological specimen.

In this study, the human colon tissue was obtained from the same lesion for the identical subjects. Though cell population was compared by vehicle, CKD-506 1 μM, and CKD-506 3 μM, there was no significant difference among the three groups. Notably, smooth muscle cells were one of the major components (Figure 17A). The epithelial cells and endothelial cells were also observed as expected from the visual observation of biopsy samples (Figure 17B, C).

The immune score informs about the potential immune attributes of the sample, supporting possible involvement in diverse biological processes or disease conditions. The immune score was also similar among vehicle or CKD-506 treated groups (Figure 17D). There was a substantial portion of monocytes and neutrophils (Figure 17E, F). The M1 macrophage occupied more proportion than the M2 macrophage (Figure 17H, I). The Th1 cell was more abundant than the Th2 cell or Treg cells (Figure 17J, K, I).

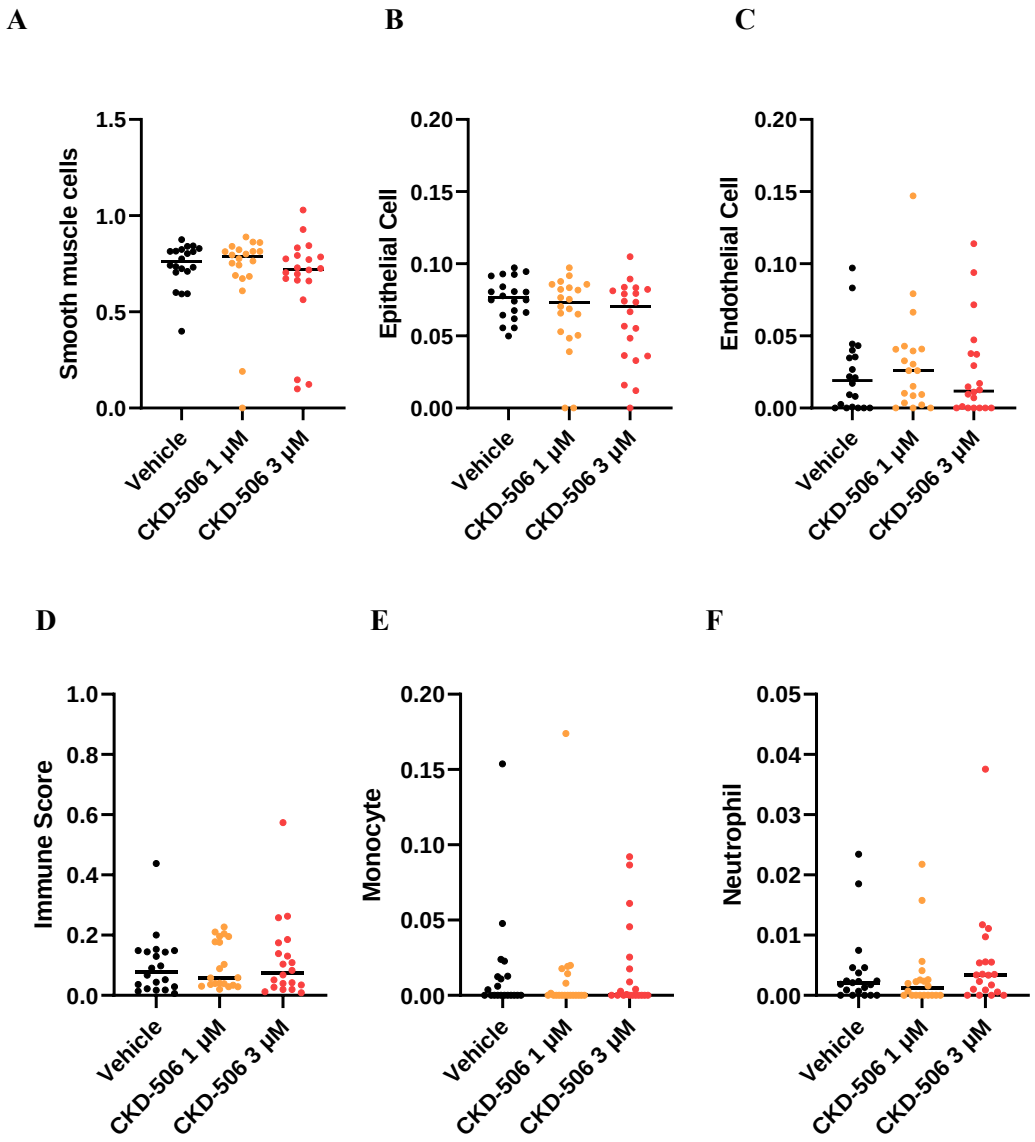

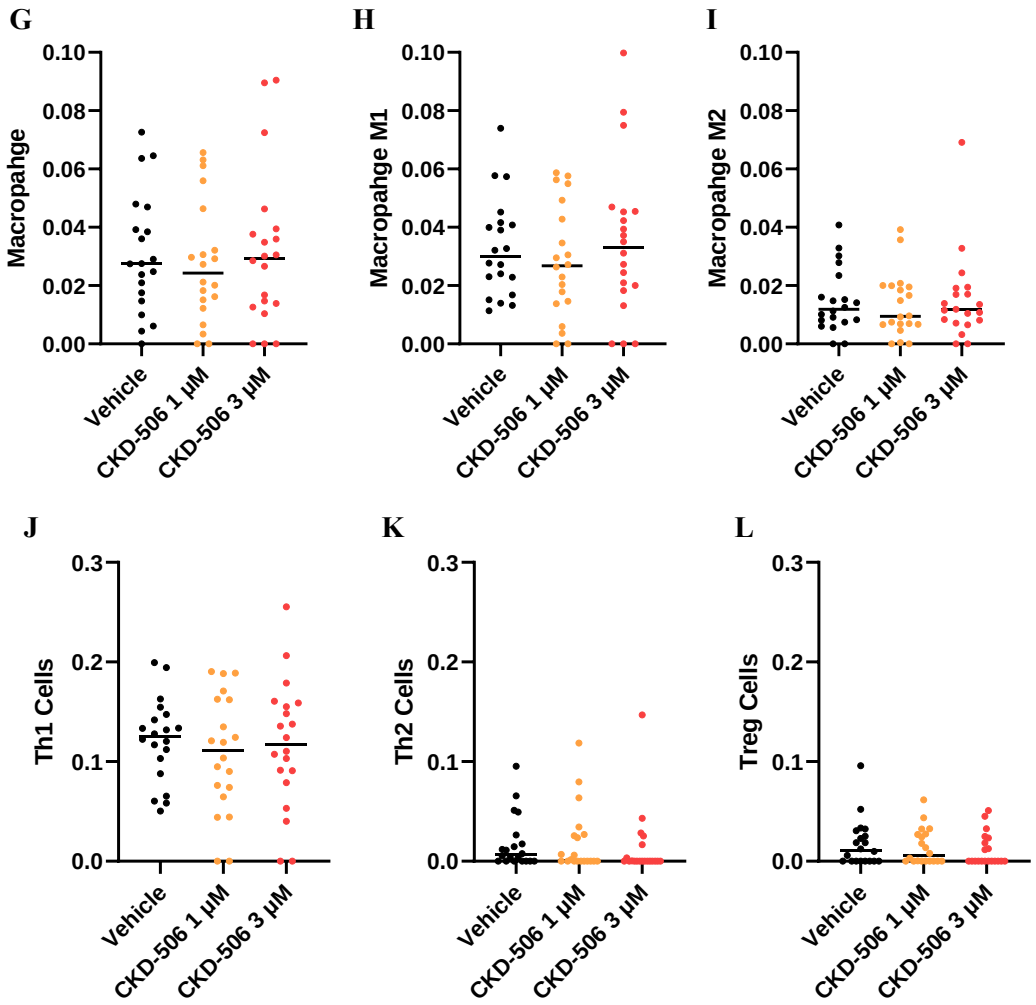

Figure 17. Deconvoluted cell population analysis

xCell deconvolution cell population analysis was done for all the RNA-seq samples. Stromal cell (A, B, C) as well as overall immune score was rated (D). The monocyte (E), neutrophil (F), macrophage (G, H, I), and T cell (J, K, L) distribution were also investigated.

8. Network-based gene ontology analysis

There were constraints in performing intricate and comprehensive network analysis only by extracted DEGs. Consequently, we expanded the gene set by utilizing an established database. Network-based GO analysis was only done for anti-TNF non-responders due to a higher quality of DEGs and better clustering than conventional non-responders.

The SAFE network analysis of CKD-506 1 μM treated anti-TNF non-responders classified extended gene sets into mainly 7 domains (Figure 18). These domains contained G protein-coupled receptor pathway, protein endoplasmic insertion or degradation network, chemical detection, and barrier micellar blood-brain (BBB) assembly. The same evaluation was done for CKD-506 3 μM treated anti-TNF non-responders. The extended gene sets were subdivided into 12 categories including cell adhesion, differentiation, mitosis, histone deacetylation, transcriptional regulation, and glycosylation of lactosylceramide (Figure 19). The pathway related to protein transportation and G protein-coupled receptor was again found to be correlated.

The general GO analysis using the GOBP and KEGG datasets was performed. The GOBP-based GO analysis of the CKD-506 1 μM treated group showed a strong correlation G protein-coupled receptor pathway, cell migration, chemotaxis, cell junction, and inflammatory cytokine-related pathway (Figure 20). The KEGG-based GO analysis of the same gene set displayed mainly chemokine signaling, cAMP (cyclic adenosine 3’,5’-monophosphate) signaling, inflammatory cytokine pathways, and components related to the kinase pathway (Figure 21). For the CKD-506 3 μM treated anti-TNF refractory group, GOBP-based GO analysis exhibited significant association with MAPK (mitogen-activated protein kinase) cascade, wound healing, cell adhesion, and migration (Figure 22). Using the KEGG dataset, PI3K (phosphoinositide 3-kinase)-AKT (also known as protein kinase B) signaling pathway, JAK (Janus kinase)-STAT (signal transducer and activator of transcription) pathway, RAS pathway, infection-

related pathways, chemokine signaling, and focal adhesion were noted to be relevant pathways (Figure 23).

Especially for the CKD-506 3 μM treated group, not only the extended gene set but also original DEGs were assessed for the GO study. With the native DEGs, GOBP-based GO analysis identified wound healing, oxygen response, cell proliferation, and interaction as meaningful biological processes (Figure 24). Applying the KEGG database, PI3K-AKT signaling, hypoxia-inducible factor-1 (HIF-1) signaling, P53 signaling, coagulation cascade, and cancer-related pathways were found to be noteworthy connections to the original DEGs (Figure 25).

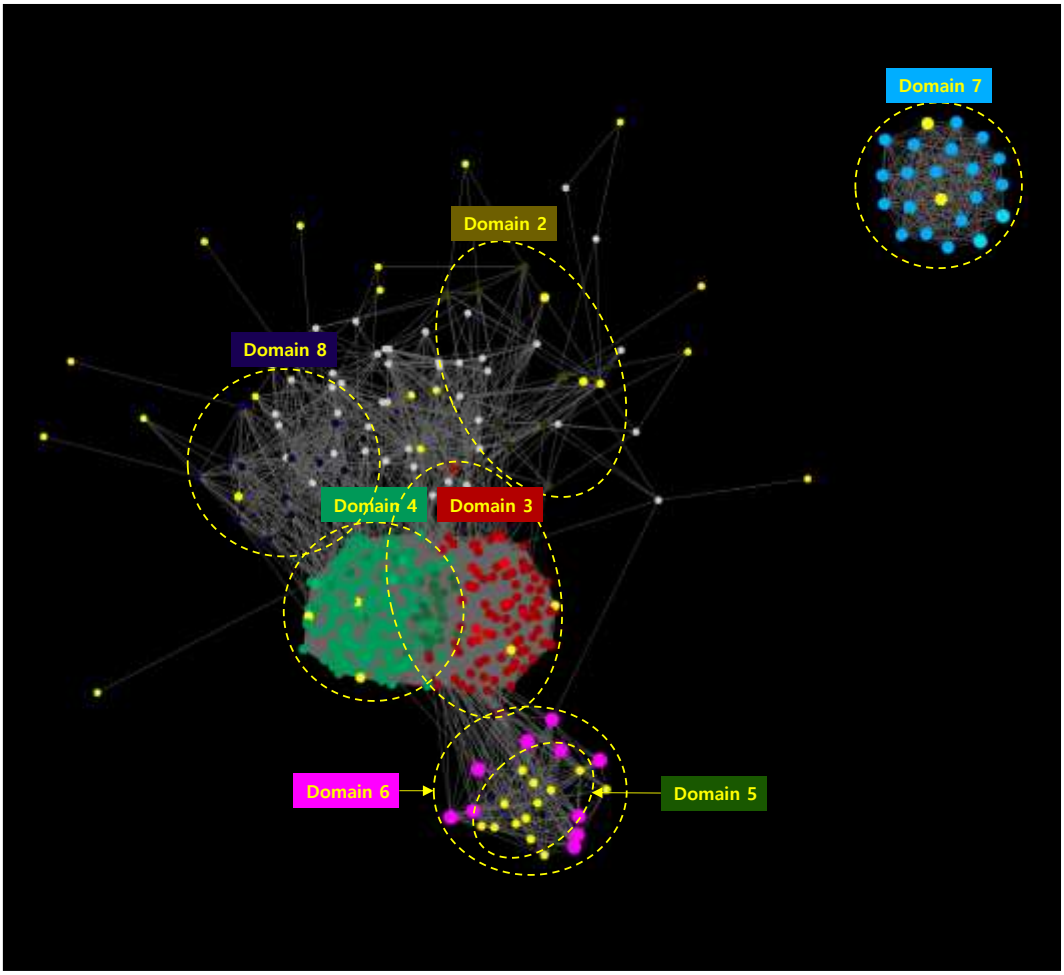

Figure 18. Network-based GO analysis of CKD-506 1 μM treated Anti-TNF non-responders

Domain 2: catabolic modification-dependent protein

Domain 3: adenylate G pathway protein-coupled receptor

Domain 4: pathway signaling chemotaxis G protein-coupled

Domain 5: membrane protein endoplasmic insertion network

Domain 6: chemical detection involved the perception sensory

Domain 7: adhesion assembly barrier bicellular blood-brain

Domain 8: activity endopeptidase negative regulation

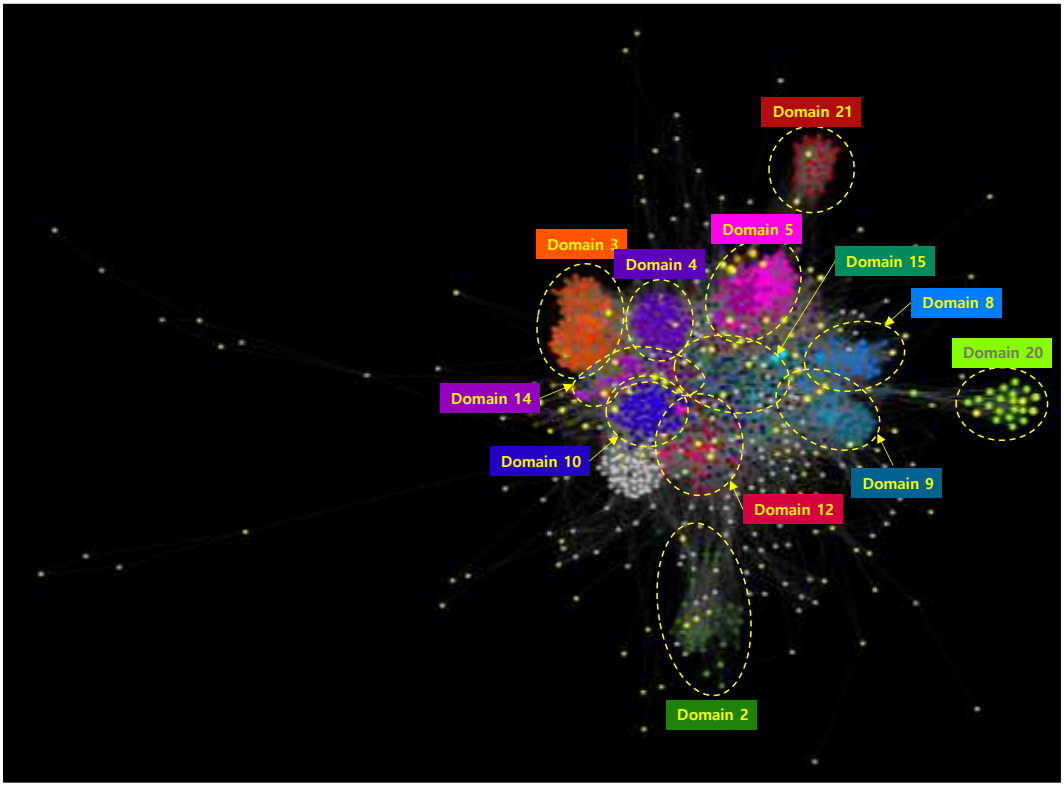

Figure 19. Network-based GO analysis of CKD-506 3 μM treated Anti-TNF non-responders

Domain 2: biosynthetic ganglioside glycosylation keratan lactosylceramide

Domain 3: Golgi transport vesicle-mediated endoplasmic protein

Domain 4: endocytosis membrane vesicle exocytosis regulation

Domain 5: protein catabolic cell mitotic positive

Domain 8: deacetylation histone regulation chromatin negative

Domain 9: II polymerase regulation RNA transcription

Domain 10: signaling pathway G protein-coupled receptor

Domain 12: cell adhesion differentiation adhesion-dependent animal

Domain 14: pathway receptor regulation signaling activity

Domain 15: positive regulation signaling 3-kinase cascade

Domain 20: adhesion assembly barrier bicellular blood-brain

Domain 21: cell adhesion cardiac regulation action

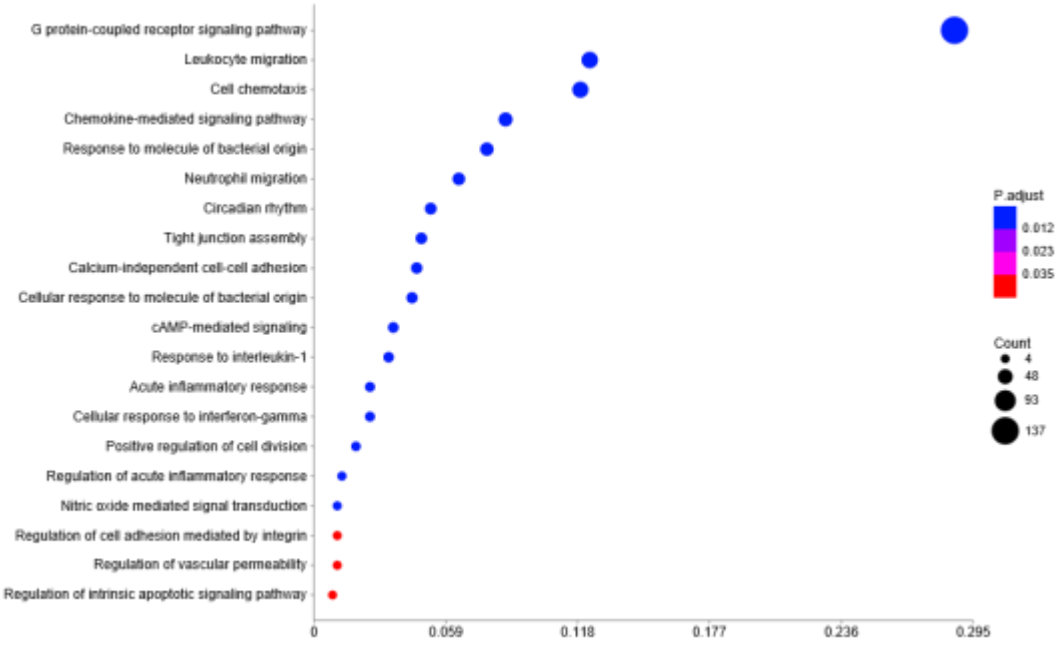

Figure 20. GOBP-based GO analysis of CKD-506 1 μM treated anti-TNF non-responders in the extended gene set

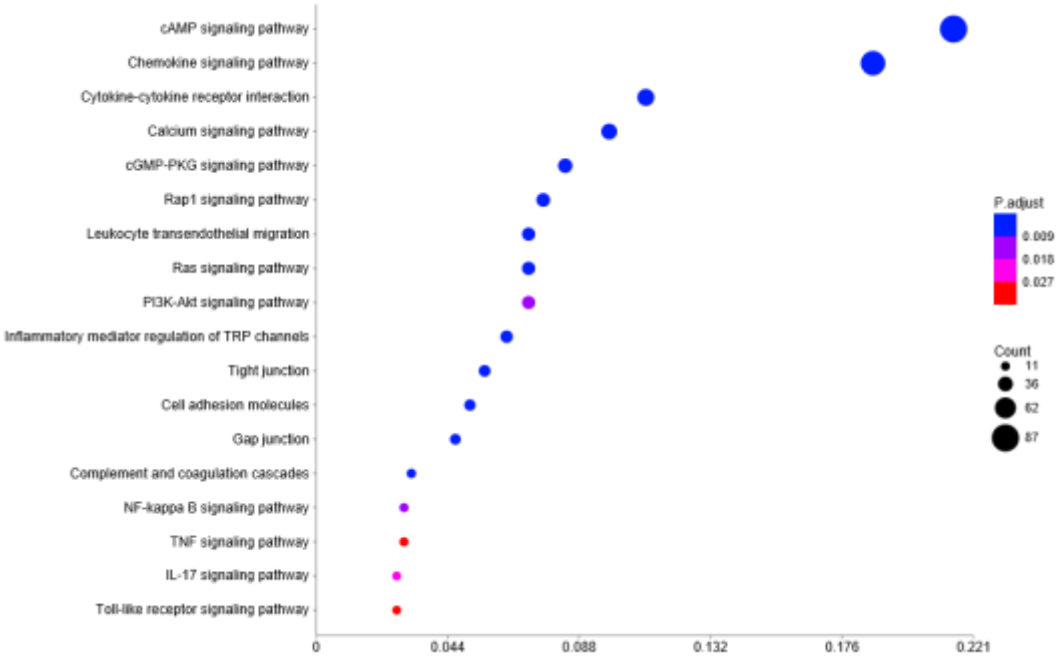

Figure 21. KEGG-based GO analysis of CKD-506 1 μM treated anti-TNF non-responders in the extended gene set

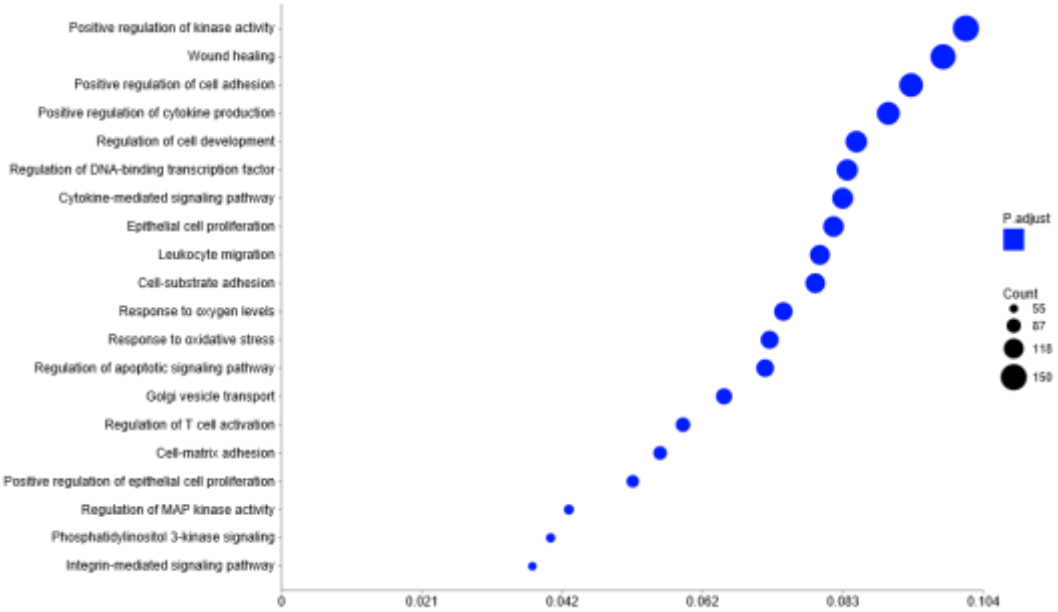

Figure 22. GOBP-based GO analysis of CKD-506 3 μM treated anti-TNF non-responders in the extended gene set.

P adjusted value was not denoted due to all the pathways presented less than 0.05×10^{-10}.

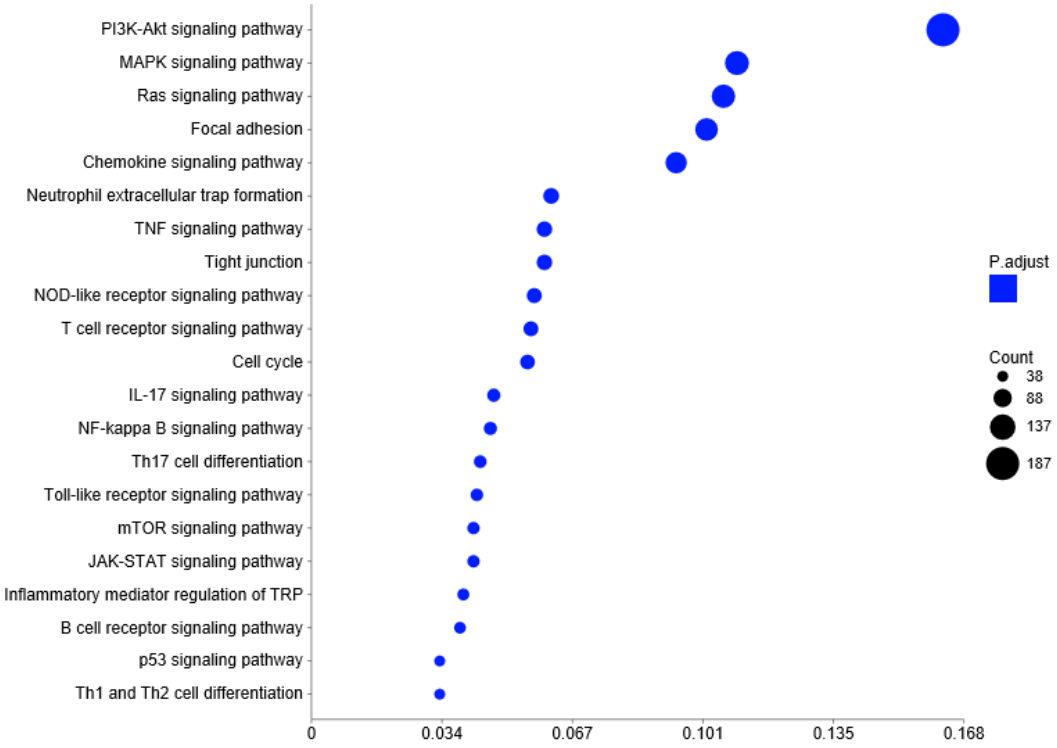

Figure 23. KEGG-based GO analysis of CKD-506 3 μM treated anti-TNF non-responders in the extended gene set

P adjusted value was not denoted due to all the pathways presented less than 0.05×10^{-10}.

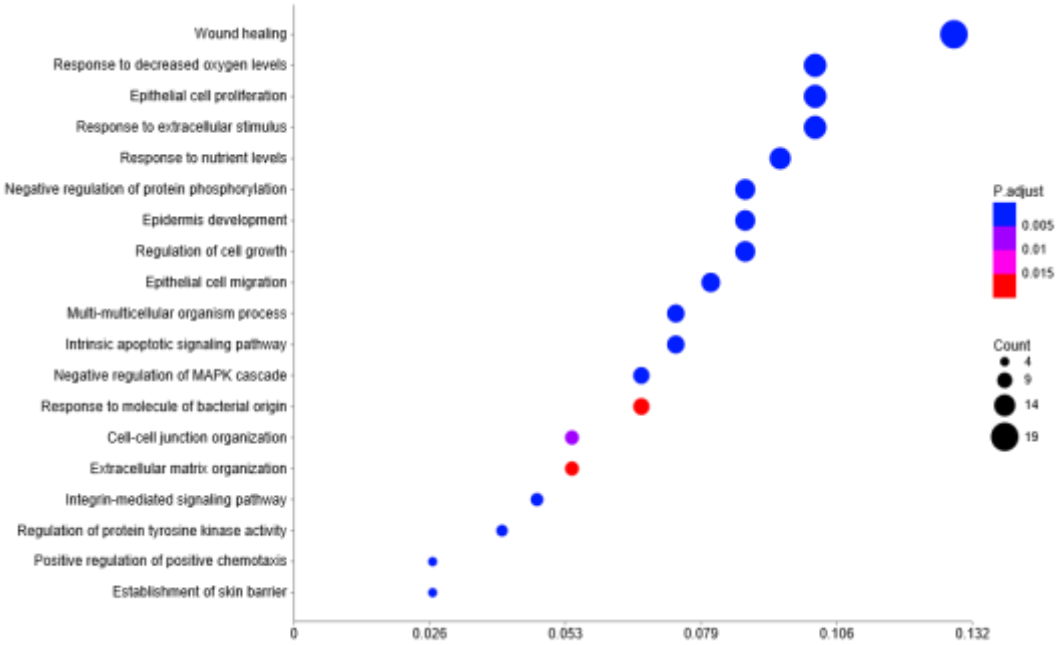

Figure 24. GOBP-based GO analysis of CKD-506 3 μM treated anti-TNF non-responders in the original DEG set

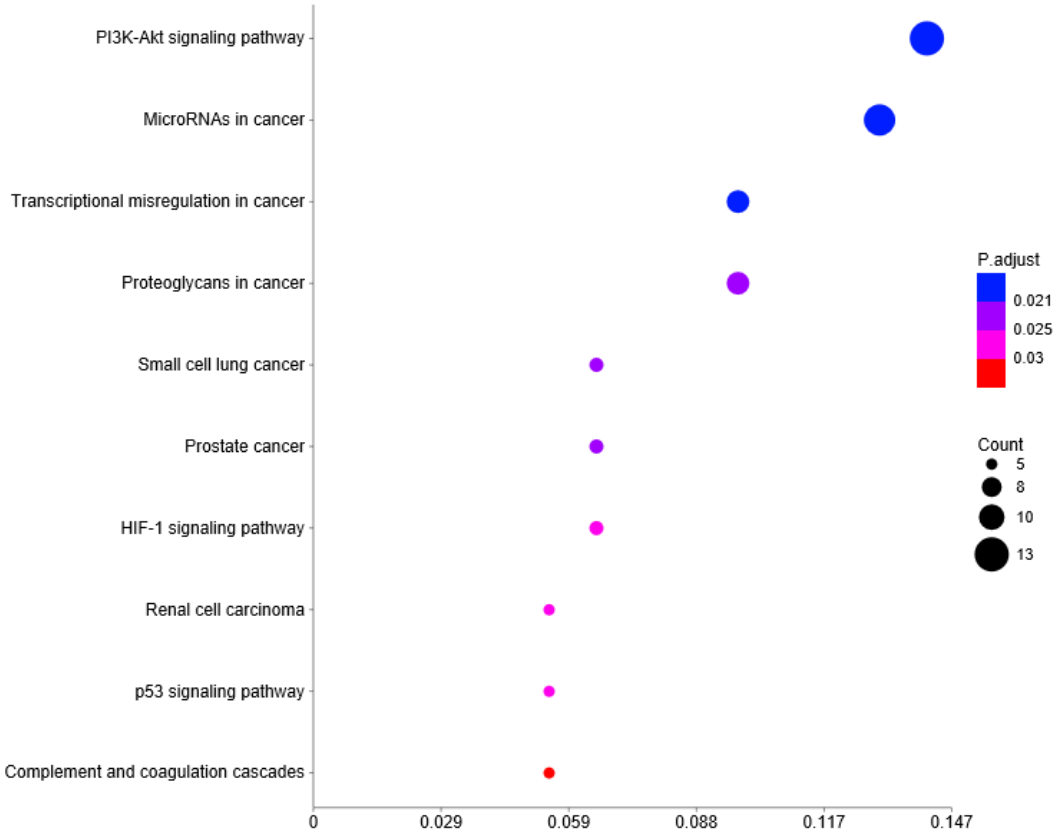

Figure 25. KEGG-based GO analysis of CKD-506 3 μM treated anti-TNF non-responders in the original DEG set

9. Gene set enrichment assay

Traditional GSEA including hallmark, ontology, immunologic signature, regulatory target, and cell type signature gene sets supported by MSigDB were also applied for further investigation. For the advanced research, all the gene lists and all the samples including both conventional non-responders and anti-TNF non-responders were included.

The hallmark-based GSEA discovered that IL6-JAK-STAT3 signaling, MYC targets, PI3K-AKT-MTOR signaling, reactive oxygen species (ROS) pathway, and tumor growth factor-beta (TGF-β) signaling were all negatively correlated with CKD-506-treated groups compared to vehicle (Figure 26). In KEGG-based GSEA, MTOR signaling pathway and apoptosis were all negatively correlated with CKD-506-treated groups compared to vehicle (Figure 27).

A

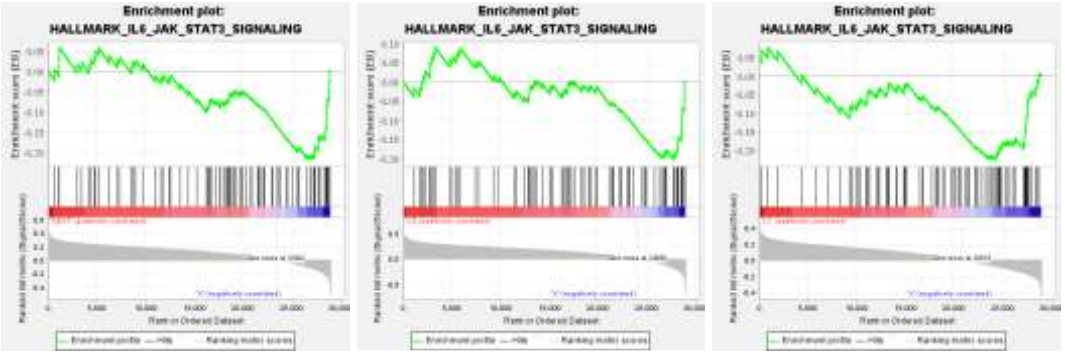

B

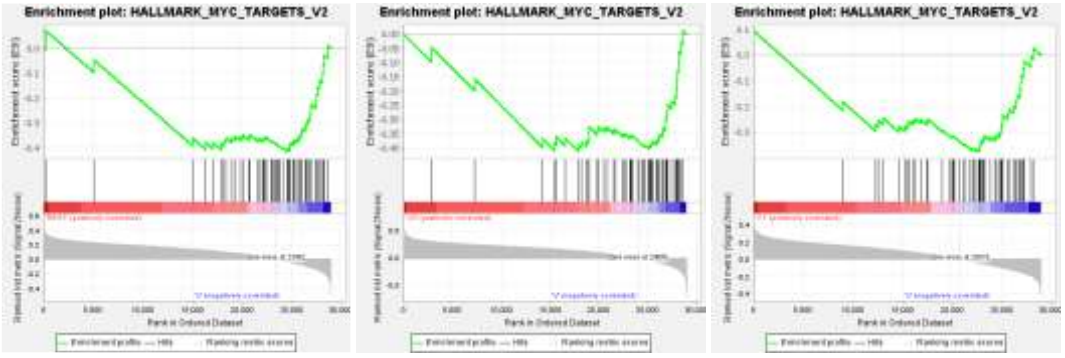

C

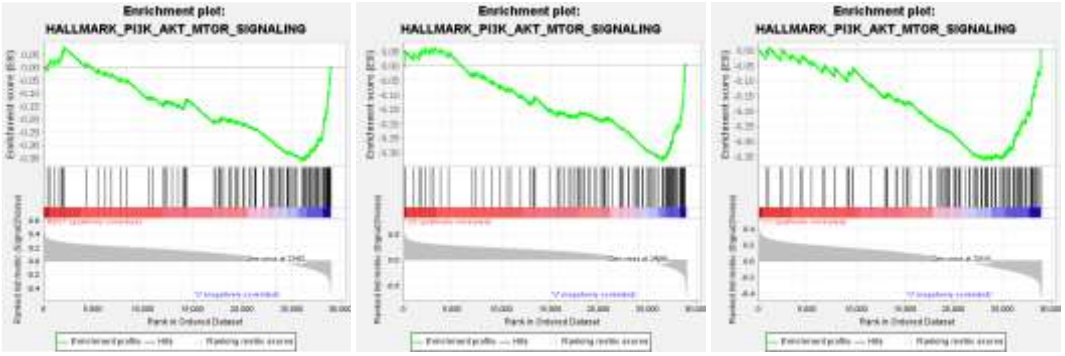

D

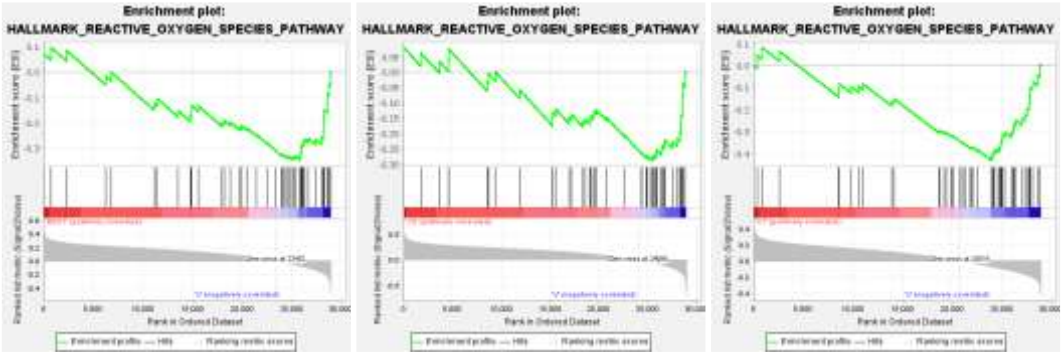

E

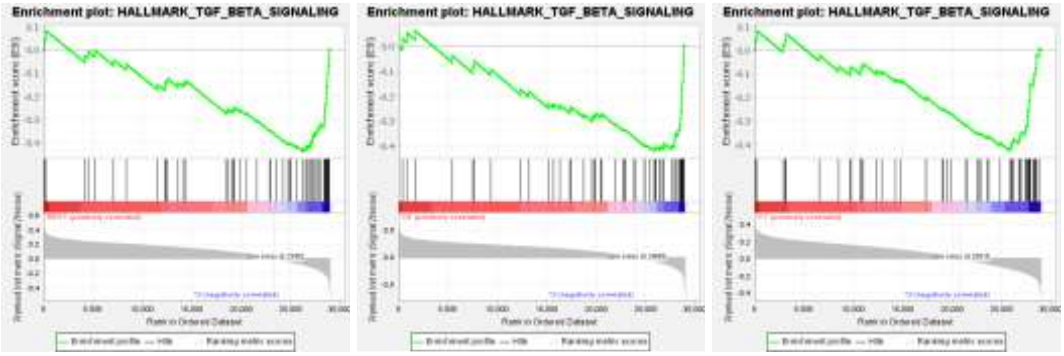

Figure 26. Hallmark-based GSEA

Hallmark-based GSEA was done for all the patients and gene lists. Enrichment plot was depicted for CKD-506 both 1 μM and 3 μM vs vehicle (left), CKD-506 3 μM vs vehicle (middle) and CKD-506 3 μM vs vehicle (right). IL6-JAK-STAT3 signaling(A), MYC targets(B), PI3K-AKT-MTOR signaling(C), reactive oxygen species pathway(D), and TGF-β signaling(E) were all negatively correlated with CKD-506-treated groups compared to vehicle.

A

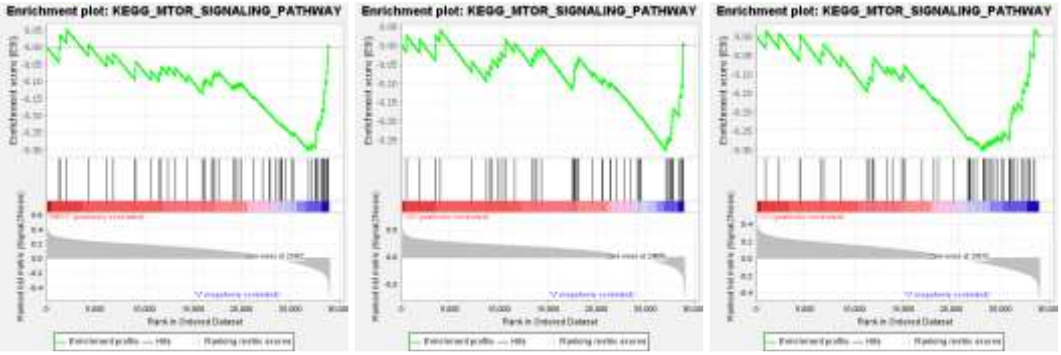

B

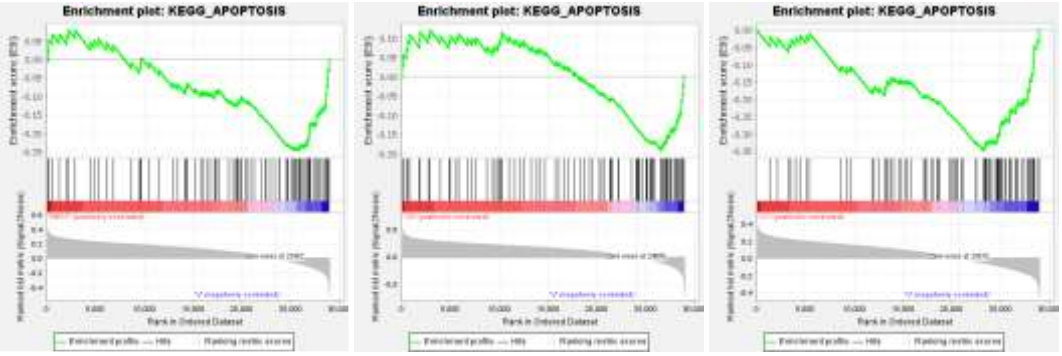

Figure 27. KEGG-based GSEA

KEGG-based GSEA was done for all the patients and gene lists. Enrichment plot was depicted for CKD-506 both 1 μM and 3 μM vs vehicle (left), CKD-506 3 μM vs vehicle (middle) and CKD-506 3 μM vs vehicle (right). MTOR signaling pathway(A) and apoptosis(B) were all negatively correlated with CKD-506-treated groups compared to vehicle.

10. Validation of target genes in vitro and ex-vivo

Several target genes and pathways extracted from the various analysis tools were validated via qRT-PCR after in-vitro culture of the human colon cell line and ex-vivo culture of mouse colon tissue. To mimic the inflammatory environment, either TNF-α or IFN-γ was treated in human cell lines or mouse tissue.

The HAS3 showed a decrease in transcription level under inflammatory conditions and CKD-506 treatment exhibited a dose-dependent increment in both human and mouse colitis models (Figure 28A, Figure 29A). The SLC26A2 did not display significant changes at the transcriptional level under inflammatory induction, but CKD-506 treatment provoked meaningful escalation compared to the vehicle (Figure 28B, Figure 29B). The YOD1 showed no noticeable transcription alterations in both human and mouse colitis models under inflammatory conditions. Following CKD-506 treatment in a human colon cell line, the transcription level was raised in a dosage-dependent manner; nevertheless, when compared to the vehicle-treated group, it either declined or remained relatively unchanged (Figure 28C). In the mouse model, there was an evident YOD1 transcriptional elevation in CKD-506 treatment samples compared to the vehicle, yet it did not demonstrate a dosage-dependent manner (Figure 29C). The transcriptional level of CD177 was elevated in IFN-γ treated mouse model. Upon CKD-506 treatment, there was a meaningful increment in both human and mouse models compared to vehicle treatment (Figure 28D, Figure 29D). The IL1R2 was decreased in the mouse colitis model and CKD-506 treatment elevated transcriptional levels in both human and mouse samples though the significance was only confirmed in the human cell line (Figure 28E, Figure 29E). The MIER3 was reduced in inflammatory surroundings. In the human colon cell line, CKD-506 declined transcriptional level in a dose-dependent manner, however, the mouse model did not show meaningful modifications (Figure 28F, Figure 29F).

The transcriptional reduction of C-MYC was prominent in colitis-mimicking conditions, and CKD-506 induced further decrement in both human and mouse models

(Figure 28G, Figure 29G). The JAK2-STAT3 pathway showed CKD-506-dependent transcriptional decrement in both human and mouse models. However, STAT3 displayed a significant reduction only in the mouse colitis model (Figure 28H-I, Figure 29H-I). Each component of the PI3K-AKT-MTOR pathway presented a similar transcription level even in an inflammatory situation. Both in human and mouse models, the CKD-506 treatment induced significant decrement in a dose-dependent manner (Figure 28J-L, Figure 29J-L).

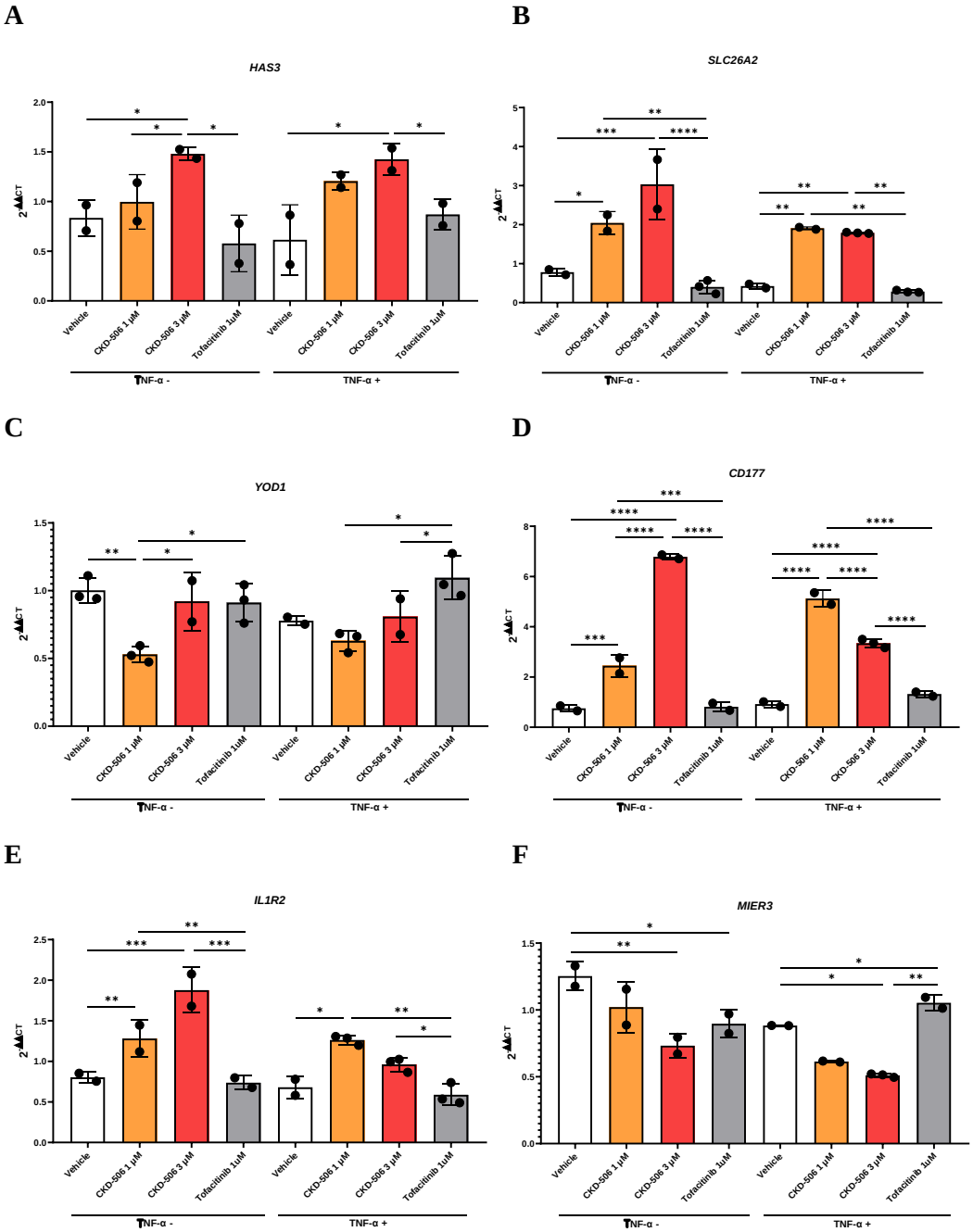

G

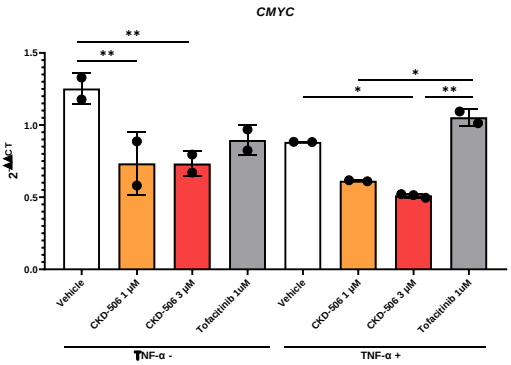

H

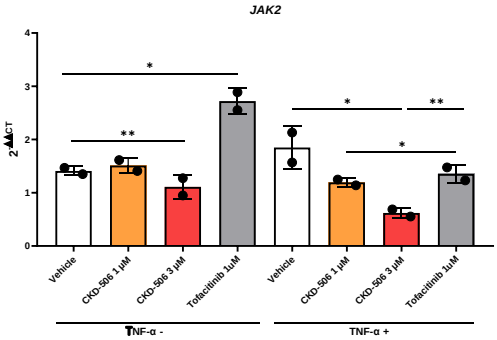

I

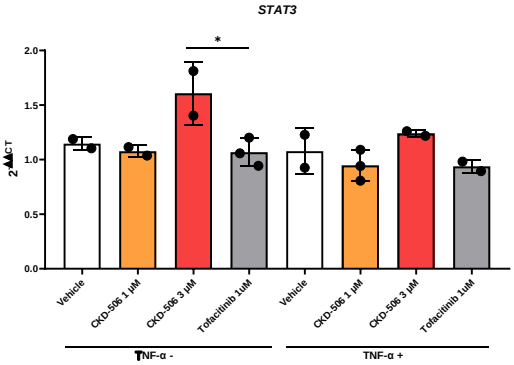

J

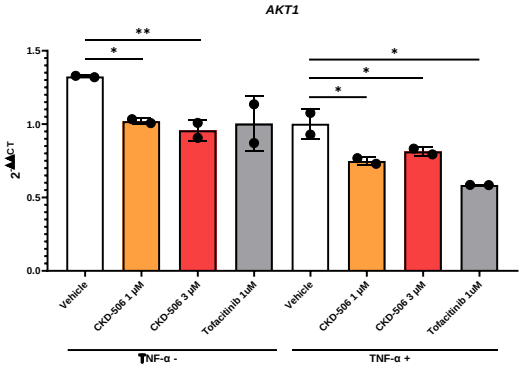

K

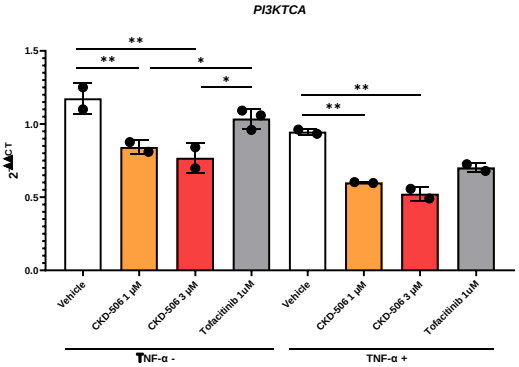

L

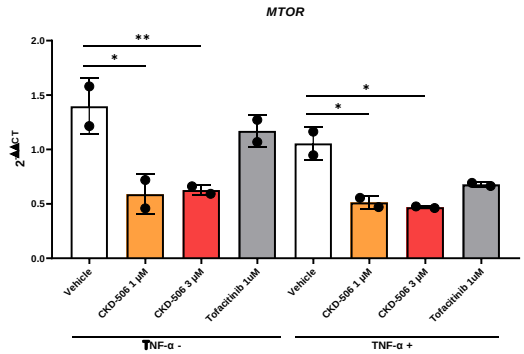

Figure 28. Validation of revealed CKD-506 targets in human colon in vitro culture

Several candidates or downstream targets of CKD-506 identified in RNA-sequencing analysis were validated on the HT-29 human colon cell line. Significance is indicted by * $p < 0.05$, ** $p < 0.005$, *** $p < 0.0005$, **** $p < 0.0001$.

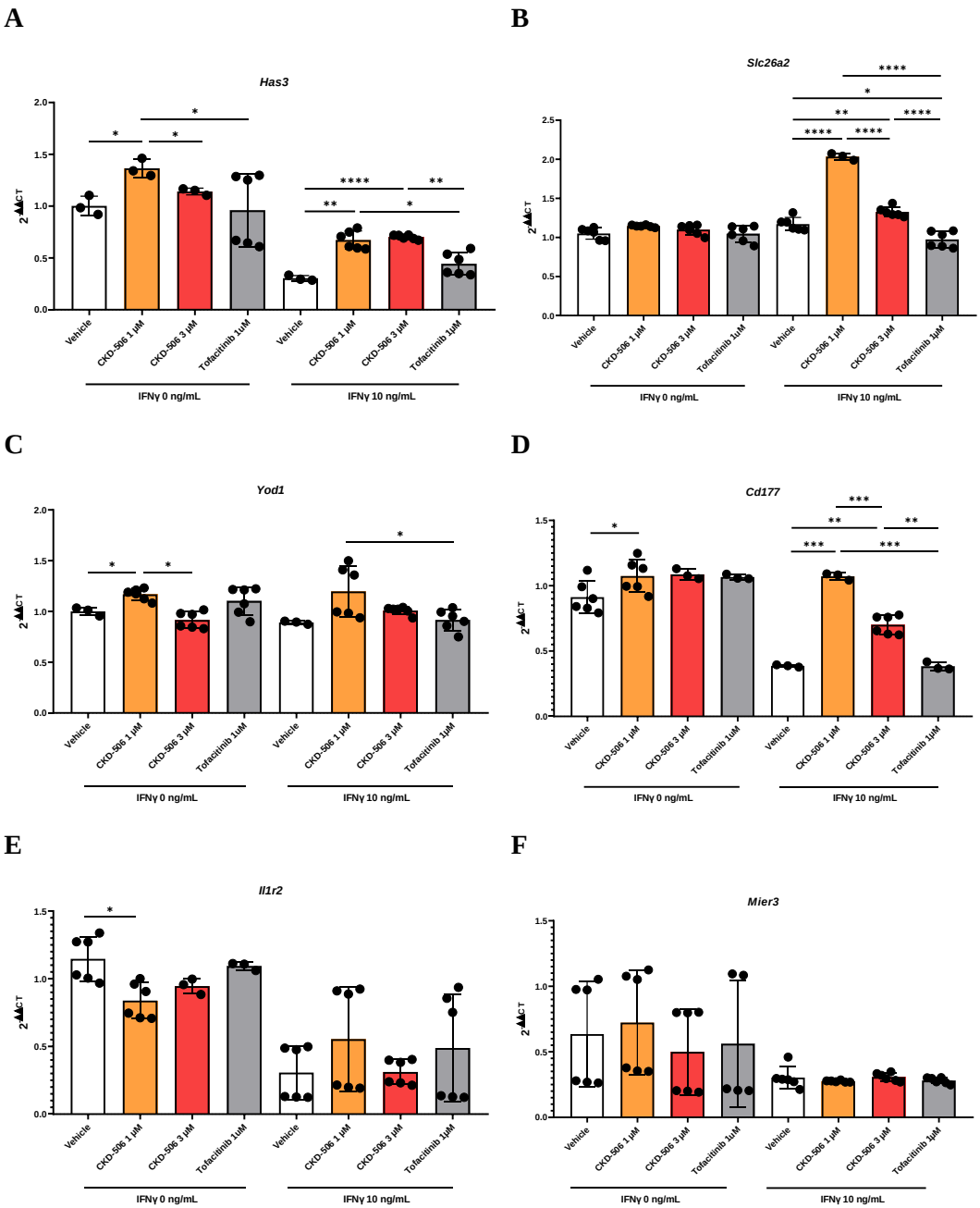

G

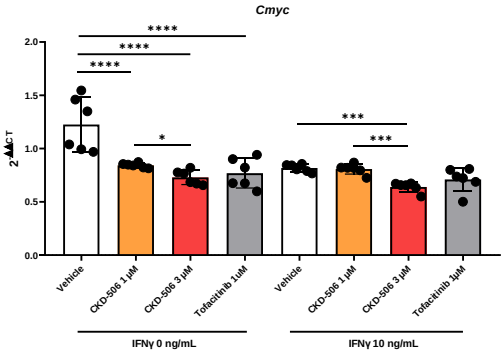

H

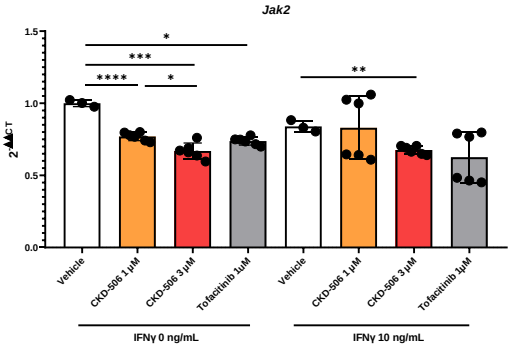

I

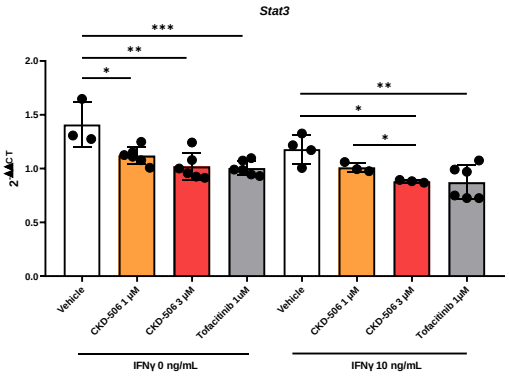

J

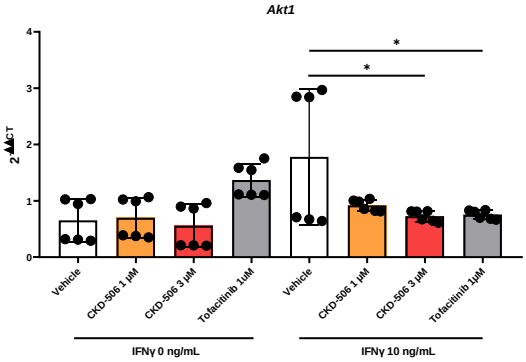

K

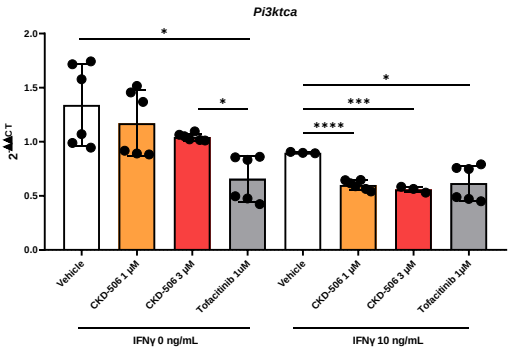

L

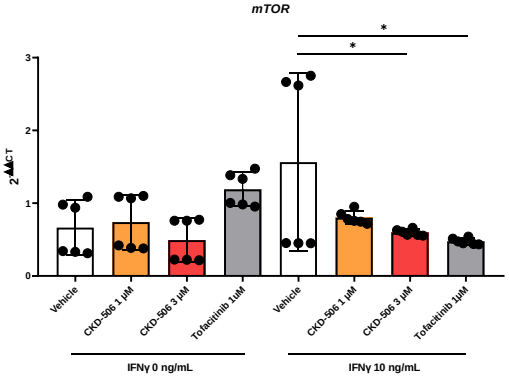

Figure 29. Validation of revealed CKD-506 targets in mouse colon ex-vivo culture

Several candidates or downstream targets of CKD-506 identified in RNA-sequencing analysis were validated on mouse colon tissue. Significance is indicted by * $p < 0.05$, ** $p < 0.005$, *** $p < 0.0005$, **** $p < 0.0001$.

IV. DISCUSSION

IBD including CD and UC is a chronic and relapsing intestinal inflammatory disorder affecting a larger population recently. The conventional aminosalicylic acid with immunosuppressant and the most representative biologics, anti-TNF inhibitor is a well-known therapeutic option. However, the number of patients refractory to the current regimen is increasing and there is a need for novel therapy.

The CKD-506 is a a contemporary HDAC6 selective inhibitor, which has been proven to be effective in other autoimmune diseases. Though CKD-506 alleviated intestinal inflammation in animal models or blood samples, there was no further research on human-derived colon samples.

There was no published data about the HDAC6 expression profile. In this study, HADC6 expression and its activity were first confirmed through IHC staining. Though the recruited patients group showed heterogeneous features in terms of age and immunomodulator use, there was no significant association with the IHC score. It was clear that IBD patients illustrated higher levels of HDAC6 expression compared to healthy controls. However, there was no meaningful variation between disease subtypes or treatment responses. Rather IHC score was correlated with the Mayo score or disease activity.

Unlike expectation, α-tubulin acetylation was also increased in IBD patients as the HDAC6 expression level escalated. The acetylation and deacetylation of α-tubulin are mainly regulated by alpha-tubulin acetyltransferase 1 (ATAT1) and HADC6 in mammals; however, underlying mechanisms or interactions are still unclear. Other genetic or environmental factors other than HADC6 may also play a crucial role in the modification of α-tubulin acetylation level. Though α-tubulin acetylation was increased in IBD patients compared to healthy controls, the relative expression level was lower than HDAC6 in paired analysis. Through this initial study, it can be assumed that HDAC6 inhibitors could be effective in IBD patients with high HDAC6 expression.

The colon is a complicated and multi-layered structure. There were several limitations in adopting animal models or cell cultures to mimic human intestines. Therefore, an ex-vivo culture system was developed to reproduce an environment closer to the human colon. Referring to previous publications, oxygen level, growth factor, antibiotics, and antifungals were modified for optimized conditions. Since excessive artifacts may harm or conceal the physiologic response, only essential chemicals and supports remain. After the 24-hour incubation, the cell structure was hardly recognized. Considering at least the time required for transcriptional regulation after chemical treatment, the incubation time was determined as 3 hours. The microscopic cell structure was well maintained and morphological defensive effects of CKD-506 were also noted in this period. Before the ex-vivo culture of human colon samples and RNA-seq, several inflammatory cytokines and epithelial barrier markers were explored in mouse colon punch specimens after ex-vivo incubation with CKD-506.

IL-10, a regulatory cytokine, restrained both the presentation of antigens and the subsequent release of pro-inflammatory cytokines. Numerous studies have investigated the utilization of IL-10 as a therapeutic approach for IBD and IL-10 mutations were correlated with early onset IBD.[53,54] Interestingly CKD-506 treatment elevated IL-10 transcription and expression levels, and seems to repress pro-inflammatory cascades.

The intestinal lining is coated with a layer of mucus primarily composed of heavily O-glycosylated MUC2 mucin. This mucus serves as the initial protective barrier, helping to minimize contact between the epithelium and potential hazards like ingested substances, digestive processes, or substantial microorganisms. Malfunctions in mucus enable bacteria to access the epithelium and trigger an immune response contributing to intestinal inflammation. In cases of acute inflammation in CD and UC, both adults and children showed a reduction in MUC2 expression and a consistent decrease in goblet cells. Furthermore, varying levels of expression could be observed depending on the presence or severity of inflammation.[55,56] The qRT-PCR results implied that CKD-506 may increase MUC2 transcriptional level. By these results, the following gene ontology

study on RNA sequencing data presented a strong correlation with epithelial barrier or mucus protective activity.

There is no doubt that TNF-α is one of the most prominent pivotal inflammatory factors in IBD. For about a quarter of a century, anti-TNF antibodies have been extensively utilized for various categories of diseases. Despite the introduction of novel biological treatments, a significant number of patients initially select an anti-TNF inhibitor due to their current affordability. When dealing with fistulizing CD, anti-TNF antagonists continue to be the favored therapeutic option. In cases of severe acute UC, the preferred choice of treatment remains the anti-TNF inhibitor, primarily due to its rapid impact and the potential for adjusting dosage.[57,58] In the CKD-506-treated mouse colon presented a radical reduction in TNF-α transcription level.

IL-33 belongs to the IL-1 cytokine family and is known for its diverse functions, acting either as a conventional extracellular cytokine or as a nuclear transcription factor.[59] It has been elevated in the inflamed mucosa of the intestines in patients with IBD. Clinical observations suggest that IL-33 primarily contributes to the mucosal inflammation seen in IBD, acting as a signal that triggers a pro-inflammatory response. In addition, IL-33, along with its receptor suppression of tumorigenicity 2 (ST2), has interactions with both innate and adaptive immune systems and is considered a crucial controller of inflammatory conditions.[60,61] The CKD-506 significantly alleviated IL-33 transcription in the mouse colon.

Significantly elevated levels of IL-1β are found in the intestines of individuals afflicted with IBD.[62] IL-1β is an inflammatory cytokine known for its broad impact on both systemic and local processes. Predominantly synthesized by innate white blood cells, IL-1β can regulate the activities of immune cells as well as cells not directly related to the immune system.[63] Research on infection has confirmed the pivotal role of IL-1β in adjusting intestinal inflammation. Blocking IL-1β has been shown to mitigate inflammatory disorders in conditions such as Clostridium difficile–associated colitis and Salmonella typhimurium–induced enteritis.[64] The treatment of CKD-506 induced

suppressed transcription of IL-1β.

LRG1 belongs to the leucine-rich repeat (LRR) protein family and was initially identified in human serum. LRG1 is a versatile and pathogenic signaling molecule that regulates the TGFβ pathway in inflammatory circumstances.[65] IL-6 triggers the production of LRG1, and it is also induced by other pro-inflammatory cytokines. Furthermore, LRG1 expression rises not only in the liver but also at localized sites of inflammation. In individuals with active UC, serum levels of LRG1 were notably elevated compared to those with UC in remission or healthy individuals.[66] The high dose of CKD-506 seems to diminish LRG1 transcription level in the mouse colon.

IL-2 is primarily generated by activated T cells and plays a role in stimulating the proliferation of lymphocytes, macrophages, and natural killer (NK) cells. It is also important in driving $CD4^+$ T cells to differentiate into Th1 and Th2 effector subsets, while simultaneously impeding Th17 differentiation. Elevated levels of IL-2 were observed in biopsies of mucosal IBD.[67] However, some studies described that inflammatory lesions in CD, but not UC, exhibited higher IL-2 mRNA transcript levels, suggesting the relevance of T-cell activation and lymphocyte-induced cytokine secretion in the development of CD.[68] In addition, the expression of IL-22 showed a notable decline in CD patients treated with anti-TNF therapy compared to untreated CD patients and controls.[69] In this research statistically significant reduction of IL-2 by CKD-506 was observed in the CBA assay.

IL-4, a cytokine originating from T cells which was once referred to as B-cell growth factor, has been identified to suppress actions of monocyte effectors including the generation of IL1β, TNF-α, and superoxide anions. Furthermore, IL-4 triggers the production of the interleukin-1 receptor antagonist, contributing to anti-inflammatory impacts.[70] Reduced IL-4 production in IBD could lead to impaired immune regulation and anti-inflammatory processes and aggravated disease pathogenesis.[71] Though IL-4 transcription level seemed to be higher in the mucosa of IBD patients compared to healthy control in several studies, the tendency varied according to the cell population

and severity of inflammation.[71,72] The co-incubation with CKD-506 lessened the IL-4 expression in mouse colon.

In experimental colitis and individuals with IBD, heightened production of IL-6 from lamina propria macrophages and $CD4^+$ T cells was observed. IL-6 can initiate pro-inflammatory actions by activating other inflammatory cells including APCs and T cells.[73] However, IL-6 might also serve crucial roles in epithelial homeostasis by promoting the growth and expansion of intestinal epithelial cells (IECs).[74] In specific subsets of CD patients, clinical improvements were observed through the interruption of IL-6 signaling using antibody-based blockade.[75] The CKD-506 treatment dramatically dropped the IL-6 expression in CBA study.

IFN-γ holds a pivotal function in both immune reactions and inflammatory processes. Immune cells, specifically T cells and natural killer cells are responsible for its production. It is a well-known cytokine that causes IBD in mice models and is understood as a pro-inflammatory cytokine, increased in IBD patients.[76,77] In this CBA analysis, as expected CKD-506 declined IFN-γ expression level.

Numerous investigations have examined the presence of Th17 cell-related cytokines in the mucosa of patients with IBD. These examinations have revealed elevated expression of Th17 cell-related cytokines such as IL-17, by lamina propria T cells in both CD and UC.[78] IL-17 demonstrated potent pro-inflammatory effects in IBD, and increased levels of IL-17 has been identified in both mucosa and serum in IBD patients.[79,80] In this mouse colon CBA study, CKD-506 subsided IL-17 expression level.

Through the overall qRT-PCR and CBA analysis of IFN-γ and CKD-506 treated mouse colon punch samples, potential of CKD-506 to alleviate colonic inflammation was observed. Based on these findings, human colon biopsy samples were ex-vivo cultured and RNA-seq was executed. A total of 20 patients were enrolled, and the analysis was focused on treatment-refractory patients with high disease activity. Among several criteria for DEG extraction, cutoff values of significance or fold change were defined under consultation with the Bioinformatics Collaboration Unit (BiCU) in the

Department of Biomedical Systems Informatics, Yonsei University College of Medicine. The batch effect and individual patient factor were adjusted before the DEG selection process

The UC and CD, or conventional and anti-TNF non-responders expressed a substantial number of DEGs. Anti-TNF non-responders presented lower *p*-values and higher fold change than conventional non-responders. However, the distinctive clustering of DEGs within a certain group was not well recognized. Therefore, an extended gene set was prepared for the network-based pathway analysis, and individual genes filtered by Venn diagram or volcano plot were also delicately evaluated for therapeutic target screening. Several possible targets of CKD-506 are abbreviated below. The validation was done by qRT-PCR of revealed genes after CKD-506 treated inflammation-induced human colon cell line in-vitro culture and mouse colon ex-vivo culture.

Solute carrier family 26 member 2 (SLC26A2) presented significant escalation in all the UC groups including both anti-TNF and conventional non-responders, both CKD-506 1 μM and 3 μM group. Though the underlying mechanism is not fully understood, the SLC26A2 gene was specific to IBD compared to irritable bowel syndrome (IBS) patients in the multigene analysis.[81] Two genome-wide associations study (GWAS) presented that SLC26A2 was downregulated in both UC and CD.[82,83] CKD-506 may normalize depressed SLC26A2 expression and contribute to the recovery of intestinal homeostasis. In both human and mouse models, CKD-506 increased SLC26A2 transcriptional levels in inflammatory situations. Accumulated oxalate in IBD contributes to pathogenesis, and SLC26A2 is known to regulate intestinal oxalate and anion secretion.[84,85] Modulating metabolites via this mechanism might enable immune modulation.

Hyaluronan synthase (HAS) 3 exhibited significant transcriptional amplification in anti-TNF non-responders with CD and UC patients treated with CKD-506 at concentrations of 1 μM and 3 μM. In particular, the CKD-506 3 μM treatment showed

notably enhanced transcription of HAS3 in anti-TNF non-responders from both CD patients and UC patients. HAS3 expression is predominantly localized to the nucleus and Golgi complex within cellular structures. Among various organs, the gastrointestinal tract, encompassing the colon, stomach, and esophagus, demonstrated heightened expression of HAS3. Hyaluronan (HA) has emerged as a novel regulator in the context of IBD. HA secretion from microvascular endothelial cells, smooth muscle cells, and epithelial cells reinforced the epithelial barrier by contributing to extracellular matrix formation. On the other hand, HA also exhibited a pro-inflammatory role by promoting excessive angiogenesis and fibrosis.[86] Notably, in a mouse colitis model induced by dextran sulfate sodium (DSS), increased endothelial HAS3 activity exacerbated colitis symptoms.[87] In a similar context, intestinal inflammation showed improvement in mice lacking the HAS3 gene.[88] In the 2,4-dinitrobenzene sulfonic acid (DNBS) induced mouse colitis model, accumulation of hyaluronan at the myenteric plexus was observed.[86] Intriguingly, HAS3 transcription escalated in both CD and UC anti-TNF non-responder groups, contrasting with the previous findings from the mouse colitis model. This apparent discrepancy can be attributed to the dual role of HA in mucosal barrier maintenance and intestinal inflammation. The opposite trends may be explained by the reinforcing effect of HA on the epithelial barrier and its potential to modulate the immune response through increased expression. In the following qRT-PCR analysis, CKD-506 elevated HAS3 transcriptional levels in the both human and mouse models despite the basal reduction of HAS3 in TNF-α or IFN-γ treatment.

The YOD1 deubiquitinase transcription was elevated in CD patients who did not respond to anti-TNF treatment. This increment was observed in cases where CKD-506 was administered at both 1 μM and 3 μM concentrations. Furthermore, a similar increase was noted in patients with UC who were non-responsive to anti-TNF treatment and received CKD-506 at a concentration of 3 μM. YOD1 is primarily distributed within the cytosol and nucleus, with its expression detected in the small intestine and colon. In laboratory-cultured human oral keratinocytes, the overexpression of YOD1 led to

improved cell migration and heightened expression of TGF-β3.[89] M2 macrophage-derived extracellular vesicles from a mouse model of hepatocellular carcinoma, inhibition of miR-21-5P and the overexpression of YOD1 suppressed the YAP/β-catenin pathway and induced exhaustion of CD8+ T cells.[90] Within both CD and UC patients who were unresponsive to anti-TNF treatment, the CKD-506 treatment led to an augmentation in YOD1 transcription levels. Previous studies implied that YOD1 may be involved in cell proliferation and migration, suggesting its potential significance in colitis. Though there were no definite alterations between the vehicle and CKD-506 treated group in both human in-vitro and mouse ex-vivo model, the YOD1 transcriptional level presented incremental tendency as CKD-506 reached a higher concentration.

Interleukin 1 receptor type 2 (IL1R2) exhibited high transcription levels in the CD anti-TNF non-responder group treated with CKD-506 at 1 μM, particularly pronounced in both CD and UC anti-TNF non-responders treated with CKD-506 at 3 μM. IL1R2 was detected in both the nucleus and cytoplasm. Among the organs, the colon presented elevated expression levels compared to the stomach and esophagus. IL1R type 2 functions as a decoy receptor that exerts inhibitory effects on interleukin-1 alpha (IL1A), interleukin-1 beta (IL1B), and interleukin-1 receptor type 1 (IL1R1) by binding to these ligands. IL1, including TNF-α, is among the most prominent pro-inflammatory cytokines. It plays a pivotal role in the inflammation and tissue damage associated with IBD. Interestingly, IL1R2 was identified as one of the susceptible loci through an IBD GWAS.[91] Following CKD-506 treatment, IL1R2 levels increased in both CD and UC anti-TNF non-responders. Elevated IL1R2 expression may mitigate inflammation in the disease's pathogenesis by inhibiting pro-inflammatory cytokines like IL1 or TNF-α. Though there was no significant change in a mouse model, the human colon cell line displayed a meaningful elevation of IL1R2 transcriptional level in the CKD-506 treated group even in inflammatory surroundings.

Mesoderm induction early response 1 family member 3 (MIER3) displayed an

elevated level of transcription in both CD and UC anti-TNF non-responders following treatment with CKD-506 at 3 μM, and only in the CD group after CKD-506 treatment at 1 μM. In the context of colorectal cancer cell lines, MIER3 exhibited the ability to suppress epithelial-mesenchymal transition (EMT) by downregulating Sp1, leading to a noticeable reduction in the proliferation, migration, and invasion of colorectal cancer cells.[92] In non-small cell lung cancer (NSCLC), MIER3 was found to inhibit the recruitment of HDAC1/2 and the Wnt/β-catenin pathway, thereby contributing to the mitigation of disease progression.[93] However, in breast cancer, MIER3 seemed to exert the opposite effect, accelerating cell proliferation, migration, and invasion through the recruitment of the HDAC1/2 and SNAIL complex.[94] For both CD and UC anti-TNF non-responders, CKD-506 treatment resulted in an upregulation of MIER3 transcription. Drawing from the findings of a previous study, it can be inferred that MIER3 may play a role in regulating HDAC activity, which in turn impacts cell proliferation, migration, invasion, and EMT. Contrary to previous findings, MIER3 was decreased in the human colon cell line and there was no meaningful change in the mouse colon tissue model when CKD-506 was treated. There may exist more complicated interactions between different types of cells in real human colon niches regulating the MIER3 level.

CD177 demonstrated an elevated level of transcription in CD anti-TNF non-responders following treatment with CKD-506 at both 1 μM and 3 μM. CD177 is predominantly localized in the extracellular space and is expressed in the stomach, esophagus, and colon. CD177 is a glycosyl-phosphatidylinositol (GPI)-linked cell surface glycoprotein that plays a significant role in neutrophil activation. Moreover, CD177 contributes to neutrophil transmission through its interaction with endothelial cell adhesion molecule-1 (ECAM-1).[95] Notably, mutations or overexpression of CD177 have been documented in certain hematologic disorders. CD177-positive neutrophils have demonstrated a protective effect in mouse colitis models, and our research team has unveiled that the triggering receptor expressed on myeloid cells-1 (TREM1) agonist contributes to colitis relief through the regulation of CD177-positive neutrophils.[96]

Numerous studies have underscored the pivotal role of neutrophil activity in the regulation of IBD. In CD anti-TNF non-responders, CD177 transcription was significantly increased. CD177-positive neutrophils are already recognized as a pivotal factor in relieving IBD. It is plausible that CKD-506 may also exert control over neutrophil activation, thereby influencing intestinal inflammation. In accordance with previous studies, CD177 was significantly increased when CKD-506 was treated in both human and mouse models. The CD177 protein was expressed by epithelial cells from the colon, breast, and prostate in the previous study, though functional studies were focused on mainly neutrophils.[97] It is interesting that even a single colon epithelial cell line showed transcriptional activation of CD177.

To indirectly assess the cell population of acquired human colon biopsy samples, xCell deconvolution was performed. Since the biopsy samples were obtained at the same lesion, it seems trivial that there were no significant differences between the vehicle or CKD-506 treated specimen. Predicting the overall cell population is still meaningful for the estimation of related signaling pathways. Smooth muscle cell was one of the major components. It is well known that macrophage M1/M2 disequilibrium is observed in IBD patients.[98] M1 macrophages and proinflammatory cytokines aggravate IBD, whereas M2 macrophages facilitate wound repair and inflammation alleviation. The Th1/Th2 imbalance is also a well-understood pathogenesis of IBD. The CD is Th1 dominant and UC is known to be Th2 dominant.[99] In this study, M1 macrophage was abundant compared to M2 macrophage, and Th1 T cell was prominent than Th2 T cell.

To identify common trends of selected DEGs, network-based and general GO analyses were performed. Intestinal barrier and cell adhesion were some of the popular pathways that appeared to be correlated with DEGs in this analysis. In the pathophysiology of IBD, epithelial barrier function as well as cell adhesion and interaction are well described.[100] Both CD and UC exhibit similar characteristics, including an epithelial break, a decrease in the integrity of tight junctions, and the atrophy of glands.[101] In individuals with active CD, there is an elevated level of intestinal

permeability. The impairment of the barrier function is probably a result of epithelial harm, such as apoptosis, erosion, and ulceration, which are distinct traits of gut inflammation. Inflammatory cytokines linked to gut inflammation modify the permeability of the epithelial layer by influencing the junctional complexes.[102] The intestinal epithelium should be viewed as more than just a basic physical barrier. Instead, it is a remarkably active tissue that reacts to a variety of cues, including the gut microbiota and the immune system. This epithelial reaction to these signals controls functions like barrier integrity, the composition of the microbiota, and mucosal immune homeostasis in the lamina propria.[103] This dynamic feature of the epithelial barrier is one of the major components contributing to the pathogenesis of IBD and CKD-506 seemed to affect epithelial homeostasis.

Recovery from hypoxia and the HIF-1 signaling pathway were also listed in GO analysis results. Hypoxia has a crucial role in inflammatory diseases such as IBD. The group of HIFs functions as transcription factors that facilitate the cellular and tissue response to hypoxia.[104] HIFs manage a transcriptional program encompassing an extensive range of physiological processes, including angiogenesis, erythropoiesis, cell metabolism, autophagy, and apoptosis. Consequently, HIFs guarantee optimal functional, metabolic, and vascular adjustment to reduced oxygen levels.[105] The HIF-1 signaling has significant impacts on preserving gut barriers and regulating immune responses.[106] It is feasible that extracted DEGs from the CKD-506 treatment group present an association with HIF-1 signaling or O_2-related pathways.

The ER (endoplasmic reticulum) stress and protein transportation or folding was one of the repeatedly mentioned GO terms. In eukaryotic organisms, disruption of endoplasmic reticulum homeostasis can result in the accumulation of unfolded and misfolded proteins within the ER lumen, a state termed ER stress. This cellular mechanism triggers the unfolded protein response, which serves to boost the ER protein folding capacity, alleviates the burden of protein synthesis and refinement, and initiates ER-related protein breakdown. Paneth and goblet cells, two types of secretory epithelial

cells in the intestinal tract, demonstrate heightened sensitivity to ER stress. Recent research indicated that epithelial ER stress might contribute to the development of CD and UC. This could occur through compromised protein secretion, prompting apoptosis in epithelial cells, and activating inflammatory reactions within the gastrointestinal system.[107] ER stress is also known to be involved in the intestinal barrier function of IBD and CKD-506 may play a pivotal role in the regulation of ER stress as well.[108]

G protein-coupled receptors (GPCR) are essential signaling components in immune reactions, cellular growth, control of inflammation, and epithelial barrier maintenance. Progress in comprehending the configurations and functions of GPCRs has fueled investigations into roles in disease development, resulting in the development of GPCR-targeted medication. Currently, several GPCRs have been shown to be associated with IBD, providing significant advances in the drug discovery process of IBD.[109] GPCRs are recognized as critical regulators of the intestinal mucosal immune system and CKD-506 also seemed to be involved in this mechanism.[110]

The PI3K-AKT and mammalian target of rapamycin (mTOR) pathway is a crucial internal signaling process that holds significant physiological functions in cell-programmed cell apoptosis, protein metabolism, chemokine production, and angiogenesis. This pathway has been found to participate in the control of forkhead box P3 (Foxp3) expression, which subsequently affects the development of regulatory T-cells (Tregs).[111,112] The PI3K-AKT pathway was activated in mice colitis models, and further studies approved that also elevated CD and UC.[113] Though there is a controversy on the relationship between IBD pathogenesis and PI3K-AKT, inhibitors of this pathway relieved inflammation. The CKD-506 may contribute to the alleviation of intestinal inflammation via up or down streams of the PI3K-AKT signaling pathway. In the following qRT-PCR analysis, the PI3K-AKT-mTOR axis was depressed in CKD-506 treatment samples compared to vehicle treated group in a dose-dependent manner for both human and mouse experimental models.

The interaction between JAKs and STATs, orchestrating cellular responses, holds

pivotal roles in both intestinal homeostasis and inflammation. Compounds disrupting these interactions, particularly those aimed at JAK1 and JAK3, have shown promising effectiveness and safety profiles in treating IBD, even in patients unresponsive to TNF antagonist treatment. In contrast to monoclonal antibody therapies, JAK inhibitors can be taken orally, possess predictable pharmacokinetics, and do not evoke immune responses. While inhibiting STATs could offer another approach to combat inflammation, clinical trials for IBD treatment in this regard have not been initiated thus far.[114] The JAK-STAT pathway is not only recognized as a key mechanism of pathogenesis but also an innovative approach for novel therapy. The CKD-506 showed statistically significant enrichment with JAK-STAT and shared a crucial mechanism with tofacitinib. In the human and mouse models, the higher CKD-506 concentration treated group presented lower JAK2 and STAT3 transcriptional levels.

Glycosphingolipid is a prominent subgroup of cellular glycoconjugates and is found throughout cell membrane lipid microdomains contributing to protein interactions and signaling processes.[115] Previous studies have shown that glucosylceramide content in the intestinal mucosa is related to the pathogenesis of colitis and glucosylceramide alleviated intestinal inflammation in mice colitis models.[116,117] On the other hand, sphingolipid lactosylceramide is indicated as a biomarker of IBD in children.[118] The level of lactosylceramide was elevated in inflamed mucus, and glucosylceramide form was more abundant in the healthy control. Therefore, glycosylation of lactosylceramide might present anti-inflammatory effects on IBD and positively correlated with DEGs extracted from CKD-506 treated gene sets.

Neurologic pathways were also frequently associated with the GO term. A significant amount of evidence indicates that α-tubulin acetylation could play a major role in neurodegenerative disorders like Huntington's and Parkinson's diseases. Additionally, there was HDAC6 accumulation in Lewy bodies within the nerve cells of patients with Parkinson's disease.[119] Importantly, the targeted blocking of HDAC6 has been shown to improve nerve cell damage caused by oxidative stress-related neurodegeneration and

inadequate axonal regrowth.[120] Recently therapeutic potentials of various HDAC6 inhibitors are currently under research on neurodegenerative diseases.[121] However, it is unclear whether α-tubulin acetylation and neurologic synapse-related gene set contribute to intestinal inflammation.

HDAC inhibition by gut microbe-generated short-chain fatty acids entrains circadian entrainment.[122] In this point of view, circadian entrains enrichment results are also explainable. HDAC6 appears to be involved in microbial or viral infections.[123] It is feasible that CKD-506 contributes to the pathway related to CMV, HSV, shigellosis, or E. coli infection. The network-based and conventional GO analysis suggested possible pathways related to DEGs extracted from anti-TNF non-responders in this study. Previous studies and clinical practices supported that listed GO terms are reliable mechanisms that could be induced by HDAC6 inhibitor, CKD-506.

Instead of anti-TNF non-responders only, all the patients were included in GSEA, and the enrichment score was calculated by providing a vector of correlation. The CKD-506 treatment was negatively correlated with IL6-JAK-STAT3 signaling, PI3K-ATK-mTOR signaling, and apoptosis compared to the vehicle. These trends were consistent with GO analysis data. Interestingly, MYC, TGF- β signaling, and ROS were also found to be negatively correlated with the CKD-506 treatment group compared to the vehicle. MYC is a well-known proto-oncogene and expression was increased in biopsies of both UC and CD.[124] MYC amplifications have been reported in IBD-associated carcinoma and contributed to IBD pathogenesis via altered cell cycle control.[125] In the human and mouse model, C-MYC was depressed in the CKD-506 treatment group compared to the vehicle treated group as expected. The TGF-β plays a key role in numerous cellular activities, encompassing the regulation of cell growth, differentiation, embryonic development, wound healing, angiogenesis, and immune modulation. Within the digestive system, TGF-β exhibits the ability to either stimulate or restrain inflammation and the development of cancer.[126] Dysfunctional TGF-β signaling has been associated with the emergence of intestinal inflammation in both experimental models and

individuals with IBD. Substances that restore TGF-β signaling are being examined as potential therapeutic candidates for treating IBD.[127] Though transcription or expression levels in UC and CD are ambiguous, it is still meaningful that CKD-506 also participates in this pathway.

It is widely recognized that reactive oxygen molecules are generated in various pathological conditions, disrupting multiple cellular processes, and eventually causing cellular damage. Following intestinal ischemia, ROS are produced upon reperfusion of the ischemic tissue. This leads to increased permeability of the endothelium and mucosa, enabling inflammatory leukocytes to infiltrate the ischemic region. Additionally, ROS indirectly contributes to leukocyte activation. Consequently, these inflammatory cells respond by generating oxygen radicals, which significantly contribute to tissue damage. Hence, intestinal ischemia and reperfusion trigger an inflammatory reaction. Furthermore, in chronic intestinal inflammatory diseases, reactive oxygen molecules are believed to have a crucial role in the disease progression. Consequently, eliminating these reactive species would be advantageous in managing these disorders.[128] Reduction ROS alleviates intestinal inflammation and CKD-506 was negatively correlated with ROS gene sets.

Through a volcano plot, a Venn diagram literature study of single genes was done and candidate genes of CKD-506 were selected one by one. Network-based and general GO analysis provided guidance on where to focus among signaling pathways and biological processes based on selected DEGs. In addition to DEGs, all the gene lists were included in GSEA. The dataset applied in GO analysis and GSEA were identical, however, GSEA exhibited enrichment scores according to ranked genes without exceptions.

V. CONCLUSION

In this study, increased HDAC6 expression and its activity were analyzed in human colon biopsy samples for the first time. The ex-vivo culture system for mouse and human colon biopsy samples was successfully established with minimized artifacts. The application of this system to a chemical-induced mouse colitis model, the anti-inflammatory and epithelial barrier strengthening potential of CKD-506 was confirmed through qRT-PCR and CBA analysis. Through the RNA-seq of human colon biopsy specimens of current treatment-refractory patients, a rough cell population was estimated and possible therapeutic targets of CKD-506 were elucidated. Network-based investigation and diverse approaches to enrichment analysis revealed relevant pathways and signals of CKD-506 and validated through qRT-PCR of in-vitro and ex-vivo samples

It is meaningful that this is the first research uncovering the effects of HDAC6 selective inhibitor, CKD-506 on human-derived colon specimens. A stabilized ex-vivo culture format can be utilized for different drugs or various types of other organs. The limited number of patients and heterogenous individual characteristics of IBD patients constrained the interpretation or deduction of intended target genes. However, still, even the bulk RNA-seq was beneficial for screening potential candidate genes or a comprehensive understanding of related upstream or downstream pathways.

The results of RNA-seq data suggested that novel HDAC inhibitors modulating epigenetic, transcriptional, and post-translational levels could alleviate human intestinal inflammation through various mechanisms. Still, there are a lot more steps to forge ahead, these kinds of efforts will provide brand-new therapeutic options for patients resistant to recent regimens with high disease activity.

REFERENCES

1. Xavier RJ, Podolsky DK. Unravelling the pathogenesis of inflammatory bowel disease. Nature 2007;448:427-34.
2. Mizoguchi E, Low D, Ezaki Y, Okada T. Recent updates on the basic mechanisms and pathogenesis of inflammatory bowel diseases in experimental animal models. Intest Res 2020;18:151-67.
3. Kaplan GG, Windsor JW. The four epidemiological stages in the global evolution of inflammatory bowel disease. Nat Rev Gastroenterol Hepatol 2021;18:56-66.
4. D'Haens GR, Sartor RB, Silverberg MS, Petersson J, Rutgeerts P. Future directions in inflammatory bowel disease management. J Crohns Colitis 2014;8:726-34.
5. Nakase H, Uchino M, Shinzaki S, Matsuura M, Matsuoka K, Kobayashi T, et al. Evidence-based clinical practice guidelines for inflammatory bowel disease 2020. J Gastroenterol 2021;56:489-526.
6. Levin AD, Wildenberg ME, van den Brink GR. Mechanism of Action of Anti-TNF Therapy in Inflammatory Bowel Disease. J Crohns Colitis 2016;10:989-97.
7. Cui G, Fan Q, Li Z, Goll R, Florholmen J. Evaluation of anti-TNF therapeutic response in patients with inflammatory bowel disease: Current and novel biomarkers. EBioMedicine 2021;66:103329.
8. Gisbert JP, Chaparro M. Primary Failure to an Anti-TNF Agent in Inflammatory Bowel Disease: Switch (to a Second Anti-TNF Agent) or Swap (for Another Mechanism of Action)? J Clin Med 2021;10.
9. Baumgart DC, Le Berre C. Newer Biologic and Small-Molecule Therapies for Inflammatory Bowel Disease. N Engl J Med 2021;385:1302-15.
10. 2020 Inflammatory bowel disease fact sheet in Korea. Korean Association for the Study of Intestinal Diseases; 2022.
11. Cheng C, Shan W, Huang W, Ding Z, Cui G, Liu F, et al. ACY-1215 exhibits anti-inflammatory and chondroprotective effects in human osteoarthritis chondrocytes

via inhibition of STAT3 and NF-kappaB signaling pathways. Biomed Pharmacother 2019;109:2464-71.

12. Choi EW, Song JW, Ha N, Choi YI, Kim S. CKD-506, a novel HDAC6-selective inhibitor, improves renal outcomes and survival in a mouse model of systemic lupus erythematosus. Sci Rep 2018;8:17297.
13. Bae D, Lee JY, Ha N, Park J, Baek J, Suh D, et al. CKD-506: A novel HDAC6-selective inhibitor that exerts therapeutic effects in a rodent model of multiple sclerosis. Sci Rep 2021;11:14466.
14. Ran J, Zhou J. Targeted inhibition of histone deacetylase 6 in inflammatory diseases. Thorac Cancer 2019;10:405-12.
15. Pulya S, Amin SA, Adhikari N, Biswas S, Jha T, Ghosh B. HDAC6 as privileged target in drug discovery: A perspective. Pharmacological Research 2021;163.
16. Do A, Reid RC, Lohman RJ, Sweet MJ, Fairlie DP, Iyer A. An HDAC6 Inhibitor Confers Protection and Selectively Inhibits B-Cell Infiltration in DSS-Induced Colitis in Mice. Journal of Pharmacology and Experimental Therapeutics 2017;360:140-51.
17. Park JK, Jang YJ, Oh BR, Shin J, Bae D, Ha N, et al. Therapeutic potential of CKD-506, a novel selective histone deacetylase 6 inhibitor, in a murine model of rheumatoid arthritis. Arthritis Research & Therapy 2020;22.
18. M TT, Shen S. Recent innovative advances in the discovery of selective HDAC6 inhibitors. Future Med Chem 2021;13:1017-9.
19. Lee JW, Lee SM, Chun J, Im JP, Seo SK, Ha N, et al. Novel Histone Deacetylase 6 Inhibitor CKD-506 Inhibits NF-kappa B Signaling in Intestinal Epithelial Cells and Macrophages and Ameliorates Acute and Chronic Murine Colitis. Inflammatory Bowel Diseases 2020;26:852-62.
20. Pan FG, Han L, Zhang Y, Yu YD, Liu JB. Optimization of Caco-2 and HT29 co-culture in vitro cell models for permeability studies. International Journal of Food Sciences and Nutrition 2015;66:680-5.

21. Roeselers G, Ponomarenko M, Lukovac S, Wortelboer HM. Ex vivo systems to study host-microbiota interactions in the gastrointestinal tract. Best Practice & Research Clinical Gastroenterology 2013;27:101-13.
22. Autrup H, Barrett LA, Jackson FE, Jesudason ML, Stoner G, Phelps P, et al. Explant culture of human colon. Gastroenterology 1978;74:1248-57.
23. Kelly CJ, Colgan SP. Breathless in the Gut: Implications of Luminal O2 for Microbial Pathogenicity. Cell Host Microbe 2016;19:427-8.
24. Jepson MA, Clark MA. The role of M cells in Salmonella infection. Microbes and Infection 2001;3:1183-90.
25. Schwerdtfeger LA, Nealon NJ, Ryan EP, Tobet SA. Human colon function ex vivo: Dependence on oxygen and sensitivity to antibiotic. PLoS One 2019;14:e0217170.
26. Moldoveanu AC, Diculescu M, Braticevici CF. Cytokines in inflammatory bowel disease. Rom J Intern Med 2015;53:118-27.
27. Gajendran M, Loganathan P, Jimenez G, Catinella AP, Ng N, Umapathy C, et al. A comprehensive review and update on ulcerative colitis. Dm Disease-a-Month 2019;65.
28. Torres J, Mehandru S, Colombel JF, Peyrin-Biroulet L. Crohn's disease. Lancet 2017;389:1741-55.
29. Crohn’s Disease: Developing Drugs for Treatment. 2022.
30. Ulcerative Colitis: Developing Drugs for Treatment. 2022.
31. Schroeder KW, Tremaine WJ, Ilstrup DM. Coated Oral 5-Aminosalicylic Acid Therapy for Mildly to Moderately Active Ulcerative-Colitis - a Randomized Study. New England Journal of Medicine 1987;317:1625-9.
32. Rutgeerts P, Sandborn WJ, Feagan BG, Reinisch W, Olson A, Johanns J, et al. Infliximab for induction and maintenance therapy for ulcerative colitis. N Engl J Med 2005;353:2462-76.
33. Best WR, Becktel JM, Singleton JW, Kern F, Jr. Development of a Crohn's disease activity index. National Cooperative Crohn's Disease Study. Gastroenterology

1976;70:439-44.

34. Daperno M, D'Haens G, Van Assche G, Baert F, Bulois P, Maunoury V, et al. Development and validation of a new, simplified endoscopic activity score for Crohn's disease: the SES-CD. Gastrointest Endosc 2004;60:505-12.

35. Hanauer SB, Feagan BG, Lichtenstein GR, Mayer LF, Schreiber S, Colombel JF, et al. Maintenance infliximab for Crohn's disease: the ACCENT I randomised trial. Lancet 2002;359:1541-9.

36. Erben U, Loddenkemper C, Doerfel K, Spieckermann S, Haller D, Heimesaat MM, et al. A guide to histomorphological evaluation of intestinal inflammation in mouse models. International Journal of Clinical and Experimental Pathology 2014;7:4557-U27.

37. Jauregui-Amezaga A, Geerits A, Das Y, Lemmens B, Sagaert X, Bessissow T, et al. A Simplified Geboes Score for Ulcerative Colitis. Journal of Crohns & Colitis 2017;11:305-13.

38. Almradi A, Ma C, D'Haens GR, Sandborn WJ, Parker CE, Guizzetti L, et al. An expert consensus to standardise the assessment of histological disease activity in Crohn's disease clinical trials. Aliment Pharmacol Ther 2021;53:784-93.

39. Bolger AM, Lohse M, Usadel B. Trimmomatic: a flexible trimmer for Illumina sequence data. Bioinformatics 2014;30:2114-20.

40. Kim D, Landmead B, Salzberg SL. HISAT: a fast spliced aligner with low memory requirements. Nature Methods 2015;12:357-U121.

41. Li H, Handsaker B, Wysoker A, Fennell T, Ruan J, Homer N, et al. The Sequence Alignment/Map format and SAMtools. Bioinformatics 2009;25:2078-9.

42. Pertea M, Pertea GM, Antonescu CM, Chang TC, Mendell JT, Salzberg SL. StringTie enables improved reconstruction of a transcriptome from RNA-seq reads. Nature Biotechnology 2015;33:290-+.

43. Pertea M, Kim D, Pertea GM, Leek JT, Salzberg SL. Transcript-level expression analysis of RNA-seq experiments with HISAT, StringTie and Ballgown. Nature

Protocols 2016;11:1650-67.

44. Goedhart J, Luijsterburg MS. VolcaNoseR is a web app for creating, exploring, labeling and sharing volcano plots. Scientific Reports 2020;10.

45. Oliveros JC. VENNY. An interactive tool for comparing lists with Venn Diagrams. http://bioinfogp. cnb. csic. es/tools/venny/index. html 2007.

46. Aran D, Hu ZC, Butte AJ. xCell: digitally portraying the tissue cellular heterogeneity landscape. Genome Biology 2017;18.

47. Szklarczyk D, Gable AL, Lyon D, Junge A, Wyder S, Huerta-Cepas J, et al. STRING v11: protein-protein association networks with increased coverage, supporting functional discovery in genome-wide experimental datasets. Nucleic Acids Research 2019;47:D607-D13.

48. Ashburner M, Ball CA, Blake JA, Botstein D, Butler H, Cherry JM, et al. Gene Ontology: tool for the unification of biology. Nature Genetics 2000;25:25-9.

49. Baryshnikova A. Spatial Analysis of Functional Enrichment (SAFE) in Large Biological Networks. Methods Mol Biol 2018;1819:249-68.

50. Shannon P, Markiel A, Ozier O, Baliga NS, Wang JT, Ramage D, et al. Cytoscape: A software environment for integrated models of biomolecular interaction networks. Genome Research 2003;13:2498-504.

51. Yu GC, Wang LG, Han YY, He QY. clusterProfiler: an R Package for Comparing Biological Themes Among Gene Clusters. Omics-a Journal of Integrative Biology 2012;16:284-7.

52. Yu G. Enrichplot: visualization of functional enrichment result. R package version 2021;1.

53. Li MC, He SH. IL-10 and its related cytokines for treatment of inflammatory bowel disease. World Journal of Gastroenterology 2004;10:620-5.

54. Zhu L, Shi T, Zhong C, Wang Y, Chang M, Liu X. IL-10 and IL-10 Receptor Mutations in Very Early Onset Inflammatory Bowel Disease. Gastroenterology Res 2017;10:65-9.

55. Johansson MEV. Mucus Layers in Inflammatory Bowel Disease. Inflammatory Bowel Diseases 2014;20:2124-31.
56. Kang Y, Park H, Choe BH, Kang B. The Role and Function of Mucins and Its Relationship to Inflammatory Bowel Disease. Frontiers in Medicine 2022;9.
57. Vulliemoz M, Brand S, Juillerat P, Mottet C, Ben-Horin S, Michetti P, et al. TNF-Alpha Blockers in Inflammatory Bowel Diseases: Practical Recommendations and a User's Guide: An Update. Digestion 2020;101:16-26.
58. D'Haens GR, van Deventer S. 25 years of anti-TNF treatment for inflammatory bowel disease: lessons from the past and a look to the future. Gut 2021;70:1396-405.
59. Andoh A, Nishida A. Pro- and anti-inflammatory roles of interleukin (IL)-33, IL-36, and IL-38 in inflammatory bowel disease. Journal of Gastroenterology 2023;58:69-78.
60. Aggeletopoulou I, Tsounis EP, Triantos C. Molecular Mechanisms Underlying IL-33-Mediated Inflammation in Inflammatory Bowel Disease. International Journal of Molecular Sciences 2023;24.
61. Beltran CJ, Nunez LE, Diaz-Jimenez D, Farfan N, Candia E, Heine C, et al. Characterization of the Novel ST2/IL-33 System in Patients with Inflammatory Bowel Disease. Inflammatory Bowel Diseases 2010;16:1097-107.
62. McCabe RP, Secrist H, Botney M, Egan M, Peters MG. Cytokine mRNA expression in intestine from normal and inflammatory bowel disease patients. Clin Immunol Immunopathol 1993;66:52-8.
63. Coccia M, Harrison OJ, Schiering C, Asquith MJ, Becher B, Powrie F, et al. IL-1beta mediates chronic intestinal inflammation by promoting the accumulation of IL-17A secreting innate lymphoid cells and CD4(+) Th17 cells. J Exp Med 2012;209:1595-609.
64. Friedrich M, Pohin M, Powrie F. Cytokine Networks in the Pathophysiology of Inflammatory Bowel Disease. Immunity 2019;50:992-1006.

65. Camilli C, Hoeh AE, De Rossi G, Moss SE, Greenwood J. LRG1: an emerging player in disease pathogenesis. Journal of Biomedical Science 2022;29.
66. Naka T, Fujimoto M. LRG is a novel inflammatory marker clinically useful for the evaluation of disease activity in rheumatoid arthritis and inflammatory bowel disease. Immunological Medicine 2018;41:62-7.
67. Brynskov J, Tvede N, Andersen CB, Vilien M. Increased concentrations of interleukin 1 beta, interleukin-2, and soluble interleukin-2 receptors in endoscopical mucosal biopsy specimens with active inflammatory bowel disease. Gut 1992;33:55-8.
68. Mullin GE, Lazenby AJ, Harris ML, Bayless TM, James SP. Increased interleukin-2 messenger RNA in the intestinal mucosal lesions of Crohn's disease but not ulcerative colitis. Gastroenterology 1992;102:1620-7.
69. Katz LH, Kopylov U, Fudim E, Yavzori M, Picard O, Ungar B, et al. Expression of IL-2, IL-17 and TNF-alpha in patients with Crohn's disease treated with anti-TNF antibodies. Clin Res Hepatol Gastroenterol 2014;38:491-8.
70. Ruckert Y, Schindler U, Heinig T, Nikolaus S, Raedler A, Schreiber S. IL-4 signaling mechanisms in inflammatory bowel disease mononuclear phagocytes. Inflammatory Bowel Diseases 1996;2:244-52.
71. West GA, Matsuura T, Levine AD, Klein JS, Fiocchi C. Interleukin 4 in inflammatory bowel disease and mucosal immune reactivity. Gastroenterology 1996;110:1683-95.
72. Mullin GE, Maycon ZR, BraunElwert L, Cerchia R, James SP, Katz S, et al. Inflammatory bowel disease mucosal biopsies have specialized lymphokine mRNA profiles. Inflammatory Bowel Diseases 1996;2:16-26.
73. Atreya R, Mudter J, Finotto S, Mullberg J, Jostock T, Wirtz S, et al. Blockade of interleukin 6 trans signaling suppresses T-cell resistance against apoptosis in chronic intestinal inflammation: Evidence in Crohn disease and experimental colitis in vivo (vol 6, pg 583, 2000). Nature Medicine 2010;16:1341-.

74. Neurath MF. Cytokines in inflammatory bowel disease. Nature Reviews Immunology 2014;14:329-42.
75. Ito H, Takazoe M, Fukuda Y, Hibi T, Kusugami K, Andoh A, et al. A pilot randomized trial of a human anti-interleukin-6 receptor monoclonal antibody in active Crohn's disease. Gastroenterology 2004;126:989-96.
76. Ito R, Shin-Ya M, Kishida T, Urano A, Takada R, Sakagami J, et al. Interferon-gamma is causatively involved in experimental inflammatory bowel disease in mice. Clinical and Experimental Immunology 2006;146:330-8.
77. Strober W, Fuss IJ. Proinflammatory Cytokines in the Pathogenesis of Inflammatory Bowel Diseases. Gastroenterology 2011;140:1756-U82.
78. Rovedatti L, Kudo T, Biancheri P, Rampton DS, Sengupta N, Knowles CH, et al. Differential Regulation of Interleukin-17 and Interferon-gamma Production in Inflammatory Bowel Disease. Gastroenterology 2009;136:A258-A.
79. Fujino S, Andoh A, Bamba S, Ogawa A, Hata K, Araki Y, et al. Increased expression of interleukin 17 in inflammatory bowel disease. Gut 2003;52:65-70.
80. Catana CS, Neagoe IB, Cozma V, Magdas C, Tabaran F, Dumitrascu DL. Contribution of the IL-17/IL-23 axis to the pathogenesis of inflammatory bowel disease. World Journal of Gastroenterology 2015;21:5823-30.
81. Von Stein P, Lofberg R, Kuznetsov NV, Gielen AW, Persson JO, Sundberg R, et al. Multigene analysis can discriminate between ulcerative colitis, Crohn's disease, and irritable bowel syndrome. Gastroenterology 2008;134:1869-81.
82. Wu F, Dassopoulos T, Cope L, Maitra A, Brant SR, Harris ML, et al. Genome-wide gene expression differences in Crohn's disease and ulcerative colitis from endoscopic pinch biopsies: insights into distinctive pathogenesis. Inflamm Bowel Dis 2007;13:807-21.
83. Noble CL, Abbas AR, Lees CW, Cornelius J, Toy K, Modrusan Z, et al. Characterization of Intestinal Gene Expression Profiles in Crohn's Disease by Genome-wide Microarray Analysis. Inflammatory Bowel Diseases 2010;16:1717-

28.

84. Wang J, Wang W, Wang H, Tuo B. Physiological and Pathological Functions of SLC26A6. Front Med (Lausanne) 2020;7:618256.

85. Liu M, Devlin JC, Hu J, Volkova A, Battaglia TW, Ho M, et al. Microbial genetic and transcriptional contributions to oxalate degradation by the gut microbiota in health and disease. Elife 2021;10.

86. Filpa V, Bistoletti M, Caon I, Moro E, Grimaldi A, Moretto P, et al. Changes in hyaluronan deposition in the rat myenteric plexus after experimentally-induced colitis. Scientific Reports 2017;7.

87. Hundhausen C, Schneckmann R, Ostendorf Y, Rimpler J, von Glinski A, Kohlmorgen C, et al. Endothelial hyaluronan synthase 3 aggravates acute colitis in an experimental model of inflammatory bowel disease. Matrix Biology 2021;102:20-36.

88. Kessler SP, Obery DR, de la Motte C. Hyaluronan Synthase 3 Null Mice Exhibit Decreased Intestinal Inflammation and Tissue Damage in the DSS-Induced Colitis Model. Int J Cell Biol 2015;2015:745237.

89. Ju Q, Li MX, Chen G, Wang HX, Shi QM, Ge X, et al. Overexpression of YOD1 Promotes the Migration of Human Oral Keratinocytes by Enhancing TGF-beta3 Signaling. Biomed Environ Sci 2018;31:499-506.

90. Pu J, Xu ZM, Nian JH, Fang Q, Yang M, Huang YG, et al. M2 macrophage-derived extracellular vesicles facilitate CD8+T cell exhaustion in hepatocellular carcinoma via the miR-21-5p/YOD1/YAP/beta-catenin pathway. Cell Death Discovery 2021;7.

91. Lees CW, Barrett JC, Parkes M, Satsangi J. New IBD genetics: common pathways with other diseases. Gut 2011;60:1739-53.

92. Peng M, Hu YK, Song W, Duan SY, Xu Q, Ding YQ, et al. MIER3 suppresses colorectal cancer progression by down-regulating Sp1, inhibiting epithelial-mesenchymal transition. Scientific Reports 2017;7.

93. Zhang H, Wang L, Bai J, Jiao W, Wang M. Erratum to MIER3 suppresses the progression of non-small cell lung cancer by inhibiting Wnt/beta-Catenin pathway and histone acetyltransferase activity. Transl Cancer Res 2020;9:7379-80.

94. Huang WQ, Chen JX, Liu XH, Liu XM, Duan SY, Chen LX, et al. MIER3 induces epithelial-mesenchymal transition and promotes breast cancer cell aggressiveness via forming a co-repressor complex with HDAC1/HDAC2/Snail. Experimental Cell Research 2021;406.

95. Sachs UJH, Andrei-Selmer CL, Maniar A, Weiss T, Paddock C, Orlova VV, et al. The neutrophil-specific antigen CD177 is a counter-receptor for platelet endothelial cell adhesion molecule-1 (CD31). Journal of Biological Chemistry 2007;282:23603-12.

96. Seo DH, Che X, Kim S, Kim DH, Ma HW, Kim JH, et al. Triggering Receptor Expressed on Myeloid Cells-1 Agonist Regulates Intestinal Inflammation via Cd177(+) Neutrophils. Frontiers in Immunology 2021;12.

97. Kim MC, Borcherding N, Ahmed KK, Voigt AP, Vishwakarma A, Kolb R, et al. CD177 modulates the function and homeostasis of tumor-infiltrating regulatory T cells. Nat Commun 2021;12:5764.

98. Zhu W, Yu JB, Nie Y, Shi XK, Liu Y, Li FJ, et al. Disequilibrium of M1 and M2 Macrophages Correlates with the Development of Experimental Inflammatory Bowel Diseases. Immunological Investigations 2014;43:638-52.

99. Zundler S, Neurath MF. Immunopathogenesis of inflammatory bowel diseases: functional role of T cells and T cell homing. Clinical and Experimental Rheumatology 2015;33:S19-S28.

100. Laukoetter MG, Nava P, Nusrat A. Role of the intestinal barrier in inflammatory bowel disease. World Journal of Gastroenterology 2008;14:401-7.

101. Weber CR, Turner JR. Inflammatory bowel disease: is it really just another break in the wall? Gut 2007;56:6-8.

102. Landy J, Ronde E, English N, Clark SK, Hart AL, Knight SC, et al. Tight junctions

in inflammatory bowel diseases and inflammatory bowel disease associated colorectal cancer. World Journal of Gastroenterology 2016;22:3117-26.

103. Martini E, Krug SM, Siegmund B, Neurath MF, Becker C. Mend Your Fences The Epithelial Barrier and its Relationship With Mucosal Immunity in Inflammatory Bowel Disease. Cellular and Molecular Gastroenterology and Hepatology 2017;4:33-46.

104. Glover LE, Colgan SP. Hypoxia and Metabolic Factors That Influence Inflammatory Bowel Disease Pathogenesis. Gastroenterology 2011;140:1748-55.

105. Kerber EL, Padberg C, Koll N, Schuetzhold V, Fandrey J, Winning S. The Importance of Hypoxia-Inducible Factors (HIF-1 and HIF-2) for the Pathophysiology of Inflammatory Bowel Disease. International Journal of Molecular Sciences 2020;21.

106. Yin JH, Ren YB, Yang KQ, Wang WS, Wang T, Xiao WD, et al. The role of hypoxia-inducible factor 1-alpha in inflammatory bowel disease. Cell Biology International 2022;46:46-51.

107. Cao SS. Epithelial ER Stress in Crohn's Disease and Ulcerative Colitis. Inflammatory Bowel Diseases 2016;22:984-93.

108. Tan YR, Shen SY, Shen HQ, Yi PF, Fu BD, Peng LY. The role of endoplasmic reticulum stress in regulation of intestinal barrier and inflammatory bowel disease. Experimental Cell Research 2023;424.

109. Zeng Z, Mukherjee A, Varghese AP, Yang XL, Chen S, Zhang H. Roles of G protein-coupled receptors in inflammatory bowel disease. World Journal of Gastroenterology 2020;26:1242-61.

110. Feng ZS, Sun RC, Cong YZ, Liu ZJ. Critical roles of G protein-coupled receptors in regulating intestinal homeostasis and inflammatory bowel disease. Mucosal Immunology 2022;15:819-28.

111. Long SH, He Y, Chen MH, Cao K, Chen YJ, Chen BL, et al. Activation of PI3K/Akt/mTOR signaling pathway triggered by PTEN downregulation in the

pathogenesis of Crohn's disease. Journal of Digestive Diseases 2013;14:662-9.

112. Sauer S, Bruno L, Hertweck A, Finlay D, Leleu M, Spivakov M, et al. T cell receptor signaling controls Foxp3 expression via PI3K, Akt, and mTOR. Proceedings of the National Academy of Sciences of the United States of America 2008;105:7797-802.

113. Tokuhira N, Kitagishi Y, Suzuki M, Minami A, Nakanishi A, Ono Y, et al. PI3K/AKT/PTEN pathway as a target for Crohn's disease therapy. International Journal of Molecular Medicine 2015;35:10-6.

114. Salas A, Hernandez-Rocha C, Duijvestein M, Faubion W, McGovern D, Vermeire S, et al. JAK-STAT pathway targeting for the treatment of inflammatory bowel disease. Nature Reviews Gastroenterology & Hepatology 2020;17:323-37.

115. Lahiri S, Futerman AH. The metabolism and function of sphingolipids and glycosphingolipids. Cellular and Molecular Life Sciences 2007;64:2270-84.

116. Park EJ, Suh' M, Thomson B, Ma DWL, Ramanujam K, Thomson ABR, et al. Dietary ganglioside inhibits acute inflammatory signals in intestinal mucosa and blood induced by systemic inflammation of Escherichia coli lipopolysaccharide. Shock 2007;28:112-7.

117. Asanuma N. Effect of Dietary Ceramide and Glucosylceramide on the Alleviation of Experimental Inflammatory Bowel Disease in Mice. Journal of Oleo Science 2022;71:1397-402.

118. Filimoniuk A, Blachnio-Zabielska A, Imierska M, Lebensztejn DM, Daniluk U. Sphingolipid Analysis Indicate Lactosylceramide as a Potential Biomarker of Inflammatory Bowel Disease in Children. Biomolecules 2020;10.

119. Dompierre JP, Godin JD, Charrin BC, Cordelieres FP, King SJ, Humbert S, et al. Histone deacetylase 6 inhibition compensates for the transport deficit in Huntington's disease by increasing tubulin acetylation. Journal of Neuroscience 2007;27:3571-83.

120. Rivieccio MA, Brochier C, Willis DE, Walker BA, D'Annibale MA, McLaughlin

K, et al. HDAC6 is a target for protection and regeneration following injury in the nervous system. Proceedings of the National Academy of Sciences of the United States of America 2009;106:19599-604.

121. LoPresti P. HDAC6 in Diseases of Cognition and of Neurons. Cells 2021;10.

122. Fawad JA, Luzader DH, Hanson GF, Moutinho TJ, McKinney CA, Mitchell PG, et al. Histone Deacetylase Inhibition by Gut Microbe-Generated Short-Chain Fatty Acids Entrains Intestinal Epithelial Circadian Rhythms. Gastroenterology 2022;163:1377-+.

123. Moreno-Gonzalo O, Mayor F, Sánchez-Madrid F. HDAC6 at crossroads of infection and innate immunity. Trends in immunology 2018;39:591-5.

124. Macpherson AJ, Chester KA, Robson L, Bjarnason I, Malcolm AD, Peters TJ. Increased expression of c-myc proto-oncogene in biopsies of ulcerative colitis and Crohn's colitis. Gut 1992;33:651-6.

125. Hartman DJ, Binion DG, Regueiro MD, Miller C, Herbst C, Pai RK. Distinct Histopathologic and Molecular Alterations in Inflammatory Bowel Disease-Associated Intestinal Adenocarcinoma: c-MYC Amplification is Common and Associated with Mucinous/Signet Ring Cell Differentiation. Inflammatory Bowel Diseases 2018;24:1780-90.

126. Feagins LA. Role of transforming growth factor-beta in inflammatory bowel disease and colitis-associated colon cancer. Inflamm Bowel Dis 2010;16:1963-8.

127. Ihara S, Hirata Y, Koike K. TGF-beta in inflammatory bowel disease: a key regulator of immune cells, epithelium, and the intestinal microbiota. J Gastroenterol 2017;52:777-87.

128. Vandervliet A, Bast A. Role of Reactive Oxygen Species in Intestinal-Diseases. Free Radical Biology and Medicine 1992;12:499-513.

ABSTRACT(IN KOREAN)

염증성 장질환에서 새로운 히스톤 탈아세틸화효소 6 선택적 억제제 CKD-506의 잠재적 항염증 효과

<지도교수 천재희>

연세대학교 대학원 의학과

안 재 범

염증성 장질환은 소화기관에서 발생하는 원인 불명의 만성적이고 치료가 어려운 염증성 질환으로 항-TNF 억제제는 고식적인 치료제에 반응하지 않거나 증상이 심한 환자들을 대상으로 사용될 수 있지만, 생물학적 치료제에 반응이 없거나 효과가 있더라도 반응이 소실되는 경우 사용할 수 있는 다른 약제가 상당히 제한적인 상태이다.

히스톤 탈아세틸화효소 억제제는 다양한 자가면역 질환의 잠재적 치료제로 제기되고 있고 특히, 히스톤 탈아세틸화효소 6 (HDAC6)의 선택적 억제제인 CKD-506은 염증성 장질환의 마우스 모델에서 염증 유발에 대한 보호 효과와 함께 염증 완화 효과가 확인되었다.

본 연구에서는 HDAC6의 발현과 활성도를 염증성 장질환 환자의 장 조직에서 확인하였다. 마우스와 인간 대장 조직을 활용하여 장 점막 환경을 최대한 모방한 ex-vivo 배양시스템을 확립하고 CKD-506 처리 시 점막면역과 관련된 인자들의 변화를 관찰하였으며 고식적 치료나 항-TNF 억제제 불응 환자군의 대장 조직 ex-vivo 배양 이후 RNA-seq을 진행하였다. RNA-seq을 통해 확인한

표적유전자의 전사 단계에서의 변화를 인간 대장 유래 세포주와 마우스 ex-vivo 배양시스템에서 검증하였다.

HDAC6의 발현과 활성도가 IBD 환자에서 증가되어 있는 것을 확인하였고, 치료에 대한 반응보다는 질병의 활성도가 HDAC6 발현과 더 밀접한 연관성을 보였다. 인체 유래 대장 조직의 ex-vivo 배양 플랫폼을 안정화하여 기존 치료에 반응하지 않는 환자 대장 조직의 CKD-506 처리 후 RNA-seq을 통해 CKD-506의 표적유전자와 함께 기전을 규명하였으며, in-vitro와 ex-vivo 배양에서 전사 단계에서의 변화를 확인하였다.

본 연구에서는 CKD-506의 염증성 장질환에서 잠재적 치료제로서의 가능성을 제시하였고, 특히, 기존 치료에 반응하지 않고 높은 질병활성도를 보이는 환자군에서 유용할 것으로 판단된다.

핵심되는 말: 히스톤 탈아세틸화 효소, 염증성 장질환, 전사체 분석